

---

[All ETDs from UAB](#)

[UAB Theses & Dissertations](#)

---

2006

## Delineating the effects of mutant huntingtin on mitochondria.

Tamara Milakovic  
*University of Alabama at Birmingham*

Follow this and additional works at: <https://digitalcommons.library.uab.edu/etd-collection>

---

### Recommended Citation

Milakovic, Tamara, "Delineating the effects of mutant huntingtin on mitochondria." (2006). *All ETDs from UAB*. 5547.  
<https://digitalcommons.library.uab.edu/etd-collection/5547>

This content has been accepted for inclusion by an authorized administrator of the UAB Digital Commons, and is provided as a free open access item. All inquiries regarding this item or the UAB Digital Commons should be directed to the [UAB Libraries Office of Scholarly Communication](#).

DELINEATING THE EFFECTS OF MUTANT HUNTINGTIN ON MITOCHONDRIA

by

TAMARA MILAKOVIC

GAIL V. W. JOHNSON, COMMITTEE CHAIR  
SHANNON M. BAILEY  
PETER J. DETLOFF  
RICHARD S. JOPE  
MATHIEU J. LESORT

A DISSERTATION

Submitted to the graduate faculty of The University of Alabama at Birmingham,  
in partial fulfillment of the requirements for the degree of  
Doctor of Philosophy

BIRMINGHAM, ALABAMA

2006

UMI Number: 3227087

### INFORMATION TO USERS

The quality of this reproduction is dependent upon the quality of the copy submitted. Broken or indistinct print, colored or poor quality illustrations and photographs, print bleed-through, substandard margins, and improper alignment can adversely affect reproduction.

In the unlikely event that the author did not send a complete manuscript and there are missing pages, these will be noted. Also, if unauthorized copyright material had to be removed, a note will indicate the deletion.

**UMI<sup>®</sup>**

---

UMI Microform 3227087

Copyright 2006 by ProQuest Information and Learning Company.

All rights reserved. This microform edition is protected against unauthorized copying under Title 17, United States Code.

ProQuest Information and Learning Company  
300 North Zeeb Road  
P.O. Box 1346  
Ann Arbor, MI 48106-1346

# DELINEATING THE EFFECTS OF MUTANT HUNTINGTIN ON MITOCHONDRIA

TAMARA MILAKOVIC

## ABSTRACT

Huntington's disease (HD) is caused by a pathological expansion of polyglutamine domain in huntingtin protein. It is progressive, usually late onset disease characterized by selective striatal neurodegeneration. Several findings suggested mitochondrial dysfunction in HD. HD patients exhibit pronounced weight loss, despite sustained caloric intake. Postmortem HD brains showed reduced activities of mitochondrial complexes II, III and to a lesser extent complex IV specifically in the striatum. 3-NP (complex II inhibitor) administration resulted in HD like symptoms in rodents and nonhuman primates. Examination of HD lymphoblasts revealed reduced mitochondrial  $\text{Ca}^{2+}$  buffering capacity. Therefore, it is of great importance to determine and delineate the effects of mutant huntingtin on mitochondria.

In this dissertation, we analyzed the effects of mutant huntingtin on mitochondrial functions using genetically accurate cellular model of HD. Given the previous findings, we focused on analyses of electron transport chain and mitochondrial  $\text{Ca}^{2+}$  buffering.

In the first study, a complete analysis of respiratory chain enzyme activities and respiratory thresholds was carried out to delineate the effects of mutant huntingtin on mitochondrial electron transport chain. Our results indicate that the expression of mutant huntingtin does not affect mitochondrial electron transport chain.

In the second study, we analyzed the effects of mutant huntingtin on mitochondrial  $\text{Ca}^{2+}$  buffering function. Multiple functional assays were used to comprehensively determine  $\text{Ca}^{2+}$  effects on mitochondria. Our results indicate that

expression of mutant huntingtin impairs mitochondrial  $\text{Ca}^{2+}$  buffering. Mutant mitochondria depolarized at significantly lower  $[\text{Ca}^{2+}]$  than wild-type.  $\text{Ca}^{2+}$  uptake capacity was reduced in mutant mitochondria and respiration was more sensitive to  $\text{Ca}^{2+}$  induced changes.  $\text{Ca}^{2+}$  uptake capacity reduction was attenuated by Permeability Transition Pore (PTP) inhibitors (ADP plus oligomycin plus cyclosporine A) and  $\text{Ca}^{2+}$  induced depolarization was rescued by ADP. These results indicated PTP as the possible mechanism for mitochondrial  $\text{Ca}^{2+}$  buffering impairment in mutant huntingtin expressing cells.

Impairment of electron transport chain complexes clearly presents later event in HD. However, mitochondrial  $\text{Ca}^{2+}$  buffering impairment is likely an early and therefore important defect contributing to HD pathogenesis. Future studies should be aimed on further understanding of the mechanism of mitochondrial  $\text{Ca}^{2+}$  buffering defect and its role in HD.

## ACKNOWLEDGMENTS

I would like to acknowledge the members of my committee for their help and guidance over the course of my graduate career, Drs Richard S. Jope, Shannon M. Bailey, Peter J. Detloff and Mathieu J Lesort. I especially want to thank my mentor, Dr. Gail V. W. Johnson for without her knowledge, patience and encouragement none of this would be possible.

I would like to express great appreciation to everyone in my family who supported me. Especially, I want to thank my parents, my grandparents and my brother whose love and support kept me strong all the way. Above all, I thank my husband Vladimir for always being with me, encouraging me and trusting in me and for without whom none of this would ever happen.

## TABLE OF CONTENTS

	<i>Page</i>
ABSTRACT .....	ii
ACKNOWLEDGMENTS .....	iv
LIST OF TABLES .....	vi
LIST OF FIGURES .....	vii
INTRODUCTION .....	1
Huntington's Disease .....	1
Mitochondria .....	4
Oxidative-phosphorylation .....	4
Mitochondrial Ca <sup>2+</sup> Buffering .....	7
Huntington's Disease and Mitochondria .....	11
Excitotoxicity .....	14
MITOCHONDRIAL RESPIRATION AND ATP PRODUCTION ARE SIGNIFICANTLY IMPAIRED IN STRIATAL CELLS EXPRESSING MUTANT HUNTINGTIN .....	18
MUTANT HUNTINGTIN EXPRESSION INDUCES MITOCHONDRIAL CALCIUM HANDLING DEFECTS IN CLONAL STRIATAL CELLS: FUNCTIONAL CONSEQUENCES .....	52
CONCLUSIONS .....	89
LIST OF GENERAL REFERENCES .....	105

## LIST OF TABLES

<i>Table</i>		<i>Page</i>
	MITOCHONDRIAL RESPIRATION AND ATP PRODUCTION ARE SIGNIFICANTLY IMPAIRED IN STRIATAL CELLS EXPRESSING MUTANT HUNTINGTIN	
1.	Mitochondrial Enzyme Activities in STHdh <sup>Q7/Q7</sup> (Wild-type) and STHdh <sup>Q111/Q111</sup> (Mutant) Cells .....	45
2.	Spare Capacities and Threshold Values for Respiratory Complexes in Permeabilized Cells From STHdh <sup>Q7/Q7</sup> (Wild-type) and STHdh <sup>Q111/Q111</sup> (Mutant) Cell Lines .....	47



## LIST OF FIGURES

<i>Figure</i>	<i>Page</i>
INTRODUCTION	
1. Mitochondria and Oxidative-phosphorylation .....	6
2. Mitochondria and Ca <sup>2+</sup> .....	10
MITOCHONDRIAL RESPIRATION AND ATP PRODUCTION ARE SIGNIFICANTLY IMPAIRED IN STRIATAL CELLS EXPRESSING MUTANT HUNTINGTIN	
1. Respiratory Properties of STHdh <sup>Q7/Q7</sup> (Wild-type) and STHdh <sup>Q111/Q111</sup> (Mutant) Cells .....	43
2. ATP Levels and Mitochondrial ATP Production in Permeabilized Cells From STHdh <sup>Q7/Q7</sup> (Wild-type) and STHdh <sup>Q111/Q111</sup> (Mutant) Cells .....	44
3. Rotenone Titrations and Complex I Threshold Curves for Permeabilized Cells From STHdh <sup>Q7/Q7</sup> (Wild-type) and STHdh <sup>Q111/Q111</sup> (Mutant) Cells .....	46
4. Analysis of Complex II Threshold Profiles (By Malonate Titrations) and Catalytic Subunits Expression Levels in Permeabilized STHdh <sup>Q7/Q7</sup> (Wild-type) and STHdh <sup>Q111/Q111</sup> (Mutant) Cells .....	48
5. Antimycin Titrations and Complex III Threshold Curves for Permeabilized Cells From STHdh <sup>Q7/Q7</sup> (Wild-type) and STHdh <sup>Q111/Q111</sup> (Mutant) Cells .....	50
6. KCN Titrations and Complex IV Threshold Curves for Permeabilized Cells From STHdh <sup>Q7/Q7</sup> (Wild-type) and STHdh <sup>Q111/Q111</sup> (Mutant) Cells .....	51
MUTANT HUNTINGTIN EXPRESSION INDUCES MITOCHONDRIAL CALCIUM HANDLING DEFECTS IN CLONAL STRIATAL CELLS: FUNCTIONAL CONSEQUENCES	
1. Effects of Ca <sup>2+</sup> on Respiration in Mitochondria From STHdh <sup>Q7/Q7</sup> (Wild-type) and STHdh <sup>Q111/Q111</sup> (Mutant) Cells .....	81

## LIST OF FIGURES (continued)

<i>Figures</i>	<i>Page</i>
2. $\text{Ca}^{2+}$ Uptake Capacity Measured in Mitochondria From STHdh <sup>Q7/Q7</sup> (Wild-type) and STHdh <sup>Q111/Q111</sup> (Mutant) Cells .....	82
3. Mitochondrial and Cytosolic $\text{Ca}^{2+}$ Levels in STHdh <sup>Q7/Q7</sup> (Wild-type) and STHdh <sup>Q111/Q111</sup> (Mutant) Cells .....	83
4. Analysis of Mitochondrial Membrane Integrity Before and After $\text{Ca}^{2+}$ Addition to Mitochondria From STHdh <sup>Q7/Q7</sup> (Wild-type) and STHdh <sup>Q111/Q111</sup> (Mutant) Cells .....	84
5. Differential Effects of $\text{Ca}^{2+}$ on Mitochondrial Membrane Potential ( $\Delta\Psi_m$ ) in State 4 and State 3 Conditions in STHdh <sup>Q7/Q7</sup> (Wild-type) and STHdh <sup>Q111/Q111</sup> (Mutant) Cells .....	85
6. Effects of $\text{Ca}^{2+}$ on $\text{H}_2\text{O}_2$ Production in Mitochondria From STHdh <sup>Q7/Q7</sup> (Wild-type) and STHdh <sup>Q111/Q111</sup> (Mutant) Cells .....	86
7. Effects of Permeability Transition Pore (PTP) Inhibitors on Mitochondrial $\text{Ca}^{2+}$ Uptake Capacity in STHdh <sup>Q7/Q7</sup> (Wild-type) and STHdh <sup>Q111/Q111</sup> (Mutant) Cells .....	87
8. Effects of $\text{Ca}^{2+}$ on $\Delta\Psi_m$ and Mitochondrial $\text{Ca}^{2+}$ Accumulation in STHdh <sup>Q7/Q7</sup> (Wild-type) and STHdh <sup>Q111/Q111</sup> (Mutant) Cells in Situ.....	88

## CONCLUSIONS

1. Role of Mitochondria in Excitotoxicity .....	93
2. Proposed Model of the Mitochondrial $\text{Ca}^{2+}$ Handling Defect in Mutant Huntingtin Expressing Cells.....	98

## INTRODUCTION

### Huntington's Disease

Huntington's disease (HD) is a fatal, neurodegenerative disease inherited in an autosomal, dominant manner. In 1993, it was discovered that HD is caused by a mutation in the huntingtin gene that presents as pathological elongation of CAG repeats in exon 1 (1). Expansion of CAGs in the huntingtin gene results in expansion of polyglutamine (polyQ) region close to the N terminus of the huntingtin protein. In humans, the healthy population has between 6 and 34 CAGs, while HD develops with expansion to 40 or more CAGs. The range of 35-39 CAGs is considered diagnostically uncertain (HD carriers and some HD patients) (2). The variability of CAG repeats length, and therefore the likelihood of HD development in the family, is caused by instability of the CAG segment in the huntingtin gene, as it undergoes both decreases and increases during meiotic divisions. Larger increases are particularly noticed during paternal divisions (1). In addition, somatic instability has been described, since in different tissues CAGs length varies (3-5).

HD was first comprehensively described by George Huntington in 1872. He described it as "hereditary chorea" (6). Adult onset HD (majority of patients) is characterized by a triad of symptoms: movement abnormalities (chorea and abnormal voluntary movements), cognition decline (impaired attention, memory, speech, judgement) and psychiatric disturbances (depression, irritability, apathy). The disease onset inversely correlates with the CAG repeats length. Adult onset HD is caused by

expansions between 40 and 55 CAGs. Longer expansions are more rare and cause juvenile onset HD (age of onset before 21) (the longest expansion of 250 CAGs reported with the onset at 2.5 years of age (7)). Juvenile onset HD may have a different clinical presentation and is characterized by progressive rigidity of limbs and trunk (8).

Examination of HD patient brains revealed selective neurodegeneration as the cause for symptoms development and progression. The first region to be affected is the striatum (specifically GABAergic medium spiny neurons which comprise about 80% of striatal neurons) (2). In later stages, there is degeneration of the cortex, and to a lesser extent and regularity other brain regions (2). The striatum is the part of the basal ganglia structure located within the white matter, beneath the cerebral cortex. Basal ganglia are connected with the cortex and are involved in movement planning and coordination. The selective striatal degeneration leads to deterioration of the pathways inside the basal ganglia structure leading to dysregulation of its cortical projections (9) and causing movement disturbances and deterioration.

Another neuropathological feature of HD is aggregates found in nuclei and dystrophic neurites (10). They were detected in both HD brains and multiple mouse models (10-14). HD brains reveal aggregates in the cortex and striatum (10). Aggregates consist of ubiquitinated N-terminal fragments of mutant huntingtin, but also contain other proteins such as CREB binding protein (CBP), p53 and Sp1 (15). There is evidence suggesting both toxic and protective roles for aggregates (16). Further research is necessary to provide definite answers.

Important evidence indicates that HD is caused primarily by a toxic gain of function of the mutant huntingtin. Individuals with a heterozygous translocation

interrupting the HD gene that causes 50% reduction in the huntingtin levels do not develop HD, arguing against the major role of loss of function (17). Furthermore, transgenic mice with either truncated or full-length mutant huntingtin expressed in addition to two copies of endogenous, wild-type huntingtin develop HD like symptoms (12,18). Huntingtin knock-out mice are embryonically lethal (19-21)). Reduction of expression of expanded huntingtin (Q50) below 50% caused aberrant brain development and perinatal lethality while mice with normal levels mutant huntingtin expression developed normally (22). These findings indicated an important role of huntingtin in development but also showed that the mutant protein maintains the normal functions of huntingtin, at least during development.

Although the data clearly indicate that mutant huntingtin exhibits a toxic gain of function, it has been suggested that some loss of function could likely contribute to HD pathogenesis as well (23). Several groups have investigated the function of wild-type huntingtin. Huntingtin is a large (~350kDa) protein localized mostly in the cytosol but also found associated with a number of cellular structures: nucleus, endoplasmic reticulum (ER), Golgi complex, mitochondria, synapses, clathrin-coated vesicles and microtubules (23). Huntingtin plays an important role in embryogenesis (19-22), and likely in other processes such as neuronal survival (24), vesicular trafficking (including trafficking of mitochondria and BDNF) (25,26), BDNF transcription (27) and cholesterol synthesis (28).

The toxic functions gained by mutant huntingtin are still unclear but there is evidence suggesting that mutant huntingtin can cause: transcriptional dysfunction (15); ubiquitin-proteasome system dysfunction (16),  $\text{Ca}^{2+}$  homeostasis dysfunction (29,30) and

mitochondrial dysfunction (30-33). In order to elucidate the process of HD pathogenesis, it will be important to describe and fully understand each of the mutant huntingtin-caused dysfunctions and to determine their significance, schedule and connections in the course of the disease.

### Mitochondria

Mitochondria are cellular organelles that developed from a bacterial symbiosis with eukaryotic cells, early in evolution (34). Currently, several distinct mitochondrial functions have been recognized: energy production,  $\text{Ca}^{2+}$  buffering, apoptosis. In this dissertation, we investigated energy production and  $\text{Ca}^{2+}$  buffering mitochondrial functions in the context of HD.

### *Oxidative-phosphorylation*

Mitochondria are the most important source of energy in the cell. In the mitochondria, energy is produced through the process of oxidative-phosphorylation that takes place at the inner mitochondrial membrane (Figure 1.). Oxidative-phosphorylation machinery consists of complexes I, II, III and IV which represent the electron transport chain as they are involved in the transfer of electrons from the substrates ( $\text{NADH}$ ,  $\text{FADH}_2$ ) to  $\text{O}_2$  along the inner membrane. This process activates  $\text{H}^+$  extrusion from the matrix to the intermembrane space that establishes protonomotive force (mitochondrial membrane potential ( $\Delta\Psi_m$ ) plus pH gradient) across the inner membrane. Protonomotive force activates complex V that pumps  $\text{H}^+$  back to the matrix and synthesizes ATP from ADP and  $\text{P}^-$  (Figure 1.) (35).

Each of the complexes of the electron transport chain is a complex of proteins encoded by both mitochondrial and nuclear genes. Complex I (NADH:ubiquinone oxidoreductase) catalyzes the first step of oxidative-phosphorylation in which NADH is oxidized to  $\text{NAD}^+$  providing two electrons for the reduction of ubiquinone to ubiquinol. Complex I consists of 46 subunits (7 from mitochondrial genes). Complex II (succinate:ubiquinone oxidoreductase) catalyses the oxidation of succinate to fumarate as part of the tricarboxylic acid (TCA) cycle while transferring electrons directly to ubiquinone as part of oxidative-phosphorylation. It consists of 4 nucleus encoded subunits. Complex III (ubiquinol:cytochrome c oxidoreductase) catalyzes oxidation of ubiquinol to ubiquinone while reducing cytochrome c. It consists of 11 subunits (1 from mitochondrial genes). Complex IV (cytochrome c oxidase) catalyzes the reaction of cytochrome c oxidation while reducing  $\text{O}_2$  to  $\text{H}_2\text{O}$ . It has 13 subunits (3 from mitochondrial genes) (35). Defects of subunits of electron transport chain complexes result in impairment of oxidative-phosphorylation and manifest as late onset and progressive diseases (“primary mitochondrial diseases”) affecting brain, heart, skeletal muscle, kidney and endocrine system (34).

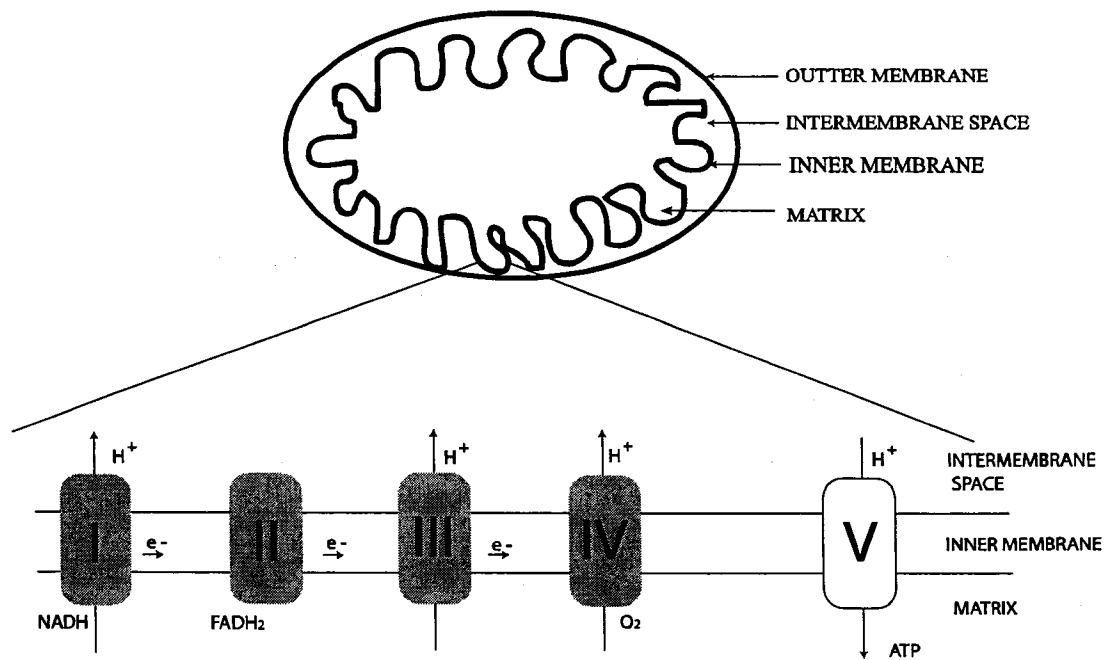


Figure 1. Mitochondria and Oxidative-phosphorylation. Mitochondria consist of several compartments: outer mitochondrial membrane, intermembrane space, inner mitochondrial membrane and matrix. Oxidative-phosphorylation takes place at the inner mitochondrial membrane. NADH and FADH<sub>2</sub> (final products of the tricarboxylic acid (TCA) cycle that takes place in the matrix) are substrates for complex I and complex II, respectively. After substrates are oxidized, electrons are transferred from complex I and II to complex III and further to complex IV where they are accepted by O<sub>2</sub> that gets reduced to water. As electrons are transferred through the inner membrane, H<sup>+</sup> gets exported from matrix to intermembrane space by complexes I, III and IV forming protonomotive force ( $\Delta\Psi_m + \text{pH gradient}$ ) across the inner membrane. The protonomotive force activates complex V that pumps H<sup>+</sup> back to the matrix and this activates synthesis of ATP from ADP and phosphate.



### *Mitochondrial $\text{Ca}^{2+}$ Buffering*

In most cells, cytosolic  $\text{Ca}^{2+}$  levels are in the range of 0.05-0.5  $\mu\text{M}$ . Cytosolic  $\text{Ca}^{2+}$  levels are tightly regulated by  $\text{Ca}^{2+}$  transport mechanisms at the plasma membrane, ER and mitochondria. At the plasma membrane,  $\text{Ca}^{2+}$  is extruded to the extracellular space by a  $\text{Ca}^{2+}$ -ATPase pump and a  $\text{Ca}^{2+}$ - $3\text{Na}^{+}$  exchanger. In addition,  $\text{Ca}^{2+}$  is taken up by the ER through a  $\text{Ca}^{2+}$ -ATPase pump and into mitochondria by a  $\Delta\Psi\text{m}$  dependent  $\text{Ca}^{2+}$ -uniporter. The outer mitochondrial membrane is permeable to  $\text{Ca}^{2+}$  and the uniporter transports  $\text{Ca}^{2+}$  through the inner membrane. The uptake of  $\text{Ca}^{2+}$  in mitochondria by the  $\text{Ca}^{2+}$ -uniporter depends on extramitochondrial  $[\text{Ca}^{2+}]$ . Further,  $\text{Ca}^{2+}$  from the mitochondria is extruded back to the cytosol by the  $\text{Na}^{+}$ - $\text{Ca}^{2+}$  exchanger, whose activity depends on free mitochondrial  $[\text{Ca}^{2+}]$ . The  $\text{Ca}^{2+}$  uptake and efflux pathways of the mitochondria are in balance at the set-point of 0.5  $\mu\text{M}$  extramitochondrial  $\text{Ca}^{2+}$  (for most cells). If extramitochondrial  $[\text{Ca}^{2+}]$  is above the set-point, mitochondria will load with  $\text{Ca}^{2+}$  and conversely, mitochondria release  $\text{Ca}^{2+}$  when the extramitochondrial  $\text{Ca}^{2+}$  is below this value (35). However, once the amount of about 10 nmol  $\text{Ca}^{2+}$ /mg (36) accumulates in mitochondria, a calcium phosphate complex starts to form in the mitochondrial matrix. This allows mitochondria to accumulate massive amounts of  $\text{Ca}^{2+}$  (800 nmol/mg at constant  $\text{Ca}^{2+}$  infusion as reported in (36)). Accumulation continues until mitochondria succeed in lowering extramitochondrial  $[\text{Ca}^{2+}]$  to the set-point. Therefore, under conditions of elevated  $\text{Ca}^{2+}$ , mitochondria can serve as temporary  $\text{Ca}^{2+}$  stores. Though very high, mitochondrial  $\text{Ca}^{2+}$  buffering capacity is not unlimited. When the limit is exceeded, opening of the permeability transition pore (PTP) occurs. This is evident by release of mitochondrial  $\text{Ca}^{2+}$ , collapse of  $\Delta\Psi$ , swelling of the matrix and rupture of the

outer membrane as shown by experiments in isolated mitochondria (36). The PTP forms at the contact sites between inner and outer mitochondrial membrane and likely consists of the voltage dependent anion channel (VDAC), adenine nucleotide translocator (ANT) and cyclophilin D. Some other proteins have been found to associate with the PTP as well (37). Interestingly, the threshold for PTP opening has been demonstrated to depend on free phosphate concentrations rather than on total amount of  $\text{Ca}^{2+}$  accumulated in the mitochondrial matrix (36). When mitochondria were incubated in the buffer with 5mM phosphate, PTP occurred at lower  $\text{Ca}^{2+}$  loads than when incubated with 2mM phosphate.

The importance of mitochondrial  $\text{Ca}^{2+}$  buffering has been attributed primarily to its role in the maintenance of cytosolic  $\text{Ca}^{2+}$  levels. Multiple studies showed that mitochondrial  $\text{Ca}^{2+}$  uptake follows stimulation with an agonist causing cytoplasmic  $[\text{Ca}^{2+}]$  increases (38). This is mostly attributed to mitochondria in close proximity to ER stores or plasma membrane where “spots” of high  $\text{Ca}^{2+}$  concentrations have been observed (38). In physiological conditions, it is suggested, mitochondrial  $\text{Ca}^{2+}$  buffering is important “in shaping spatio temporal complexity of  $\text{Ca}^{2+}$  signaling” (38).

Another important role of mitochondrial  $\text{Ca}^{2+}$  is the activation of mitochondrial metabolic enzymes. It is known that  $\text{Ca}^{2+}$  (0.1-1 $\mu\text{M}$ ) regulates three important matrix enzymes: pyruvate dehydrogenase phosphatase that activates pyruvate dehydrogenase; isocitrate dehydrogenase; 2-ketoglutarate dehydrogenase. Through this,  $\text{Ca}^{2+}$  stimulates mitochondrial ATP production. It was suggested that these events suffice  $\text{Ca}^{2+}$  uptake and efflux cycling without the requirement for accumulation of higher  $\text{Ca}^{2+}$  loads by means of phosphate (35).

The third important function of mitochondrial  $\text{Ca}^{2+}$  buffering is the opening of PTP. This is often considered an early step in apoptosis, as it can initiate the release of cytochrome c (through the induction of mitochondrial swelling and subsequent rupture of the outer mitochondrial membrane). However, the opening of PTP in situ has been questioned, especially since the precise determination of the amount of  $\text{Ca}^{2+}$  that actually loads in the mitochondria, in situ, is hard to determine. This is due to the great heterogeneity of mitochondrial response to  $\text{Ca}^{2+}$  and due to differences in sensitivity of  $\text{Ca}^{2+}$  dyes available for mitochondrial  $\text{Ca}^{2+}$  determination (38). However, the events associated with PTP, such as mitochondrial depolarization and ATP depletion are well documented during cellular  $\text{Ca}^{2+}$  overload that is usually studied in the context of excitotoxicity.

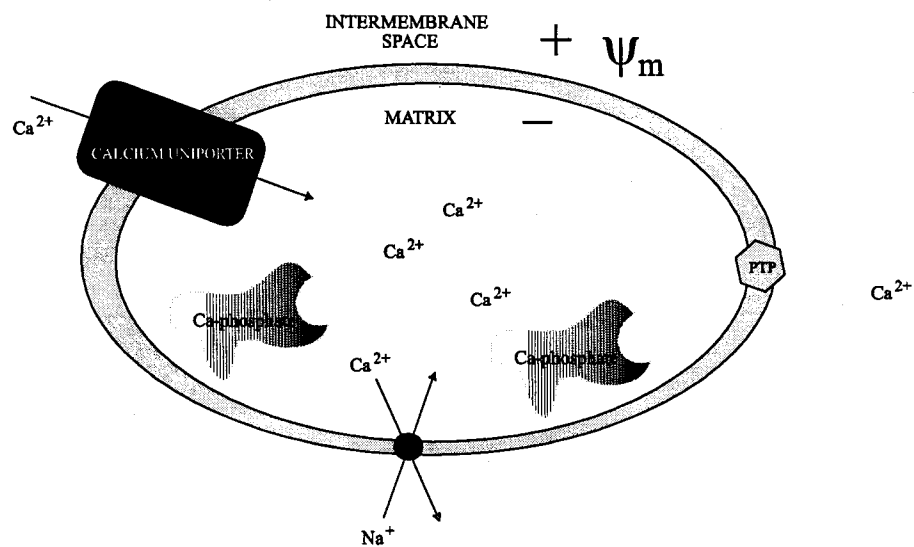


Figure 2. Mitochondria and  $\text{Ca}^{2+}$ . The major pathway of mitochondrial  $\text{Ca}^{2+}$  uptake is through the voltage dependent  $\text{Ca}^{2+}$ -uniporter.  $\text{Ca}^{2+}$  is extruded back into the cytosol through the  $\text{Ca}^{2+}$ - $\text{Na}^{+}$  exchanger. In mitochondria,  $\text{Ca}^{2+}$  is present in free form and bound form as a calcium-phosphate complex. When overloaded with  $\text{Ca}^{2+}$ , PTP opens and  $\text{Ca}^{2+}$  is released from mitochondria.

### Huntington's Disease and Mitochondria

Energetic impairment in HD was first postulated by observations of pronounced weight loss in HD patients occurring despite sustained caloric intake. Further, PET scans revealed marked reductions in glucose utilization in the striatum of symptomatic HD patients in early stages, when there was little or no evidence of striatal atrophy (39-41). The degree of striatal hypometabolism correlated well with the impairment in verbal learning and memory in HD patients, but not in normal subjects (42). Also, striatal glucose utilization was attenuated in asymptomatic subjects with increased risk of developing HD (43-45). NMR studies revealed increased lactate levels in the cortex and basal ganglia of symptomatic HD patients that suggested upregulation of glycolysis (46,47). More recently, a study demonstrated huntingtin CAG repeat length dependent decreases in the ATP/ADP ratio in lymphoblasts, both control and HD (48).

Impairment of the mitochondrial electron transport chain was proposed by studies in late stage HD patients that demonstrated decreased activities of mitochondrial complexes II, III and IV specifically in the striatum (31-33). Impaired complex I activity was reported in platelets and muscle but was unaffected in HD brain (33,49,50). Chronic administration of 3-nitropropionic acid (3-NP) (a mitochondrial complex II inhibitor) in rodents and nonhuman primates caused symptoms and neuropathology that resembled HD (51,52). It was determined that upon intraperitoneal administration in rodents, 3-NP caused marked inhibition (50-70%) of complex II activity throughout the brain but the neurodegeneration was greatly restricted to the striatum (53,54). This suggested selective vulnerability of striatal neurons to metabolic stress. These studies strongly suggested impairment of the electron transport chain in HD.

Mouse models have provided invaluable information about the pathogenesis of HD. They can be divided in the three broad groups: transgenic mice expressing exon-1 fragments of mutant huntingtin (R6/2 (144 glutamines)) being the best characterized (18)); transgenic mice expressing full length mutant huntingtin (like YAC 72) (12); mutant huntingtin knock-in mice (like HdhQ111 and Hdh 150Q) (14,55). Although all these mice were created to model HD, there are significant variations in their phenotypes. For example, R6/2 mice develop significant motor deficits, have a greatly reduced lifespan, and develop neuronal aggregates, but do not exhibit striatum specific neurodegeneration (18,56-58). The knock-in mouse models of HD develop rather subtle motor deficits, with no decrease in lifespan and no neuronal loss but do develop micro aggregates (14,55). Generally, mutant huntingtin fragments appear to be more toxic than the full length huntingtin. Also, the amount of mutant huntingtin expression is important, as the mice overexpressing full-length protein have a more severe disease phenotype than the knock-in mice.

Several studies have focused on analysis of possible energy deficits in transgenic mice. In R6/2 mice, significant reduction in complex IV and aconitase activities in the striatum and a decrease in the complex IV activity in the cortex have been shown (59). Another study showed a nonlinear drop in N-acetylaspartate (NAA) levels in R6/2 transgenic mice that coincided with the onset of symptoms (60). NAA is synthesized within mitochondria, and though its function in the brain is unknown, several studies have shown that inhibitors of the mitochondrial respiratory chain decreased NAA concentrations, which correlated with reductions in ATP and oxygen consumption (61,62). Dietary supplementation of creatine significantly improved survival, slowed

development of motor deficits, delayed the onset of weight loss and decreased gross brain and striatal atrophy in N171-82Q (expression of truncated huntingtin containing the first 171 amino acids and 82 Q) and R6/2 HD transgenic mice (63,64). In the cell, creatine gets phosphorylated by creatine kinase to phosphocreatine. Under conditions of ATP exhaustion, phosphocreatine can donate its phosphate group to ADP to resynthesize ATP (65).

Mitochondrial impairment is an important source of oxidative stress (66). Inhibition of the electron transport chain, especially complexes I and III, causes increase in reactive oxygen species (ROS) production (66). Also, mitochondrial  $\text{Ca}^{2+}$  has been suggested to affect ROS production (67). Evidence was found that implied significant oxidative damage in HD. In HD patients, elevated 8-hydroxydeoxyguanosine ( $\text{OH}^8\text{dG}$ ) (DNA oxidative damage product), increased 3-nitrotyrosine staining (peroxynitrite caused protein damage), malondyaldehyde and lipofuscin accumulation (markers for oxidative damage to lipids) were found (53). Further, significant decrease in aconitase activity (70%) was demonstrated (68). Aconitase is a TCA cycle enzyme shown to be very sensitive to oxidative damage. Age-dependent increase in oxidative damage, in the striatum, was shown in transgenic R6/1 mice (expression of exon 1 huntingtin with 115CAGs) and it paralleled the development of motor deficits (69). Recently, increased glutathione levels in cortical and striatal mitochondria from R6/2 mice were reported, suggesting oxidative stress induced upregulation of antioxidant mechanisms, glutathione peroxidase in particular (70).

In more recent studies, impairment of mitochondrial  $\text{Ca}^{2+}$  buffering has been suggested. Panov et. al. demonstrated reduced  $\text{Ca}^{2+}$  uptake capacity in mitochondria from

HD lymphoblasts and brain mitochondria from full-length huntingtin transgenic mice (YAC72) (30,71). Following these discoveries, it was demonstrated that recombinant pathologically expanded polyQ, both without and within the context of huntingtin exon 1, when added to liver mitochondria, promotes  $\text{Ca}^{2+}$  induced mitochondrial depolarization and swelling (72,73). This suggested the possibility of direct effects of mutant huntingtin on mitochondria. In support of this hypothesis, Choo et al showed that a fraction of cytosolic huntingtin directly associates with the outer mitochondrial membrane (73). Earlier this year, reduced  $\text{Ca}^{2+}$  uptake capacity was shown in muscle mitochondria from R6/2 mice (74).

Overall, these studies suggested the possibility that mutant huntingtin causes, directly or indirectly, mitochondrial dysfunction and that it may play an important role in HD pathogenesis.

#### *Excitotoxicity*

The mechanism by which mitochondrial dysfunction could contribute to neuronal dysfunction and death in HD is postulated by the model of excitotoxicity (75). Excitotoxicity is glutamate induced neuronal toxicity. Glutamate is one of the major excitatory neurotransmitters in the brain, however, overactivity of glutamate neurotransmission is characterized by  $\text{Ca}^{2+}$  mediated neuronal dysfunction. This has been described in primary neuronal cultures, where prolonged glutamate stimulation (10-15 minutes) leads to excitotoxicity (76-78). In this model, mitochondrial dysfunction could be an initiating or later (but crucial) event. If mitochondria are compromised, there is depletion of ATP levels in the cell that would lead to slowing of ATP dependent processes, including the ATP dependent  $\text{Na}^+ - \text{K}^+$  pump at the plasma membrane. This



pump utilizes about 70% of neuronal ATP to maintain resting plasma membrane potential (79-81). Therefore, its slowing would lead to plasma membrane depolarization and release of the  $Mg^{2+}$  block at NMDA receptors, lowering their threshold for stimulation by glutamate. Prolonged NMDA stimulation leads to sustained increases of cytosolic  $Ca^{2+}$  levels. This is in contrast to short NMDA stimulation, where increases of intracellular  $Ca^{2+}$  are transient because  $Ca^{2+}$  is buffered by mitochondria and the ER and successfully exported from the cell. During excitotoxicity, increase of mitochondrial  $Ca^{2+}$  levels have been demonstrated (76-78). Further, it was established that sustained increases of cytosolic  $Ca^{2+}$  levels strongly correlate with mitochondrial depolarization (77). Therefore, any mitochondrial impairment that would favor mitochondrial depolarization would likely sensitize neurons to excitotoxic insults. The importance of mitochondrial  $Ca^{2+}$  uptake in excitotoxicity has been suggested by experiments showing that inhibition of mitochondrial  $Ca^{2+}$  uptake (by rotenone (complex I inhibitor) plus oligomycin (complex V inhibitor)) significantly increases survival of primary neurons exposed to glutamate (82).

Excitotoxicity in HD has been suggested by studies demonstrating selective depletion of NMDA receptors in the striatum of HD brain, implying neurons preferentially dying in the striatum do have NMDA receptors (83). Similar reductions of NMDA receptors were also found in asymptomatic, at risk patients implying that excitotoxicity may be an early process in HD (84). Further, striatal injections of NMDA agonists, such as quinolinic acid, in primates, caused neuropathology (selective degeneration of medium spiny neurons) that resembled HD (85). Examination of HD mouse models showed differential responses to induction of excitotoxicity. YAC72 mice

(full length mutant huntingtin transgenic mice) showed increased sensitivity to excitotoxicity as quinolinic acid induced striatal lesions were larger than in wild-type mice (86). Truncated mutant huntingtin transgenic mouse model with 100 CAGs (HD100) did not show altered sensitivity to excitotoxicity (87). Further, R6/2 mice showed resistance to quinolinic acid, NMDA and 3-NP induced lesions (88,89). Even so, the glutamate release inhibitor riluzole prolonged survival in R6/2 mice (90). Despite differential response to glutamate induced toxicity, both YAC72 and R6/2 mice exhibited higher resting cytosolic  $\text{Ca}^{2+}$  levels than matching controls (12,91) and HD100 exhibited higher  $[\text{Ca}^{2+}]$  upon NMDA stimulation than control mice (92).

Selective striatal neurodegeneration is one of the important features of HD. It can be ascribed to both regional and mutant huntingtin specific factors. The striatum is very highly innervated by glutaminergic afferents from the cortex (2). However, high glutaminergic innervation is present in other brain regions as well (hippocampus, cortex, cerebellum). In the scope of the excitotoxicity model, differences in the glutamate receptor subtypes present in different brain regions could account for the selective striatal loss (2,53). Striatal medium sized spiny neurons contain NR2B NMDA receptor subtype that is suggested to be particularly responsible for excitotoxicity (93). Presence of mGlu5 receptors that when activated increase inositol triphosphate ( $\text{In}_3\text{P}$ ) leading to the release of  $\text{Ca}^{2+}$  from the ER would further contribute to great sensitivity of medium sized spiny neurons (2). Also, lower expression of the glutamate transporter (EAAC1) was found in the striatum when compared to the hippocampus and was suggested to contribute to higher striatal sensitivity to excitotoxic stress (94). Somatic instability of the

huntingtin gene was described. Large expansions of the CAG repeat region were reported in the striatum and proposed to contribute to selective striatal neurodegeneration (4).

Important evidence has suggested the involvement of mitochondrial dysfunction and excitotoxicity in HD. However, further research is necessary to provide definite answers. Given the fact that mitochondria play an essential role in cell homeostasis and well-being, it is important to determine if mitochondrial function is impaired in HD. Therefore, the goal of this study was to further investigate if mutant huntingtin impairs mitochondrial functions. To model HD, we used conditionally immortalized striatal progenitor cell lines: a wild-type (SThdh<sup>Q7/Q7</sup>) cell line expressing endogenous levels of wild-type huntingtin with 7 glutamines and a mutant (SThdh<sup>Q111/Q111</sup>) cell line expressing mutant huntingtin with 111 glutamines. The mutant cell line was derived from a mutant huntingtin knock-in mice (14,95) and represents a genetically accurate cell model of HD since it contains endogenous levels of mutant huntingtin. Based on findings from previous studies, we focused on two major questions:

1. Does mutant huntingtin affect oxidative-phosphorylation, in particular, the complexes of the electron transport chain?
2. Does mutant huntingtin affect mitochondrial Ca<sup>2+</sup> buffering and Ca<sup>2+</sup> dependent mitochondrial processes?

The results of these studies are described in the following publications.

MITOCHONDRIAL RESPIRATION AND ATP PRODUCTION ARE  
SIGNIFICANTLY IMPAIRED IN STRIATAL CELLS  
EXPRESSING MUTANT HUNTINGTIN

by

TAMARA MILAKOVIC AND GAIL V. W. JOHNSON

*Journal of Biological Chemistry*, 280 (35): 30773-82 (2005)

Copyright  
2005

by

American Society for Biochemistry and Molecular Biology

Used by permission

Format adapted and errata corrected for dissertation

### Abstract

There is significant evidence that energy production impairment and mitochondrial dysfunction play a role in the pathogenesis of Huntington disease. Nonetheless, the specific mitochondrial defects due to the presence of mutant huntingtin have not been fully elucidated. To determine the effects of mutant huntingtin on mitochondrial energy production, a thorough analysis of respiration, ATP production, and functioning of the respiratory complexes was carried out in clonal striatal cells established from Hdh<sup>Q7</sup> (wild-type) and Hdh<sup>Q111</sup> (mutant huntingtin knock-in) mouse embryos. Mitochondrial respiration and ATP production were significantly reduced in the mutant striatal cells compared with the wild-type cells when either glutamate/malate or succinate was used as the substrate. However, mitochondrial respiration was similar in the two cell lines when the artificial electron donor TMPD/ascorbate, which feeds into complex IV, was used as the substrate. The attenuation of mitochondrial respiration and ATP production when either glutamate/malate or succinate was used as the substrate was not due to impairment of the respiratory complexes, because their activities were equivalent in both cell lines. Intriguingly, in the striatum of presymptomatic and pathological grade 1 Huntington disease cases there is also no impairment of mitochondrial complexes I–IV (Guidetti, P., Charles, V., Chen, E. Y., Reddy, P. H., Kordower, J. H., Whetsell, W. O., Jr., Schwarcz, R., and Tagle, D. A. (2001) *Exp. Neurol.* 169, 340–350). To our knowledge, this is the first comprehensive analysis of the effects of physiological levels of mutant huntingtin on mitochondrial respiratory function within an appropriate cellular context. These findings demonstrate that the presence of

mutant huntingtin impairs mitochondrial ATP production through one or more mechanisms that do not directly affect the function of the respiration complexes.

### Introduction

Huntington disease (HD)<sup>1</sup> is an autosomal dominant neurodegenerative disorder caused by a pathological expansion of CAG repeats in the gene encoding for a protein called huntingtin. Disease symptomatology and progression are due to massive neuronal dysfunction and death in the striatum, and in the cerebral cortex later in the disease. Even though the identification of the gene that contains the disease-causing mutation (1) was a fundamental discovery, it is still unclear how the mutant huntingtin causes pathogenesis, which is of essential importance for the development of successful treatment strategies.

There is significant evidence that energy production is impaired in HD. Positron emission tomography scans of the striatum showed impaired glucose metabolism early in the disease (2–4). Indeed, striatal hypometabolism has been observed in presymptomatic HD cases (5). Further, NMR experiments in symptomatic HD patients found increased lactate levels in the cortex and basal ganglia (6), suggesting the possibility that glycolysis is up-regulated to compensate for impaired ATP production by the oxidative phosphorylation pathway. Several groups have also reported deficits in respiratory complexes II, III, and IV in postmortem brain tissue from HD cases in which neuronal loss was evident (7–9). Additionally, chronic treatment of rodents or nonhuman primates with 3-nitropropionic acid (3-NP) (an irreversible complex II inhibitor) caused selective damage of the striatum resulting in pathology and symptomatology that resembled HD (10, 11).

HD cell models have been extremely useful in delineating pathogenic processes caused by mutant huntingtin (12–15). Cell lines derived from the striatum of HD knock-in mice are particularly useful tools for examining the molecular mechanisms of HD pathogenesis. Trettel and colleagues (14) have established striatal cell lines from HD knock in ( $Hdh^{Q111/Q111}$ ) and wild-type ( $Hdh^{Q7/Q7}$ ) mice. The  $STHdh^{Q111/Q111}$  cell line expresses mutant huntingtin at endogenous levels, and therefore is a genetically accurate cell model of HD. As the striatum is the most affected region in HD, the striatal origin of this cell model makes it optimal for HD studies. Previous studies using the  $STHdh^{Q111/Q111}$  and  $STHdh^{Q7/Q7}$  cells have provided indirect evidence that there is mitochondrial dysfunction in the mutant huntingtin-expressing striatal cells. Reduced cAMP levels have been reported in the  $STHdh^{Q111/Q111}$  cells when compared with the  $STHdh^{Q7/Q7}$  cells (16). Further, the mutant cells were more sensitive than the wild-type cells to 3-NP induced toxicity, however both cell lines were equally sensitive to rotenone (a complex I inhibitor)-induced cell death (17). Further, treatment of the  $STHdh^{Q7/Q7}$  cells with 3-NP resulted in the initiation of apoptotic cell death, whereas cells expressing mutant huntingtin died by a nonapoptotic process when treated with 3-NP (17). Overall these and other studies clearly demonstrate that the  $STHdh^{Q111/Q111}$  and  $STHdh^{Q7/Q7}$  cell lines are appropriate models for studying HD pathogenesis.

In this study, we used these clonal striatal cell lines expressing mutant ( $STHdh^{Q111/Q111}$ ) or wild-type ( $STHdh^{Q7/Q7}$ ) huntingtin (14) to examine the effects of mutant huntingtin on energy production and mitochondrial respiration. A thorough analysis of  $O_2$  consumption, ATP production, and respiratory complex activities was carried out to delineate the effects of mutant huntingtin on mitochondrial bioenergetic

processes. Further, we performed threshold analyses to compare handling of inhibition of different respiratory complexes in the two cell lines. We found that mutant cells (STHdh<sup>Q111/Q111</sup>) have significantly reduced O<sub>2</sub> consumption and ATP production rates compared with wild-type cells (STHdh<sup>Q7/Q7</sup>). However, there were no significant differences in the respiratory complex activities. Also, the handling of mitochondrial inhibitors was similar in the two cell lines. Our findings clearly suggest that mutant huntingtin compromises oxidative phosphorylation and mitochondrial energy production, but this is not through the impairment of respiratory complexes. This is in agreement with a previous study that demonstrated in presymptomatic or grade I HD brain there are no changes in the activities of complexes I–IV in the striatum (18). Additionally, we found that the respiratory thresholds for complexes I, II, and III were low in the cultured striatal cells. These findings suggest that the striatum may be particularly sensitive to events that result in compromised mitochondrial complex activity. Overall the results of this study increase our understanding of the effects of mutant huntingtin on mitochondria and energy production and provide novel and important data regarding the bioenergetics of striatal cells.

## Materials and Methods

*Materials*—All chemicals were from Sigma-Aldrich unless otherwise noted.

*Cell Culture*—Conditionally immortalized striatal neuronal progenitor cell lines, which were obtained as a gift from Dr. M. MacDonald, were used in this study. The STHdh<sup>Q7/Q7</sup> cell line expressing endogenous normal huntingtin and the homozygous mutant STHdh<sup>Q111/Q111</sup> cell line expressing mutant huntingtin with 111 glutamines were prepared



from wild-type mice and homozygous  $Hdh^{Q111/Q111}$  knock-in mice, respectively. Both cell lines have been described previously (14). Cells were cultured in Dulbecco's modified Eagle's medium (Mediatech Inc.) supplemented with 4% fetal bovine serum (HyClone) and 4% bovine growth serum (HyClone), 2 mM L-glutamine (Mediatech Inc.), and 100 units/ml penicillin and 100  $\mu$ g/ml streptomycin (Mediatech Inc.). The cells were grown at 33 °C in a humidified atmosphere containing 5% CO<sub>2</sub>.

*Cell Permeabilization*—Cells were permeabilized as described previously (19). Briefly, cells were trypsinized, resuspended in media A (20 mM HEPES, 10 mM MgCl<sub>2</sub>, 250 mM sucrose, pH 7.3), and counted followed by permeabilization of aliquots of  $1 \times 10^7$  cells. An aliquot was resuspended in media A containing digitonin at a final concentration of 0.015% (which was found to be the optimal concentration in preliminary studies) and mixed for 1 min. After centrifugation, the digitonin-containing media A was removed, and permeabilized cells were washed with a large volume of media A to remove any remaining digitonin. For these studies commercially available digitonin was purified as described previously (20) and stored as a 10% stock in Me<sub>2</sub>SO at - 20 °C.

*Polarographic Measurements*—Respiration rates in the permeabilized cells were measured using an oxygraph (Hansatech Instruments). In this instrument a Clark-type electrode is placed at the bottom of the water-jacketed respiratory chamber. During measurements, the chamber was thermostatted at 37 °C and sealed with a plunger. An electromagnetic stirrer bar was used to mix the contents of the chamber. Permeabilized cells were resuspended in a respiration buffer (media A, 2 mM potassium phosphate (KH<sub>2</sub>PO<sub>4</sub>:K<sub>2</sub>HPO<sub>4</sub>, 1:1.78), pH 7.1, 1% bovine serum albumin) and used immediately for O<sub>2</sub> consumption measurements. A suspension of permeabilized cells ( $1 \times 10^7$  cells/ml)

was placed in the chamber and allowed to equilibrate for 2 min. This was followed by the addition of respiratory substrates: glutamate (10 mM) plus malate (10 mM), succinate (5 mM) plus rotenone (10  $\mu$ M), or ascorbate (1 mM) plus *N,N,N',N'*-tetramethylphenylenediamine dihydrochloride (TMPD) (200  $\mu$ M). State 4 respiration was monitored for 2 min after which ADP (1.5 mM) was added to initiate state 3 respiration, which was measured for a further 2–4 min. For uncoupled respiration measurements, carbonyl cyanide 4-(trifluoromethoxy)phenylhydrazone (FCCP) (20  $\mu$ M) was added to the mix of permeabilized cells and respiratory substrate (succinate plus rotenone) in the respiration medium, and O<sub>2</sub> consumption was monitored for 2 min. In the inhibitor titration experiments, rotenone (1–50 nM) to inhibit complex I, malonate (0.05–5 mM) to inhibit complex II, antimycin (1–100 nM) to inhibit complex III or KCN (1–500  $\mu$ M) to inhibit complex IV were added to the suspension of permeabilized cells in the respiratory chamber, and the mixture was incubated for 2 min. This was followed by the addition of respiratory substrates (succinate plus rotenone for complexes II, III, and IV or glutamate plus malate for complex I), and then ADP as described above. A separate incubation was performed for each inhibitor concentration. State 3 respiration rates were used for the threshold analysis.

*Enzyme Assays*—Citrate synthase, and complex I, II, and III enzyme activities were determined spectrophotometrically. All the assays were performed at 30 °C. Citrate synthase activity was determined as the rate of color change of 5,5'-dithiobis-(2-nitrobenzoic) acid at 412 nm. The reaction was initiated by the addition of oxaloacetate in the presence of acetyl-CoA (21). Complex II activity was measured by the reduction of 2,6-dichlorophenolindophenol at 600 nm. The reaction was carried out with succinate, in

the presence of KCN and rotenone and initiated by the addition of ubiquinone-2. The rate sensitive to 2-thenyltrifluoroacetone (1 mM) was taken as complex II activity (22). Complex III activity was measured by monitoring the oxidation of reduced ubiquinone-2 with cytochrome *c* as the electron acceptor at 550 nm (23). Complex I activity was determined by measuring the rate of oxidation of NADH at 340 nm using ubiquinone-2 as the electron acceptor. The rate sensitive to rotenone (10  $\mu$ M) was taken to be complex I activity (23). Because we were not able to detect complex I activity after freezethaw treatment, osmotic shock and sonication were used to prepare samples for complex I assay as described previously with modifications (24, 25). Briefly, thawed samples were centrifuged (16,000 X g for 5 min at 4 °C), and the pellet was diluted in cold water (2–4 X 10<sup>7</sup> cells/ml). After osmotic shock treatment, samples were centrifuged again, and the pellet was dissolved in media A and sonicated on ice (3 X 20 s) prior to use in the assay. Complex IV activity was determined polarographically as described previously (26). Permeabilized cells were incubated in the reaction buffer (50 mM MOPS, 0.3% Tween 80, 2 mM CCCP, pH 7.5) in the respiratory chamber for 2 min without or with KCN (1–500  $\mu$ M). Subsequently, ascorbate (3.5 mM) and TMPD (0.35 mM) were added, and O<sub>2</sub> consumption was observed.

*Threshold Curves and Determination of Thresholds and Spare Capacities*—The threshold curves were constructed from the raw data as described previously (27). To determine thresholds and spare capacities, we followed the method described in Refs. 28 and 29. As described previously, the least-square regression lines beyond the inflection point in each threshold curve were extrapolated to zero complex inhibition. The intersection of these lines with the ordinate axis was used to determine spare capacity for the complex by

subtracting 100% as the value at which respiration was unaffected by the complex inhibition. Threshold values were determined from the regression line equations, as the percentage of complex inhibition at which respiration was unaffected (100%). Spare capacity and threshold value terms are as described previously (29). In several threshold curves the inflection point was not evident; therefore, data points obtained with every inhibitor concentration were used for linear regression analysis.

*Analysis of ATP Levels and ATP Production*—ATP levels and ATP production were determined using a luciferin/luciferase assay as described previously (30) utilizing a Turner Designs TD 20/20 (Turner Designs) luminometer. To determine ATP levels, cells were collected in lysis buffer (100 mM Tris, 4 mM EDTA, pH 7.75) and boiled for 2 min. Samples were then centrifuged (1000 X g for 1min), and the supernatants were used in the luciferin/luciferase assay. ATP levels were normalized to protein content in the samples. Protein concentrations were determined from cell lysates before boiling using the bicinchoninic acid assay (Pierce) and used to calculate protein content in the amount of samples used for the ATP assay. Reaction buffer for this assay contained 70  $\mu$ M luciferin, 0.05  $\mu$ g/ml luciferase, 10 mM magnesium acetate, 0.063% bovine serum albumin, and 150 mM Tris acetate, pH 7.5. To determine mitochondrial ATP production, cells were permeabilized and resuspended in media A. The reaction buffer for this assay was respiration buffer supplemented with an adenylate kinase inhibitor (di(adenosine)pentaphosphate, 0.15 mM), respiratory substrates (glutamate (10 mM) plus malate (10 mM), or succinate (5 mM) plus rotenone (10  $\mu$ M)), luciferin (70  $\mu$ M), and luciferase (0.05  $\mu$ g/ml). After the initial luminescence reading, ADP (200  $\mu$ M) was added

to the reaction, and the increase in luminescence was monitored for 2 min in the kinetic mode.

*Western Blot Analysis*—Western blot analysis was performed according to general protocols. For this analysis, permeabilized cells samples were sonicated, and protein concentrations were determined by the bicinchoninic acid assay. Antibodies used were: complex II, a 70-kDa subunit monoclonal antibody (Molecular Probes, 5 µg of protein, 1:10,000), complex II, a 30-kDa subunit monoclonal antibody (Molecular Probes, 20 µg of protein, 1:1,000), and voltage-dependent anion channel monoclonal antibody (Calbiochem) (20 µg of protein, 1:2,000).

*Statistical Analysis*—Results were analyzed using Student's *t* test or paired *t* test as indicated. ATP production data were analyzed using Chauvenet's Criterion followed by Student's *t* test.

## Results

### *Respiratory Properties of STHdh<sup>Q7/Q7</sup> (Wild-type) and STHdh<sup>Q111/Q111</sup> (Mutant)*

*Cells*—STHdh<sup>Q7/Q7</sup> (wild-type) and STHdh<sup>Q111/Q111</sup> (mutant) cells were permeabilized with digitonin (0.015%) and used for oxygen consumption measurements. Digitonin binds to cholesterol in the eukaryotic plasma membrane and creates pores through which soluble components of the cytosol can be released and the respiratory substrates, cofactors, and inhibitors used can easily be introduced into the cell. This approach is optimal for the maintenance of coupled, metabolically active mitochondria in isolated or cultured cells (31–34). Although cholesterol is also present in the outer mitochondrial membrane, it is at substantially lower levels than in the plasma membrane (35), thus

making it possible to selectively permeabilize the plasma membrane if low enough concentrations of digitonin are used. However, if the concentration of digitonin is not high enough, the cells will be inadequately permeabilized. Therefore in preliminary studies respiration was measured in cells permeabilized with 0.005–0.02% digitonin to determine the optimal concentration for the striatal cells. These studies revealed that respiration was optimal when 0.015% digitonin was used.

State 4 (in the absence of ADP) and state 3 (in the presence of ADP) respiration rates were determined and compared between the two cell lines (Fig. 1A). All rates were expressed per unit of citrate synthase activity to normalize for the mitochondrial content. State 3 respiration was significantly reduced in the mutant cells compared with the wild-type when either succinate (with rotenone) (feeds electrons into complex II) or glutamate plus malate (feed electrons into complex I) were used as the substrates. However, when ascorbate plus TMPD (an artificial electron donor that feeds electrons into complex IV) was used as the respiratory substrate, there were no differences between the cell lines. State 4 respiration rates in the two cell lines were not significantly different when any of the respiratory substrates were used. To observe maximal respiratory capacity of the two cell lines, respiration rates were measured after the addition of the uncoupler FCCP. The uncoupled respiration rate was significantly lower in the mutant cells compared with the wild-type cells (Fig. 1A).

State 4 and State 3 respiration rates were used to calculate Respiratory Control Ratios (RCRs). RCRs were significantly reduced in the mutant cells compared with the wild-type cells when either succinate (with rotenone) or glutamate plus malate were used as the substrates (Fig. 1B). This reduction is the result of reduced state 3 respiration in the

mutant cells as shown in Fig. 1A. When ascorbate plus TMPD was used as the substrate, the RCRs were not different between the two cell lines (Fig. 1B).

*ATP Levels and Mitochondrial ATP Production in Permeabilized STHdh<sup>Q7/Q7</sup> (Wild-type) and STHdh<sup>Q111/Q111</sup> (Mutant) Cells*—To further analyze the energetic status of the STHdh<sup>Q7/Q7</sup> (wild-type) and STHdh<sup>Q111/Q111</sup> (mutant) cells, especially of their mitochondria, we measured total ATP levels and mitochondrial ATP production. To determine ATP levels, total cell lysates were prepared and ATP measured as described under “Materials and Methods.” These data demonstrate that there is no significant difference in the total ATP levels between the two cell lines (Fig. 2A). In contrast, measurement of mitochondrial ATP production revealed that the rate of mitochondrial ATP production was significantly lower in the mutant cells compared with the wild-type cells when either succinate (with rotenone) or glutamate plus malate were used as the respiratory substrates (Fig. 2B). This is consistent with the findings from the oxygen consumption experiments (Fig. 1A) where state 3 rates (with succinate plus rotenone or glutamate plus malate) were significantly lower in the mutant cell line compared with the wild-type.

*Mitochondrial Enzyme Activities in STHdh<sup>Q7/Q7</sup> (Wild-type) and STHdh<sup>Q111/Q111</sup> (Mutant) Cells*—Mitochondrial enzyme activities were measured in permeabilized STHdh<sup>Q7/Q7</sup> (wildtype) and STHdh<sup>Q111/Q111</sup> (mutant) cells. The activity of citrate synthase, a tricarboxylic acid cycle enzyme, was measured and normalized to the number of cells or protein content. Citrate synthase activity was decreased in the mutant cells (25%) when normalized to the number of cells (Table I). This corresponded to the observation that mutant cells appear smaller in size and have ~ 25% less protein content than the

wild-type cells (data not shown). When normalized to the protein content, citrate synthase activity was not different between the two cell lines (Table I). This suggests similar mitochondrial load per protein mass in the two cell lines.

To understand why the respiration rates are reduced in the mutant cells, the activity of each of the four respiratory complexes was measured and normalized to units of citrate synthase activity (Table I). No significant differences were observed between wild-type and mutant cells in the activity of any of the four respiratory complexes.

*Inhibitor Titrations and Threshold Analyses in Permeabilized STHdh<sup>Q7/Q7</sup> (Wild-type) and STHdh<sup>Q111/Q111</sup> (Mutant) Cells*—To further analyze mitochondrial respiration in the two cell lines the sensitivity of respiration and complex activities to mitochondrial inhibitors was measured and respiratory thresholds analyses were carried out. Complex I was inhibited with increasing concentrations of rotenone, and respiration rates and complex I activities were measured. Rotenone caused a dose-dependent decrease in both respiration and complex I activity (Fig. 3, *A* and *B*). When respiration rates (expressed as a percentage of respiration rate with no inhibitor) were plotted against percent inhibition of complex I activity, no significant threshold was observed (Fig. 3C). The threshold curve was further analyzed using the least squares linear regression method. Also, the calculation of thresholds and spare capacities were carried out as described under “Materials and Methods.” As previously described (29, 36), threshold values represent the extent to which complex activity can be inhibited without affecting respiration rate. Spare capacity represents the percentage of the endogenous respiration rate that could be achieved in addition to the measured endogenous respiration rate (taken as 100%) if the complex was fully utilized for respiration and respiration rate is therefore linearly



proportional to the complex activity. Hence, spare capacity is a measure of the complex reserve. Both spare capacity and threshold values were low for complex I as shown in Table II. Further, respiration and complex I activity were equally sensitive to rotenone in STHdh<sup>Q7/Q7</sup> (wild-type) and STHdh<sup>Q111/Q111</sup> (mutant) cells.

Complex II was inhibited with increasing concentrations of malonate and state 3 respiration rates (Fig. 4A), and complex II activities (Fig. 4B) were measured. Malonate was used as the complex II inhibitor for our studies because 3-NP takes ~ 20 min to inhibit complex II (37), which would make our respiration studies more difficult and less reliable. Respiration rates (expressed as percentage of respiration rate with no inhibitor) were plotted against percent inhibition of complex II activity (Fig. 4C), and the least squares linear regression was applied for analysis of respiratory thresholds. As shown in Table II, the spare capacity and threshold values for complex II were low to moderate in the striatal cultured cells, however in both cases the values were greater in the wild-type when compared with the mutant cells (23–25 for the wild-type cells and ~ 6 for the mutant cells). However, when respiration and complex II activity titration curves were analyzed (Fig. 4A and B), there was only a slight trend toward the mutant cells being more sensitive than the wild type cells, with a statistical difference occurring at only 100  $\mu$ M malonate in the respiration curve (Fig. 4A). To further examine the differences between wild-type and mutant cells with regards to complex II threshold, we also measured the sensitivity of uncoupled respiration rates to malonate in the two cell lines. Threshold curves (Fig. 4D), spare capacities, and threshold values (Table II) were obtained when uncoupled respiration was measured, and no significant differences between wild-type and mutant cells was observed. These data indicate that respiration

rate and complex II activity are not differentially sensitive to malonate in STHdh<sup>Q7/Q7</sup> (wildtype) and STHdh<sup>Q111/Q111</sup> (mutant) cells. In addition we examined expression levels of complex II catalytic subunits (30 and 70 kDa) in the STHdh<sup>Q7/Q7</sup> (wild-type) and STHdh<sup>Q111/Q111</sup> (mutant) cells. In accordance with the complex II activity data (Table I), expression levels were similar in the two cell lines (Fig. 4E).

Complex III was inhibited with increasing concentrations of antimycin, and respiration rates and complex III activities were measured. Threshold curves were constructed by plotting respiration rates (percentage of respiration rate with no inhibitor) against percentages of complex III inhibition, and spare capacities and threshold values were determined. Respiration (Fig. 5A) and complex III activity (Fig. 5B) were equally sensitive to antimycin in the both cell lines. A low threshold for both cell lines was observed as evident in Fig. 5C and Table II, similar to what was observed for complex I.

Complex IV was inhibited with increasing concentrations of KCN, and respiration rates and complex IV activities were measured. Respiration in wild-type cells showed a trend toward being more sensitive to KCN inhibition compared with the mutant cells, with statistically significant differences occurring at two KCN concentrations (Fig. 6A). However, complex IV activity was equally sensitive to KCN in both cell lines (Fig. 6B). Respiration rates (expressed as a percentage of respiration rate with no inhibitor) were plotted against percentages of inhibition of complex IV activity to obtain threshold curves (Fig. 6C). Significant thresholds were observed in both cell lines (Fig. 6C). The least-squares linear regression analysis beyond the inflection points revealed significant threshold values (39.53 in wild-type and 53.82 in mutant) and spare capacities (71.66 in

wild-type and 138.32 in mutant) in both cell lines (Table II). These data indicate that the threshold for complex IV is greater in mutant cells compared with wild-type cells.

### Discussion

To our knowledge this study represents the first complete analyses of how mutant huntingtin when expressed at physiological levels impacts mitochondrial respiratory function. In our study, we demonstrate that striatal cells derived from a precise genetic mouse model of HD show significantly diminished oxidative phosphorylation as indicated by lower respiration and mitochondrial ATP production rates compared with what was observed in wild-type cells. However, the activities of respiratory complexes and sensitivity to mitochondrial inhibitors were not different between the two cell lines. Taken together, our results suggest that mutant huntingtin compromises mitochondrial ATP production, but this effect is not through the impairment of the respiratory complexes. This is in agreement with previous findings that in presymptomatic or grade I HD brain there are no changes in the activities of complexes I–IV in the striatum (18). Also, the rather low respiratory thresholds for complexes I, II, and III in the striatal cells suggest that the striatum may be more sensitive to mitochondrial inhibitors.

Our data suggest that respiration is compromised in the striatal cells expressing endogenous levels of mutant huntingtin. Although this could not be observed during state 4 respiration, there was a significant reduction in respiration in the mutant cells at high respiration rates such as when it was coupled to ATP production (state 3) or during uncoupler-stimulated respiration. Also, there were no differences in the respiration rates (Fig. 1) or mitochondrial ATP production (data not shown) when TMPD/ascorbate was

used as the substrate. Ascorbate plus TMPD substrate is an artificial electron donor that feeds electrons directly to complex IV and is therefore more a measure of isolated complex IV activity than of respiration (38). Given the finding that complex IV activity was the same in wild-type and mutant cells, it is therefore not surprising that respiration and ATP production were not different when TMPD/ascorbate was used as the substrate.

Mitochondrial ATP production rates are significantly lower in the mutant huntingtin expressing cells compared with the wild-type cells when either glutamate plus malate or succinate are used as substrates, which is in accordance with the decreased state 3 respiration in the mutant cells. Interestingly, ATP levels measured in the whole lysates were not different between wild-type and mutant cells. The mechanism underlying this observation is not known at present but is likely not due to a compensatory up-regulation of glycolysis. This is because measurement of total ATP levels in the cells after treatment with oligomycin for 2 h (to inhibit mitochondrial ATP production) revealed that the ATP levels were decreased to the same extent in the wild-type and mutant cells. However, if the cells were treated for 2 h with pyruvate and 2-deoxyglucose (to inhibit glycolysis) the total ATP levels were decreased to a greater extent in mutant striatal cells compared with wild type striatal cells.<sup>2</sup> These data suggest that, although the overall rate of ATP production by mitochondria from the mutant cells is lower, in intact cells under control conditions the mitochondria are likely not functioning at maximal capacity, and therefore the total cellular ATP levels can be maintained despite the reduced maximal capacity. However, in the case where ATP can no longer be derived from glycolysis (pyruvate and 2-deoxyglucose), then the differences in total ATP become evident because of the fact that the capacity for ATP production by the mitochondria is lower in the mutant cells

than in the wild type cells. Therefore it can be speculated that in conditions of neuronal stress the presence of mutant huntingtin may result in a reduction in ATP levels in the cell and contribute to the pathogenic processes in HD (39). Our finding that total ATP levels are not significantly different between the wild-type and mutant cells are in contrast with a previously published study (16) that reported decreased total ATP levels in mutant huntingtin expressing striatal cells. The reason for these differences is unknown but may be due to differences in methodology. Nonetheless it is clear that in the mutant cells the ability of the mitochondria to produce ATP is impaired.

The mitochondrial respiratory complex activities were not significantly different between mutant and wild-type cells. This supports a previous finding that complex activities were not altered in the striatum of presymptomatic or lower grade HD cases in which the neuronal loss is minimal (18). It is also interesting to note that decreased respiratory complex activities were not evident in several transgenic HD mouse models (18, 40). All these data would indicate that mutant huntingtin does not impair the activity of the respiratory complexes. Decreases in complex II, III, and IV activities in the postmortem brains of higher grade HD cases, where there is substantial neuronal dysfunction and/or neuronal cell loss (7, 8), could be a consequence of changes in the ratios of cell types due to the neuronal loss and gliosis, although other factors such as oxidative stress (as a secondary effect of mitochondrial impairment) may also play role.

Respiration rates and complex activities were equally sensitive to mitochondrial inhibitors in wild-type and mutant cells, except that there was the trend of respiration being less sensitive to complex IV inhibition in the cells expressing mutant huntingtin. The trend was present at all inhibitor concentrations reaching statistical difference at two

data points. But the trend was not present in the complex IV activity titration curves. This resulted in higher values for spare capacity and respiratory threshold for the mutant cells. As demonstrated previously (29), an increase of respiratory threshold could be the compensation for the defect present elsewhere in the respiratory network. When complex II was analyzed, threshold and spare capacity were lower in the mutant compared with wild-type cells. The fact that, in the titration curves statistical difference was observed at only one inhibitor concentration, together with the fact that the differences were not significant when the uncoupled respiration was measured, led to the conclusion that the differences between wild-type and mutant cells were not of biological relevance. This is also supported by the findings that complex II activities and the expression of the catalytic subunits were equivalent in the two cell lines, therefore indicating there was no defect at the level of complex II.

There have been several reports suggesting altered sensitivity of transgenic HD mice to malonate or 3-NP (41–43). Also, a previous study from our laboratory showed that striatal cells expressing mutant huntingtin were more sensitive than wild type cells to 3-NP induced toxicity, but not to rotenone treatment (17). Interestingly, while wild-type cells die by apoptosis when treated with 3-NP, cell death in the mutant cells was nonapoptotic (17). Even though mutant huntingtin-expressing cells do have compromised mitochondrial energy production, this is not triggered by impairment of complex II. Our thorough analysis of complex II showed that mutant huntingtin does not affect complex II activity or function. However, it has been shown previously that the mitochondrial ATP-sensitive  $K^+$ -channel is composed of several proteins, including the catalytic subunits of complex II (44), and intriguingly 3-NP is known to be an activator of this channel (44).

Therefore, we could speculate that alterations in the activity of this channel could contribute to the increased sensitivity of mutant striatal cells to 3-NP. Further, activation of this channel leads to dissipation of mitochondrial membrane potential ( $\Delta\Psi_m$ ) and a decrease in the ability to retain mitochondrial calcium (45). Hence mutant huntingtin-induced alterations in the mitochondrial ATP-sensitive  $K^+$ - channel could explain the decreased  $\Delta\Psi_m$  and calcium retention capacity reported in several HD models (13), as well as the altered sensitivity of transgenic HD mice to malonate or 3-NP (41–43). Our future studies will be directed toward examining this possibility.

If the respiratory complexes are functioning properly, what could be the reason for compromised respiration in the striatal cells expressing mutant huntingtin? The dependence of oxidative phosphorylation on mitochondrial calcium concentration has been observed for different respiratory substrates, including glutamate plus malate and succinate (46). This previous study demonstrated that both state 3 respiration and ATP synthesis, but not state 4 respiration, were significantly dependent on mitochondrial calcium (46). Also, the mitochondrial calcium concentration affected the rate of uncoupler-stimulated respiration (46). Therefore it can be speculated that the compromised respiration in the striatal cells expressing mutant huntingtin could be the result of altered mitochondrial calcium concentrations. In support of this hypothesis it has been reported that calcium buffering is altered in lymphoblast mitochondria from HD patients as well as brain mitochondria from transgenic mice expressing full-length mutant huntingtin (13). However, additional research is needed to substantiate this hypothesis.

As estimated by respiratory threshold analysis, cultured striatal cells have rather low thresholds for complexes I, II, and III. This is different to what was previously found

in nonsynaptic rat brain mitochondria (complex I and III ~ 70%) (47), and in PC12 cells (complex II ~ 70%) (28). However, variations in the complex I threshold in different brain mitochondria have already been demonstrated. It was found that synaptic rat brain mitochondria have complex I threshold of ~25% (48). Also in PC12 cells the threshold for complex I was ~7% (28), which is similar to what we observed in the striatal cells (Table II). In contrast, the complex IV threshold for the striatal cells appears similar to what was previously reported for nonsynaptic brain and hippocampal mitochondria (47, 49). Low thresholds of complexes I, II, and III indicate that respiration would be easily affected by the impairment or inhibition of these complexes in the striatal cells.

In conclusion, these studies show that mutant huntingtin compromises the ability of mitochondria to produce ATP. However, this effect is not through the impairment of any of the respiratory complexes. Even though mutant huntingtin increases sensitivity to 3-NP as shown previously (17), this effect is not through the impairment of complex II respiratory activity. Additional studies fully elucidating the effects of mutant huntingtin on mitochondrial function will be important to understand HD pathogenesis.

#### References

1. The Huntington's Disease Collaborative Research Group (1993) *Cell* **72**, 971–983
2. Kuhl, D. E., Phelps, M. E., Markham, C. H., Metter, E. J., Riege, W. H., and Winter, J. (1982) *Ann. Neurol.* **12**, 425–434
3. Kuhl, D. E., Metter, E. J., Riege, W. H., and Markham, C. H. (1984) *Ann. Neurol.* **15**, (suppl.) S119–S125
4. Kuhl, D. E., Markham, C. H., Metter, E. J., Riege, W. H., Phelps, M. E., and Mazziotta, J. C. (1985) *Res. Publ. Assoc. Res. Nerv. Ment. Dis.* **63**, 199–209



5. Feigin, A., Leenders, K. L., Moeller, J. R., Missimer, J., Kuenig, G., Spetsieris, P., Antonini, A., and Eidelberg, D. (2001) *J. Nucl. Med.* **42**, 1591–1595
6. Jenkins, B. G., Koroshetz, W. J., Beal, M. F., and Rosen, B. R. (1993) *Neurology* **43**, 2689–2695
7. Gu, M., Gash, M. T., Mann, V. M., Javoy-Agid, F., Cooper, J. M., and Schapira, A. H. (1996) *Ann. Neurol.* **39**, 385–389
8. Browne, S. E., Bowling, A. C., MacGarvey, U., Baik, M. J., Berger, S. C., Muqit, M. M., Bird, E. D., and Beal, M. F. (1997) *Ann. Neurol.* **41**, 646–653
9. Mann, V. M., Cooper, J. M., Javoy-Agid, F., Agid, Y., Jenner, P., and Schapira, A. H. (1990) *Lancet* **336**, 749
10. Beal, M. F., Brouillet, E., Jenkins, B. G., Ferrante, R. J., Kowall, N. W., Miller, J. M., Storey, E., Srivastava, R., Rosen, B. R., and Hyman, B. T. (1993) *J. Neurosci.* **13**, 4181–4192
11. Brouillet, E., Hantraye, P., Ferrante, R. J., Dolan, R., Leroy-Willig, A., Kowall, N. W., and Beal, M. F. (1995) *Proc. Natl. Acad. Sci. U. S. A.* **92**, 7105–7109
12. Sanchez, I., Mahlke, C., and Yuan, J. (2003) *Nature* **421**, 373–379
13. Panov, A. V., Gutekunst, C. A., Leavitt, B. R., Hayden, M. R., Burke, J. R., Strittmatter, W. J., and Greenamyre, J. T. (2002) *Nat. Neurosci.* **5**, 731–736
14. Trettel, F., Rigamonti, D., Hilditch-Maguire, P., Wheeler, V. C., Sharp, A. H., Persichetti, F., Cattaneo, E., and MacDonald, M. E. (2000) *Hum. Mol. Genet.* **9**, 2799–2809
15. Li, S. H., Cheng, A. L., Li, H., and Li, X. J. (1999) *J. Neurosci.* **19**, 5159–5172
16. Gines, S., Seong, I. S., Fossale, E., Ivanova, E., Trettel, F., Gusella, J. F., Wheeler, V. C., Persichetti, F., and MacDonald, M. E. (2003) *Hum. Mol. Genet.* **12**, 497–508
17. Ruan, Q., Lesort, M., MacDonald, M. E., and Johnson, G. V. (2004) *Hum. Mol. Genet.* **13**, 669–681
18. Guidetti, P., Charles, V., Chen, E. Y., Reddy, P. H., Kordower, J. H., Whetsell, W. O., Jr., Schwarcz, R., and Tagle, D. A. (2001) *Exp. Neurol.* **169**, 340–350
19. Hofhaus, G., Shakeley, R. M., and Attardi, G. (1996) *Methods Enzymol.* **264**, 476–483
20. Kun, E., Kirsten, E., and Piper, W. N. (1979) *Methods Enzymol.* **55**, 115–118

21. Robinson, J. B., Brent, L. G., Sumegi, B., and Srere, P. A. (1987) in *Mitochondria a Practical Approach* (Darley-Usmar, V. M., Rickwood, D., and Wilson, M. T., eds) pp. 160–161, IRL Press, London
22. Hatefi, Y., and Stiggall, D. L. (1978) *Methods Enzymol.* **53**, 21–27
23. Ragan, C. I., Wilson, M. T., Darley-Usmar, V. M., and Lowe, P. N. (1987) in *Mitochondria, a Practical Approach* (Darley-Usmar V. M., Rickwood, D., and Wilson, M. T., eds) pp. 79–112, IRL Press, London
24. Chretien, D., Bourgeron, T., Rotig, A., Munnich, A., and Rustin, P. (1990) *Biochem. Biophys. Res. Commun.* **173**, 26–33
25. Helmerhorst, E. J., Murphy, M. P., Troxler, R. F., and Oppenheim, F. G. (2002) *Biochim. Biophys. Acta* **1556**, 73–80
26. Darley-Usmar, V. M., Capaldi, R. A., Takamiya, S., Millett, F., Wilson, M. T., Malatesta, F., and Sarti, P. (1987) in *Mitochondria, a Practical Approach* (Darley-Usmar, V. M., Rickwood, D., and Wilson, M. T., eds) pp. 113–152, IRL Press, London
27. Rossignol, R., Malgat, M., Mazat, J. P., and Letellier, T. (1999) *J. Biol. Chem.* **274**, 33426–33432
28. Mallajosyula, J. K., Andersen, J. K., and Nicholls, D. G. (2004) *On-line Abstract Viewer and Itinerary Planner, 34th Annual Meeting of the Society for Neuroscience, San Diego, California, October 23–27, 2004*, program 563.21, Society for Neuroscience, Washington, D. C.
29. Villani, G., and Attardi, G. (1997) *Proc. Natl. Acad. Sci. U. S. A.* **94**, 1166–1171
30. Drew, B., and Leeuwenburgh, C. (2003) *Am. J. Physiol.* **285**, R1259–R1267
31. Harris, S. I., Balaban, R. S., Barrett, L., and Mandel, L. J. (1981) *J. Biol. Chem.* **256**, 10319–10328
32. Granger, D. L., and Lehninger, A. L. (1982) *J. Cell Biol.* **95**, 527–535
33. Dubinsky, W. P., and Cockrell, R. S. (1975) *FEBS Lett.* **59**, 39–43
34. Fiskum, G., Craig, S. W., Decker, G. L., and Lehninger, A. L. (1980) *Proc. Natl Acad. Sci. U. S. A.* **77**, 3430–3434
35. Colbeau, A., Nachbaur, J., and Vignais, P. M. (1971) *Biochim. Biophys. Acta* **249**, 462–492

36. Rossignol, R., Faustin, B., Rocher, C., Malgat, M., Mazat, J. P., and Letellier, T. (2003) *Biochem. J.* **370**, 751–762
37. Coles, C. J., Edmondson, D. E., and Singer, T. P. (1979) *J. Biol. Chem.* **254**, 5161–5167
38. Villani, G., Greco, M., Papa, S., and Attardi, G. (1998) *J. Biol. Chem.* **273**, 31829–31836
39. Browne, S. E., and Beal, M. F. (2004) *Neurochem. Res.* **29**, 531–546
40. Higgins, D. S., Hoyt, K. R., Baic, C., Vensel, J., and Sulka, M. (1999) *Ann. N. Y. Acad. Sci.* **893**, 298–300
41. Hansson, O., Castilho, R. F., Korhonen, L., Lindholm, D., Bates, G. P., and Brundin, P. (2001) *J. Neurochem.* **78**, 694–703
42. Hickey, M. A., and Morton, A. J. (2000) *J. Neurochem.* **75**, 2163–2171
43. Bogdanov, M. B., Ferrante, R. J., Kuemmerle, S., Klivenyi, P., and Beal, M. F. (1998) *J. Neurochem.* **71**, 2642–2644
44. Ardehali, H., Chen, Z., Ko, Y., Mejia-Alvarez, R., and Marban, E. (2004) *Proc. Natl. Acad. Sci. U. S. A.* **101**, 11880–11885
45. Holmuhamedov, E. L., Wang, L., and Terzic, A. (1999) *J. Physiol.* **519**, 347–360
46. Moreno-Sanchez, R. (1985) *J. Biol. Chem.* **260**, 4028–4034
47. Davey, G. P., and Clark, J. B. (1996) *J. Neurochem.* **66**, 1617–1624
48. Davey, G. P., Peuchen, S., and Clark, J. B. (1998) *J. Biol. Chem.* **273**, 12753–12757
49. Davey, G. P., Canevari, L., and Clark, J. B. (1997) *J. Neurochem.* **69**, 2564–2570

#### Footnotes

Acknowledgments--We are grateful to Dr. M. E. MacDonald for providing us with STHdh<sup>Q7/Q7</sup> and STHdh<sup>Q111/Q111</sup> cell lines. We are also thankful to Dr. M. J. Kumar for explanations and suggestions regarding threshold analysis and Dr. M. Lesort for his constructive comments on the manuscript and also for sharing his unpublished data with us.

1 The abbreviations used are: HD, Huntington disease; 3-NP, 3-nitropropionic acid; TMPD, *N,N,N',N'*-tetramethylphenylenediamine dihydrochloride; FCCP, carbonyl cyanide 4-(trifluoromethoxy)phenylhydrazone; RCR, respiratory control ratio; MOPS, 3-(*N*-morpholino)propanesulfic acid; CCCP, carbonyl cyanide *m*-chlorophenylhydrazone.

2 Z. Mao and M. Lesort, manuscript in preparation.

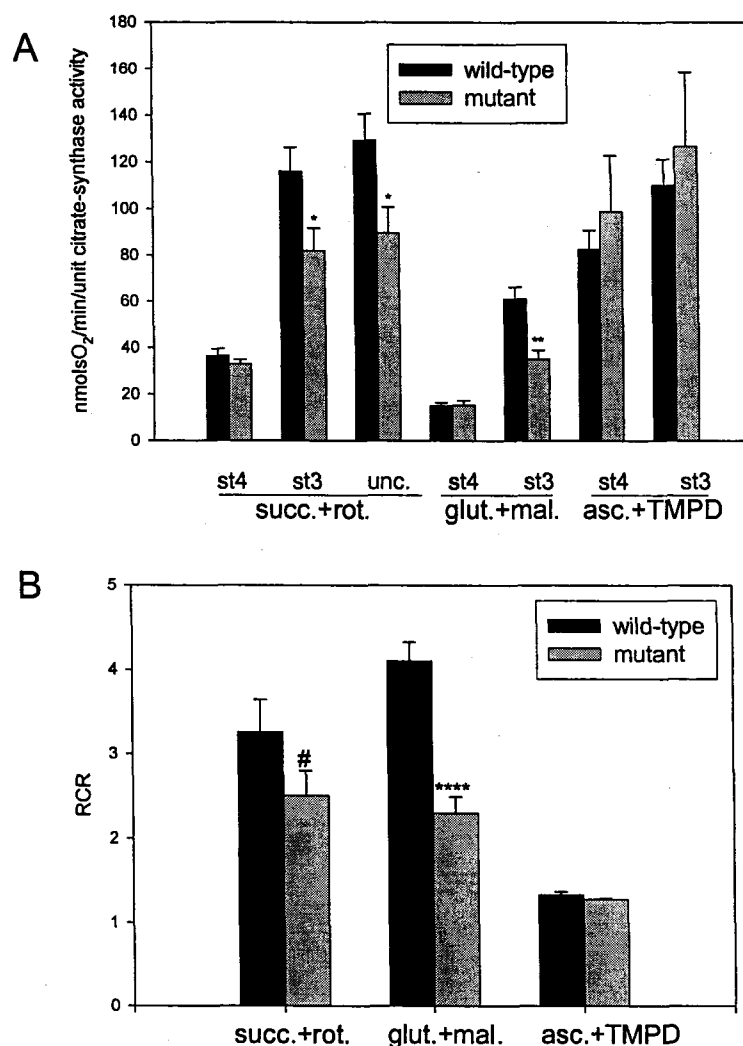


**FIG. 1. Respiratory properties of STHdh<sup>Q7/Q7</sup> (wild-type) and STHdh<sup>Q111/Q111</sup> (mutant) cells.** *A*, State 3 (*st3*), state 4 (*st4*), and uncoupled respiration rates (*unc.*). Cells were permeabilized, incubated with the indicated respiratory substrates (succinate plus rotenone (*succ.+rot.*), glutamate plus malate (*glut.+mal.*), or ascorbate plus TMPD (*asc+TMPD*)), and respiration rates were determined as described under “Materials and Methods.” For uncoupled respiration, permeabilized cells were incubated with succinate plus rotenone plus FCCP as described. All rates were normalized to citrate synthase activity measured in the same samples. In the presence of glutamate plus malate or succinate plus rotenone, state 3 rates were significantly lower in the mutant cells. The uncoupled respiration rate was also lower in the mutant cells. Rates were not different between the two cell lines when ascorbate plus TMPD was used as the substrate. *B*, respiratory control ratios (*RCRs*). *RCRs* were calculated as the ratios between state 3 and state 4 rates. *RCRs* were significantly lower in the mutant cells when either succinate plus rotenone (*succ+rot.*) or glutamate plus malate (*glut.+mal.*) were used as respiratory substrates. All data are mean  $\pm$  S.E. of 4–5 independent experiments. For statistical analyses either the Student *t* test (\*,  $p < 0.05$ ; \*\*,  $p < 0.01$ ; \*\*\*\*,  $p < 0.001$ ) or paired *t* test (#,  $p < 0.05$ ) was used.

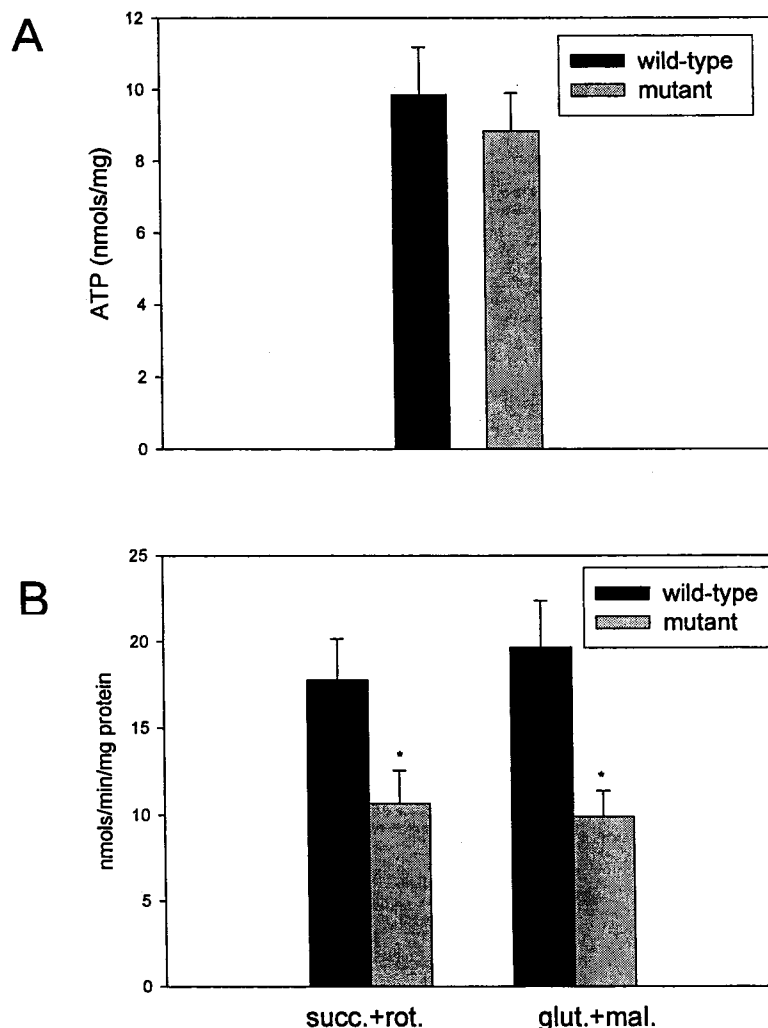


**FIG. 2. ATP levels and mitochondrial ATP production in permeabilized cells from STHdh<sup>Q7/Q7</sup> (wild-type) and STHdh<sup>Q111/Q111</sup> (mutant) cells.** *A*, ATP levels. ATP levels were determined in the whole cell lysates as described under "Materials and Methods." No significant differences in ATP levels between the two cell lines were observed. Results are mean  $\pm$  S.E. of three independent experiments. *B*, mitochondrial ATP production. Mitochondrial ATP production was measured in permeabilized cells as described under "Materials and Methods." When either succinate (with rotenone) or glutamate plus malate were used as respiratory substrates, ATP production rates were significantly lower in mutant cells compared with wild-type cells. Results are means  $\pm$  S.E. of 13–16 measurements from five independent experiments. Data are analyzed using Chauvenet's Criterion followed by Student *t* test (\*,  $p < 0.05$ ).

Enzyme	Units	Wild-type (mean±SEM)	Mutant (mean±SEM)
Citrate synthase	nmols/min/1*10 <sup>7</sup> cells	545.18±25.96	407.62±20.2*
Citrate synthase	nmols/min/mg protein	467.29±29.14	463.64±30.07
NADH dehydrogenase	nmols/min/unit citrate synthase activity	35.06±4.22	35.54±1.98
Succinate dehydrogenase	nmols/min/unit citrate synthase activity	8.862±0.66	8.278±1.54
Ubiquinone cytochrome c oxidoreductase	μmols/min/unit citrate synthase activity	77.84±11.77	54.61±10.44
Cytochrome c oxidase	nmolsO <sub>2</sub> /min/unit citrate synthase activity	159.39±10.89	182.51±22.65

TABLE I. Mitochondrial enzyme activities in *STHdh*<sup>Q7/Q7</sup> (wild-type) and *STHdh*<sup>Q111/Q111</sup> (mutant) cells. Permeabilized cells were used to measure mitochondrial enzyme activities as described under "Materials and Methods." All results are presented as mean ± S.E. of at least four independent experiments. The activity of citrate synthase was lower in the mutant cell line when normalized to the number of cells but not when normalized to the protein content. Respiratory complexes enzyme activities were normalized to the units of citrate synthase activity (unit = 1 μmol/min/ml) and were not different between the two cell lines. Data were analyzed using Student *t* test.

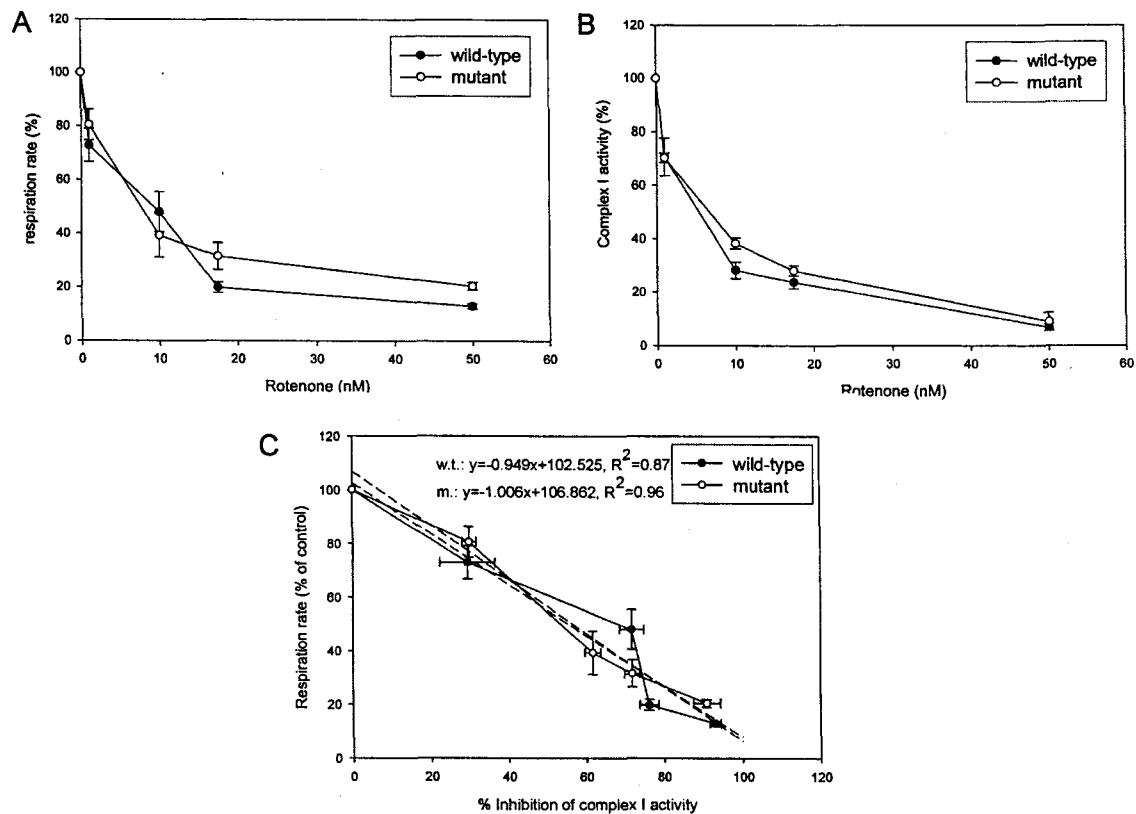
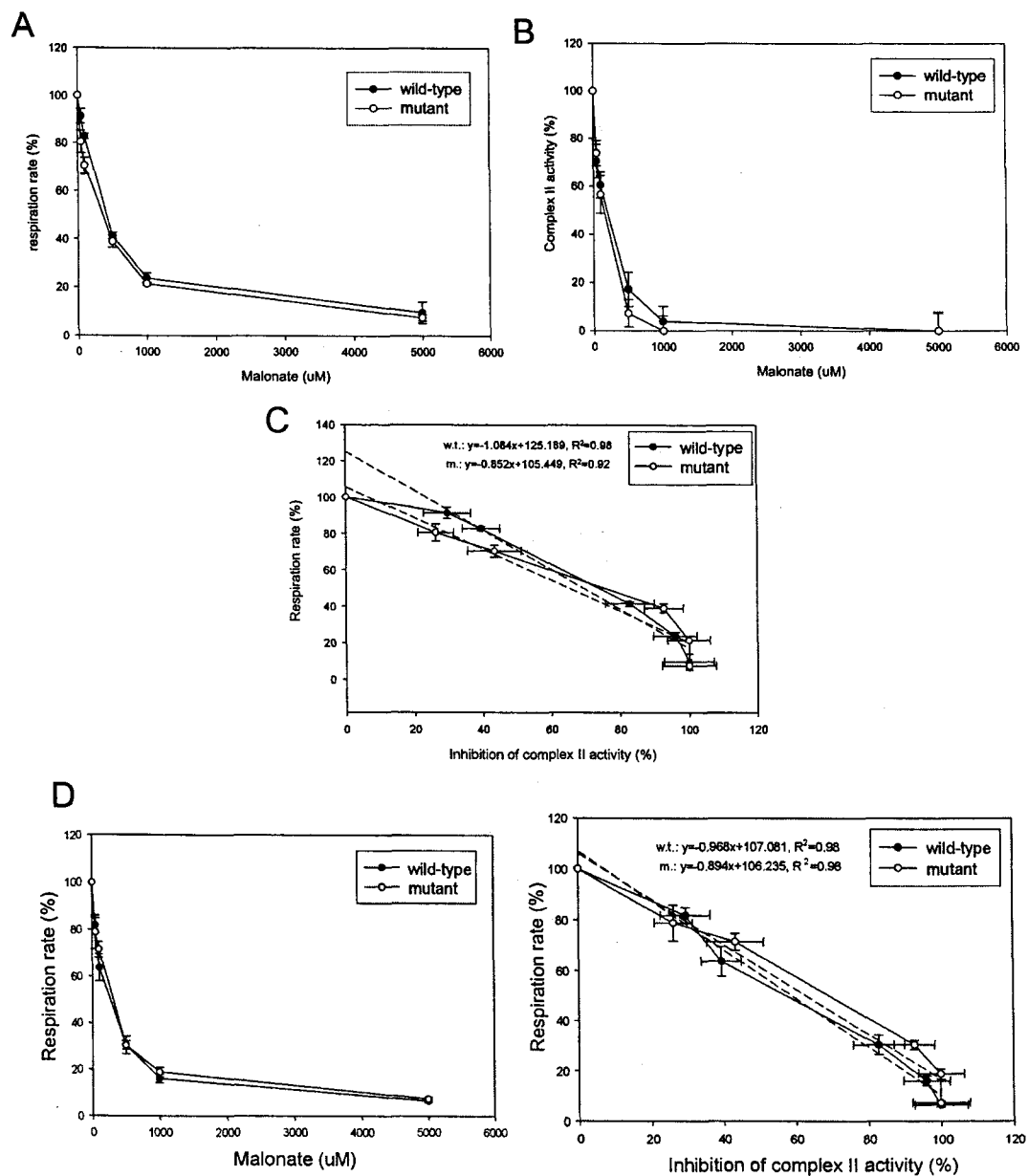


**FIG. 3. Rotenone titrations and complex I threshold curves for permeabilized cells from STHdh<sup>Q7/Q7</sup> (wild-type) and STHdh<sup>Q111/Q111</sup> (mutant) cells.** *A*, rotenone titration of respiration. Permeabilized cells were incubated with increasing concentrations of rotenone and state 3 respiration rates were determined polarographically as described under "Materials and Methods." Measured rates were expressed as a percentage of the control rate (no inhibitor present). *B*, rotenone titration of complex I activity. Complex I activity was determined spectrophotometrically as described under "Materials and Methods," and activities obtained after incubation with the indicated concentrations of rotenone were expressed as a percentage of the control activity (no inhibitor present). *C*, threshold curves for complex I. Data from *panels A* and *B* were used to construct the threshold curves, by plotting respiration rates (percentage of control) *versus* percent inhibition of complex I activity obtained at each concentration of rotenone. No true threshold was observed for complex I in either cell line. Therefore, linear regression was performed for data points at all inhibitor concentrations.  $R^2$  values and regression equations are shown for both the wild-type (*w.t.*) and mutant (*m.*) cells. Respiration and complex I activity from both cell lines were equally sensitive to inhibition by rotenone. All data are means  $\pm$  S.E. of at least four independent experiments.



	Spare capacity		Threshold value	
	Wild-type	Mutant	Wild-type	Mutant
Complex I	2.53	6.86	2.66	6.82
Complex II	25.19	5.45	23.24	6.4
Complex II (uncoupled)	7.08	6.23	7.32	6.97
Complex III	0	0	0	0
Complex IV	71.66	138.32	39.53	53.82

TABLE II. *Spare capacities and threshold values for respiratory complexes in permeabilized cells from  $STHdh^{Q7/Q7}$  (wild-type) and  $STHdh^{Q111/Q111}$  (mutant) cell lines. Spare capacities and threshold values are calculated from threshold curves as described under “Materials and Methods.”*



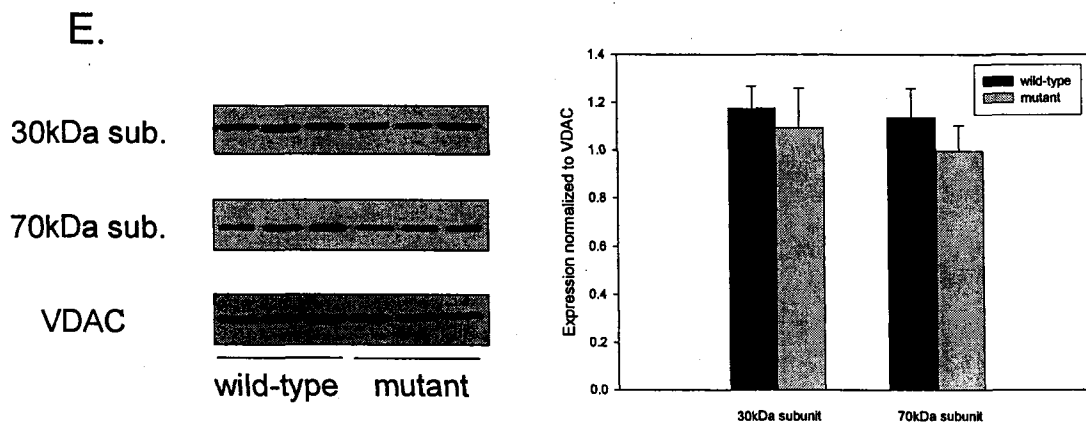
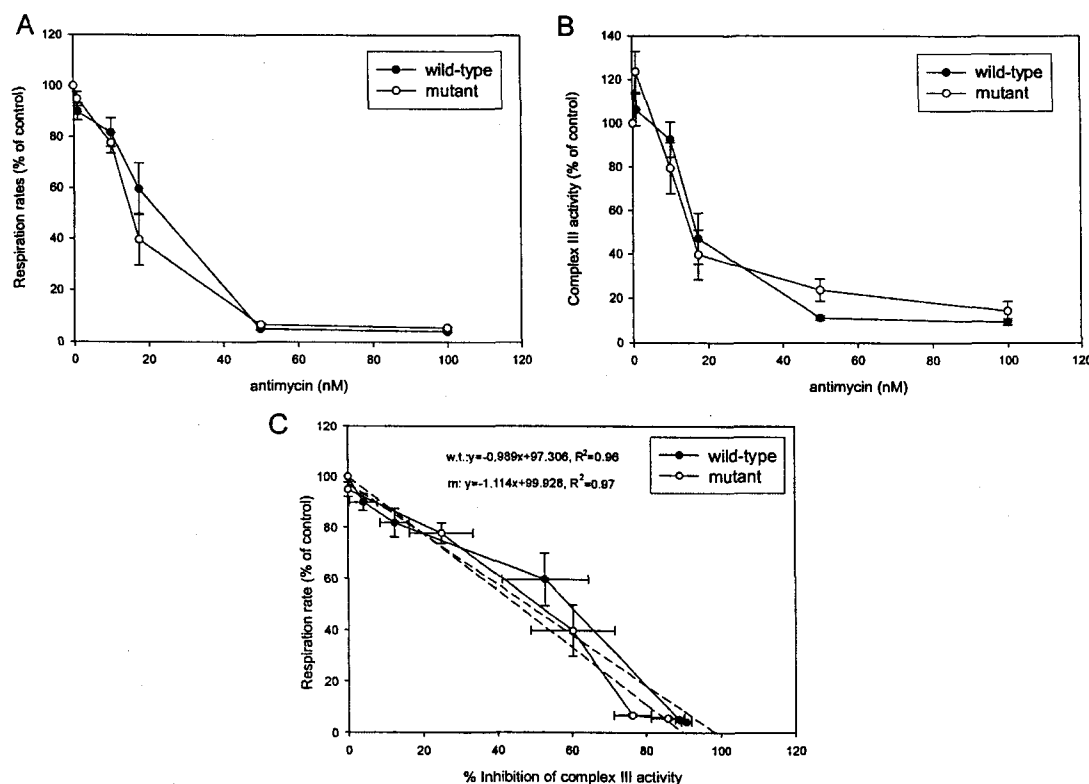
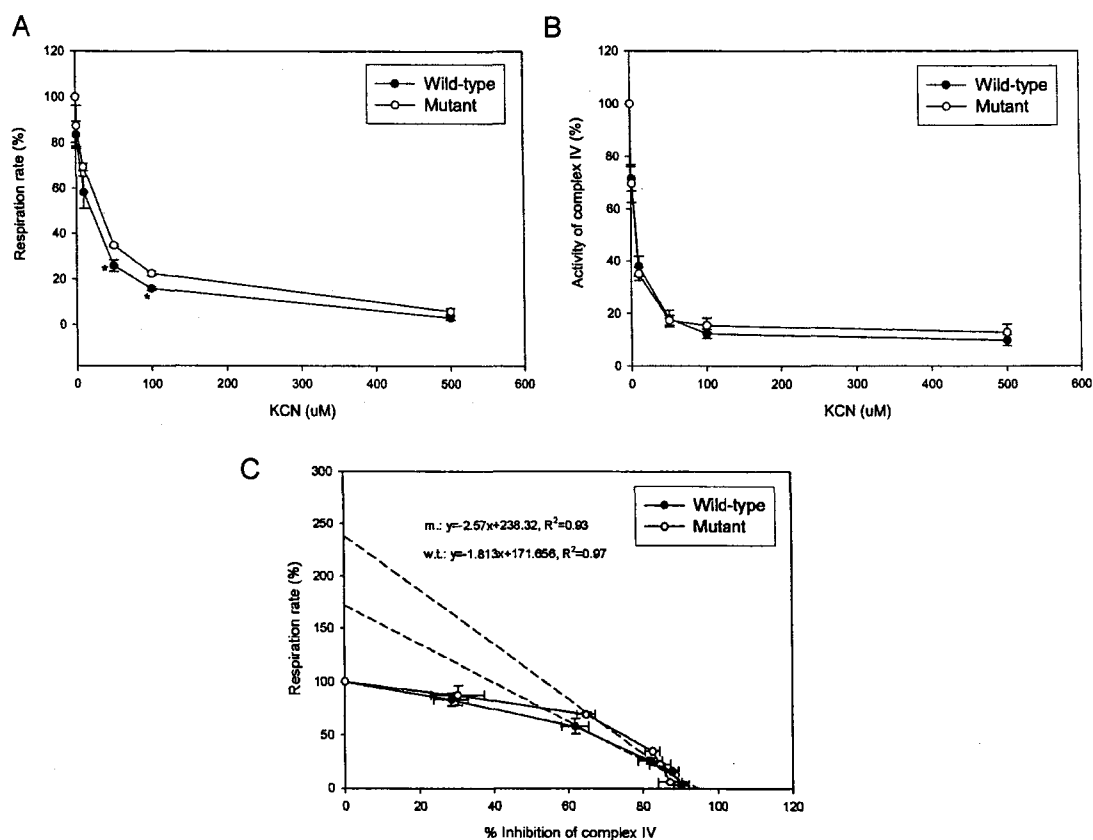


FIG. 4. Analysis of complex II threshold profiles (by malonate titrations) and catalytic subunits expression levels in permeabilized  $\text{STHdh}^{Q7/Q7}$  (wild-type) and  $\text{STHdh}^{Q111/Q111}$  (mutant) cells. *A*, malonate titration of respiration. Permeabilized cells were incubated with the indicated concentrations of malonate and state 3 respiration rates were determined polarographically as described under "Materials and Methods." Measured rates were expressed as a percentage of the control rate (no inhibitor present). *B*, malonate titration of complex II activity. Complex II activity was determined spectrophotometrically as described under "Materials and Methods," and activities obtained after incubation with each malonate concentration were expressed as a percentage of the control activity (no inhibitor present). *C*, threshold curves for complex II. Data from *panels A* and *B* were used to construct threshold curves. Linear regression was performed for data points at all inhibitor concentrations.  $R^2$  values and regression equations are shown for both wild-type (*w.t.*) and mutant (*m.*) cells. Respiration and complex II activity from both cell lines were equally sensitive to inhibition by malonate. All data are means  $\pm$  S.E. of at least four independent experiments. *D*, malonate titration of uncoupled respiration and obtained threshold curves. Permeabilized cells were incubated with FCCP, succinate, rotenone, and increasing concentrations of malonate and uncoupled respiration rates were determined. Data from *panels B* and *D* (*left*) were used to construct threshold curves (*D*, *right*). Threshold curves were very similar to the curves obtained with state 3 respiration rates. *E*, expression levels of complex II catalytic subunits (30 and 70 kDa) in  $\text{STHdh}^{Q7/Q7}$  (wild-type) and  $\text{STHdh}^{Q111/Q111}$  (mutant) cells. Cell lysates were blotted for 30- and 70-kDa complex II subunits and voltage-dependent anion channel (VDAC). Representative immunoblots are shown in *E* (*left*). Densitometric analysis was used to quantify complex II subunits expression levels normalized to voltage-dependent anion channel from at least five different preparations (*right*). No significant differences were observed in the expression of either of the complex II catalytic subunits.



**FIG. 5. Antimycin titrations and complex III threshold curves for permeabilized cells from STHdh<sup>Q7/Q7</sup> (wild-type) and STHdh<sup>Q111/Q111</sup> (mutant) cells.** *A*, antimycin titration of respiration. Permeabilized cells were incubated with increasing concentrations of antimycin, and state 3 respiration rates were determined polarographically as described under "Materials and Methods." Measured rates were expressed as a percentage of the control rate (no inhibitor present). *B*, antimycin titration of complex III activity. Complex III activity was determined spectrophotometrically as described under "Materials and Methods," and activities obtained after incubation with the indicated concentrations of antimycin were expressed as a percentage of the control activity (no inhibitor present). *C*, threshold curves for complex III. Data from *panels A* and *B* were used to construct threshold curves. No true threshold was observed for complex III in both cell lines. Therefore, linear regression was performed for data points at all inhibitor concentrations.  $R^2$  values and regression equations are shown for both wild-type (*w.t.*) and mutant (*m.*) cells. Respiration and complex III activity from both cell lines were equally sensitive to inhibition by antimycin. All data are means  $\pm$  S.E. of six independent experiments.



**FIG. 6. KCN titrations and complex IV threshold curves for permeabilized cells from STHdh<sup>Q7/Q7</sup> (wild-type) and STHdh<sup>Q111/Q111</sup> (mutant) cells.** *A*, KCN titration of respiration. Permeabilized cells were incubated with increasing concentrations of KCN, and state 3 respiration rates were determined polarographically as described under “Materials and Methods.” Measured rates were expressed as a percentage of the control rate (no inhibitor present). *B*, KCN titration of complex IV activity. Complex IV activity was determined polarographically as described under “Materials and Methods,” and activities obtained after incubation with different concentrations of KCN were expressed as a percentage of the control activity (no inhibitor present). *C*, threshold curves for complex IV. Data from *panels A* and *B* were used to construct threshold curves, by plotting respiration rates (percentage of control) *versus* percent inhibition of complex IV activity obtained at each concentration of KCN. Data points below the inflection point in each curve were used for linear regression. Linear equations and  $R^2$  values are shown. Significant thresholds were observed in each cell line, as shown in Table II. Complex IV activity from both cell lines was equally sensitive to complex IV inhibition by KCN. Respiration in wild-type cells showed a trend toward being more sensitive to KCN inhibition compared with the mutant cells, with statistically significant differences at two KCN concentrations (Student’s *t* test, \*,  $p < 0.05$ ). All data are means  $\pm$  S.E. of at least three independent experiments.

MUTANT HUNTINGTIN EXPRESSION INDUCES MITOCHONDRIAL CALCIUM  
HANDLING DEFECTS IN CLONAL STRIATAL CELLS: FUNCTIONAL  
CONSEQUENCES

by

TAMARA MILAKOVIC, RODRIGO A. QUINTANILLA AND GAIL V. W.  
JOHNSON

Submitted to *Journal of Biological Chemistry*

Format adapted for dissertation

### Abstract

Huntington's disease (HD) is caused by the pathological elongation of CAG repeats in the huntingtin protein gene and is characterized by atrophy and neuronal loss primarily in the striatum. Mitochondrial dysfunction and impaired  $\text{Ca}^{2+}$  homeostasis in HD have been suggested previously. Here, we elucidate the effects of  $\text{Ca}^{2+}$  on mitochondria from the wild-type (STHdh<sup>Q7/Q7</sup>) and mutant (STHdh<sup>Q111/Q111</sup>) huntingtin expressing cells of striatal origin. When treated with the increasing  $\text{Ca}^{2+}$  concentrations, mitochondria from mutant huntingtin expressing cells showed enhanced sensitivity to  $\text{Ca}^{2+}$ , as they were more sensitive to  $\text{Ca}^{2+}$  induced decreases in state 3 respiration and  $\Delta\Psi_m$  than mitochondria from wild-type cells. Further, mutant huntingtin expressing cells had a reduced mitochondrial  $\text{Ca}^{2+}$  uptake capacity in comparison with wild-type cells. Decreases in state 3 respiration were associated with increased mitochondrial membrane permeability. The  $\Delta\Psi_m$  defect was attenuated in the presence of ADP and the decreases in  $\text{Ca}^{2+}$  uptake capacity were abolished in the presence of Permeability Transition Pore (PTP) inhibitors. Basal mitochondrial  $\text{Ca}^{2+}$  levels were similar in wild-type and mutant cells, but mutant huntingtin expressing cells showed increased mitochondrial  $\text{Ca}^{2+}$  accumulation when challenged with the increasing loads of  $\text{Ca}^{2+}$ . These findings clearly indicate that mutant huntingtin expressing cells have mitochondrial  $\text{Ca}^{2+}$  handling defects and that the increased sensitivity to  $\text{Ca}^{2+}$  induced mitochondrial permeabilization may be a contributing mechanism to the mitochondrial dysfunction in HD.

## Introduction

Huntington's disease (HD)<sup>1</sup> is a neurodegenerative disease that is inherited in an autosomal dominant manner. It belongs to a family of CAG expansion diseases, and is caused by the pathological elongation of the CAG repeats in exon one of the huntingtin protein gene (1). Symptoms and disease progression are due to dysfunction and loss of neurons starting in the striatum (specifically medium spiny neurons), but progressing to cortex and to a lesser extent to other brain regions in the later stages of the disease (2). Disease is caused by the toxic gain of function of mutant protein but some loss of function may also contribute to the pathogenesis (for review see (3)). The toxic gain of function of mutant huntingtin has not been clearly defined, but there are findings suggesting that mutant huntingtin causes transcriptional dysregulation (4), ubiquitinproteasome system dysfunction (5),  $\text{Ca}^{2+}$  homeostasis dysfunction (6,7) and mitochondrial dysfunction (7-10).

Mitochondrial dysfunction in HD has been suggested primarily by the studies showing impairment of mitochondrial complexes (II, III and IV) specifically in the striatum in the late stages HD patients (8-10). Administration of the mitochondrial complex II inhibitor 3-nitropropionic (3-NP) in both rodents and non human primates resulted in symptoms and neuropathology that resemble HD (11,12). Further, studies have shown impairment of mitochondrial  $\text{Ca}^{2+}$  buffering in HD lymphoblast cell line and brain mitochondria from the full-length mutant huntingtin transgenic mice (YAC72) (7,13).

Striatum, the primary region to get affected in HD is highly innervated by cortical glutaminergic projections (2). Previously it has been demonstrated that mitochondrial



dysfunction can lead to neuronal sensitization to glutamate leading to excitotoxic cellular dysfunction and cell death (14,15). Hence, even though HD is not a classic mitochondrial disease (16), elucidation of mitochondrial dysfunction mechanisms would likely provide important insight in HD pathogenesis.

To study the effects of mutant huntingtin on mitochondrial function, conditionally immortalized cells of striatal origin that express endogenous, comparable levels of either wild-type (STHdh<sup>Q7/Q7</sup>) or mutant (STHdh<sup>Q111/Q111</sup>) huntingtin were used (17). These cell lines are prepared from wild-type (Hdh<sup>Q7/Q7</sup>) and mutant huntingtin knock-in mice (Hdh<sup>Q111/Q111</sup>) (17) and therefore the STHdh<sup>Q111/Q111</sup> cell line is a genetically accurate cell model of HD. In our previous study (18), we investigated the effects of mutant huntingtin on mitochondrial electron transport chain complexes using STHdh<sup>Q7/Q7</sup> and STHdh<sup>Q111/Q111</sup> cell lines. Given the fact that the metabolic thresholds and enzyme activities of electron transport chain complexes were not different between the two cell lines, it is likely that the mitochondrial complex deficits are a later event in the course of HD pathogenesis, indeed in low grade HD cases no deficits in the enzyme activities of electron transport chain complexes were observed (19).

In the present study, we examined the effects of Ca<sup>2+</sup> on mitochondria from STHdh<sup>Q7/Q7</sup> and STHdh<sup>Q111/Q111</sup> cells. Isolated mitochondria were treated with increasing Ca<sup>2+</sup> concentrations and mitochondrial function was assessed using different assays. We determined that mutant huntingtin expressing cells have decreased Ca<sup>2+</sup> uptake capacity, and exhibit increased sensitivity to Ca<sup>2+</sup> induced decreases in respiration and  $\Delta\Psi_m$ . The  $\Delta\Psi_m$  defect was attenuated in the presence of ADP and the decrease in Ca<sup>2+</sup> uptake capacity was abolished in the presence of PTP inhibitors. In the whole cell setting

increased mitochondrial  $\text{Ca}^{2+}$  accumulation was observed in response to increasing extracellular  $\text{Ca}^{2+}$  concentrations, but the basal mitochondrial  $\text{Ca}^{2+}$  levels were similar between the two cell lines. This study clearly demonstrates that mitochondrial  $\text{Ca}^{2+}$  buffering capacity in STHdh<sup>Q111/Q111</sup> cells is compromised, and suggests increased sensitivity to  $\text{Ca}^{2+}$  induced mitochondrial permeabilization as a mechanism of mitochondrial dysfunction in HD.

### Materials and Methods

*Materials* – All chemicals were from Sigma-Aldrich unless otherwise noted. All the buffers used in experiments with crude mitochondrial preparations were prepared in water (Sigma; catalogue # 95305) that is standardized for  $\text{Ca}^{2+}$  content ( $\text{Ca}^{2+} \leq 0.000001\%$ ).

*Cell Culture* – In this study, conditionally immortalized striatal progenitor cell lines: STHdh<sup>Q7/Q7</sup> cell line expressing endogenous wildtype huntingtin and the homozygous mutant STHdh<sup>Q111/Q111</sup> cell line expressing comparable levels of mutant huntingtin with 111 glutamines were used. Cell lines were prepared from wildtype mice and homozygous Hdh<sup>Q111/Q111</sup> knock-in mice and were described previously (17). Culturing conditions were the same as described in our previous study (18).

*Isolation of Mitochondria* – Cells were grown on 150 mm plates until  $\approx 80\text{-}90\%$  confluency, washed twice with cavitation buffer (250 mM sucrose, 5 mM HEPES, 3 mM  $\text{MgCl}_2$ , 1 mM EGTA, pH 7.3 corrected with 5 M KOH) and scraped into cavitation buffer using soft rubber scrapers. Cells were opened using  $\text{N}_2$  cavitation for 5 min at 250 psi on ice and samples were additionally homogenized with 1 stroke in a glass Dounce

homogenizer. Homogenates were centrifuged at 7000 xg for 10 min at 4°C. Supernatants were aspirated and pellets were resuspended in cavitation buffer and used as crude mitochondrial preparations. Protein concentrations in crude mitochondrial preparations were determined using the bicinchoninic acid assay (Pierce) and aliquots were then prepared that contained the indicated protein content for each measurement. Aliquots were centrifuged at 7000 xg for 10 min and kept on ice in cavitation buffer until use in each assay.

*Measurement of Mitochondrial Respiration* – Respiration rates were measured using an oxygraph (Hansatech Instruments) as described previously (18). Crude mitochondrial preparations (0.5mg aliquots) were resuspended in respiration buffer (130 mM KCl, 20 mM HEPES, 2 mM MgCl<sub>2</sub>, 2 mM EGTA, 2 mM potassium phosphate [KH<sub>2</sub>PO<sub>4</sub>:K<sub>2</sub>HPO<sub>4</sub>, 1:1.78], 1% essentially fatty acids free bovine serum albumin (BSA), pH 7.2 adjusted with 5 M KOH) to a final concentration of 1mg/ml. The mitochondrial suspension (0.5ml volume) was placed in the respiratory chamber and allowed to equilibrate for 2 min. Respiratory substrate (glutamate (10 mM) plus malate (10 mM) or succinate (5 mM) with rotenone (10 μM)) was then added and state 4 respiration was measured for 2 min, ADP (1.5 mM) was then added and state 3 respiration was measured for a further 2-4 min. Rates were normalized to citrate synthase activity in the same samples. Citrate synthase activity was determined as previously described (18).

*Ca<sup>2+</sup> Titration Experiments* – Respiration buffers containing specific free Ca<sup>2+</sup> concentrations (Ca<sup>2+</sup>-EGTA respiration buffers) were prepared on the day of the experiment. To calculate the amount of total Ca<sup>2+</sup> that was needed to achieve the appropriate free Ca<sup>2+</sup> concentration in the respiration buffer that contained 2 mM EGTA

we used MaxChelator software (downloadable at: <http://www.stanford.edu/cpatton/maxc.html> (20)). Each  $\text{Ca}^{2+}$ -EGTA respiration buffer was prepared separately by diluting each specific 100X  $\text{CaCl}_2$  stock in the respiration buffer and correcting its pH to 7.2 using 0.1 M KOH in the respiration buffer.  $\text{CaCl}_2$  stocks were prepared from  $\text{CaCl}_2 \cdot 2\text{H}_2\text{O}$  (minimum 99%), that was dried overnight and stored in a desiccation chamber until use. Crude mitochondrial preparations were dissolved in prepared  $\text{Ca}^{2+}$ -EGTA respiration buffers and respiration rates were measured as described above. The period between buffer addition to the mitochondrial preparation and initiation of state 3 was approximately 5 min. Free  $\text{Ca}^{2+}$  concentrations in the  $\text{Ca}^{2+}$ -EGTA buffers were checked using a calibrated  $\text{Ca}^{2+}$  electrode on the day of the experiment. Measured concentrations were averaged and presented on the X-axis of  $\text{Ca}^{2+}$  titration experiments graphs. Actually concentrations were always slightly higher than those calculated by software.

*Cytochrome c and NADH Respiration Experiments* – Respiration experiments were performed as described above. State 3 respiration was measured for 2 min prior to the addition of cytochrome c (30  $\mu\text{M}$ ) and respiration was monitored for another 2 min. This was followed by the addition of NADH (5 mM) and respiration was monitored for an additional 2 min.

*Determination of Mitochondrial  $\text{Ca}^{2+}$  Uptake Capacity* –  $\text{Ca}^{2+}$  uptake capacities were measured using a  $\text{Ca}^{2+}$  electrode (World Precision Instruments). Crude mitochondrial preparation was resuspended in  $\text{Ca}^{2+}$  uptake buffer (130 mM KCl, 20 mM HEPES, 2 mM  $\text{MgCl}_2$ , 2 mM potassium phosphate [ $\text{KH}_2\text{PO}_4:\text{K}_2\text{HPO}_4$ , 1:1.78], 1% BSA, pH 7.2 adjusted with 5 M KOH) and placed in the oxygraph respiratory chamber. The

respiratory chamber was thermostatted at 37°C and its contents were constantly mixed with an electromagnetic stirrer bar. Glutamate (10 mM) and malate (10 mM) were added as respiratory substrates.  $\text{Ca}^{2+}$  and reference electrodes were added to the chamber from the top. Starting volume of the reaction was 2 ml. The chamber was kept open during an experiment.  $\text{Ca}^{2+}$  additions were performed using fine tubing and a Hamilton syringe. 5 mM, 10 mM and 20 mM  $\text{CaCl}_2$  stocks were used to make 10 nmols, 20 nmols, 40 nmols or 80 nmols  $\text{Ca}^{2+}$  additions. The  $\text{Ca}^{2+}$  electrode measures extramitochondrial  $\text{Ca}^{2+}$  and increases in the signal present as downward deflections on the traces. To observe the effects of PTP inhibition on  $\text{Ca}^{2+}$  uptake capacity we used cyclosporine A (1  $\mu\text{M}$ ) plus ADP (50  $\mu\text{M}$ ) plus oligomycin (2  $\mu\text{g/ml}$ ). The PTP inhibitors were added to the respiratory chamber prior to  $\text{Ca}^{2+}$  additions (21). To calculate  $\text{Ca}^{2+}$  uptake capacity, we counted number of  $\text{Ca}^{2+}$  additions until the addition after which no uptake was observed (trace horizontal). The number of additions was multiplied by the nmols  $\text{Ca}^{2+}$  per addition, and normalized to protein content.

*Cytoplasmic and Mitochondrial Calcium Imaging* – Cells grown on poly-L-lysine-coated plates were loaded for 30 min (37°C) with 5  $\mu\text{M}$  Fluo-3 AM (Molecular Probes), and 10  $\mu\text{M}$  Rhod-2 AM (Molecular Probes) in Krebs-Ringer-Hepes (KRH) supplemented with 5 mM glucose, containing 0.02 % pluronic acid. The fluorescence changes in Fluo-3 AM represent the cytoplasmic calcium changes (22), while changes in Rhod-2 AM fluorescence are a measure of calcium changes in the mitochondria (23,24). Cells were washed three times and left in KRH-glucose for 10 min until cell fluorescence had reached a plateau. Fluorescence was imaged with a confocal laser scanning microscope (Leica model TCS SP), using an 40x water-immersion lens. Images were

acquired using a 488-nm Argon laser to excite Fluo-3 AM fluorescence and a 561-nm He-Ne laser to excite Rhod-2 AM fluorescence. The signals were collected at 505-530 nm (Fluo-3 AM) and at 590 nm (Rhod-2 AM). The images were analyzed with LCS Leica confocal software (Leica Microsystems, Heidelberg, Germany). Background was measured in parts of the field devoid of cells and found to be not significantly different from the signal recorded in cells depleted of dye with 100  $\mu$ M digitonin. This value was subtracted from cell measurements. The fluorescence intensity variation was recorded from 8-15 cells on average per experiment. Estimation of fluorescence intensity of Fluo-3 AM and Rhod-2 AM was presented as a pseudoratio ( $\Delta F/F_0$ ) as calculated by the following formula:  $\Delta F/F_0 = (F - F_{\text{base}})/(F_{\text{base}} - B)$ , where F is the measured fluorescence intensity of the indicator,  $F_{\text{base}}$  is the fluorescence intensity before the stimulation, and B is the background signal determined from the average of areas adjacent to the cells (25,26).

*Mitochondrial Membrane Potential ( $\Delta\Psi_m$ ) Determination in Live Cells –*

Mitochondrial membrane potential was estimated using the specific mitochondrial probe CM-H2TMRos (Mitotracker Red) (Molecular Probes) (27,28). Cells were grown on poly-L-lysine-coated plates and cultured for 3 days. The cells were then loaded for 30 min with CM-H2TMRos in KRH-glucose, washed, and allowed to equilibrate for 15 min. Coverslips were then mounted in a chamber on the stage of a confocal laser scanning microscope 4 (Leica model TCS SP5). Quantitative measurements of CM-H2TMRos fluorescence were performed by confocal microscopy (Leica model TCS SP5), using a 40X water-immersion lens. CM-H2TMRos fluorescence images were obtained by excitation at 563 nm, reflection off a dichroic mirror with a cut-off wavelength at 564

nm, and longpass emission filtering at 590 nm. Signal from control cells and cells treated with different stimuli were compared using identical settings for laser power, confocal thickness and detector sensitivity (27,28). The images were analyzed with LCS Leica confocal software and recorded as the mean Mitotracker red signal per live cell.

*Measurement of Mitochondrial Membrane Potential ( $\Delta\Psi_m$ ) in Mitochondrial Preparations* –  $\Delta\Psi_m$  was measured using 5,5',6,6'-tetrachloro-1,1',3,3'-tetraethylbenzimidazolylcarbocyanine iodide (JC-1; Molecular Probes) according to a published protocol with modifications (29). Modifications were made so that method could be used with isolated mitochondria. To measure  $\Delta\Psi_m$  at different  $\text{Ca}^{2+}$  concentrations, crude mitochondrial preparation was aliquoted into the wells of 96-well plate (50  $\mu\text{g}/\text{well}$ ). The plate was centrifuged at 3220 xg for 10 min at 4°C and supernatants were carefully aspirated. Ca-EGTA respiration buffers with 0, 0.4 or 0.6  $\mu\text{M}$  (software calculated) free  $\text{Ca}^{2+}$  or  $\text{Ca}^{2+}$  uptake buffer with 150, 500 or 1000  $\mu\text{M}$   $\text{Ca}^{2+}$  each supplemented with glutamate (10 mM), malate (10 mM), and with (for state 3) or without (for state 4) ADP (1.5 mM) were added to separate wells in duplicates (50  $\mu\text{l}/\text{well}$ ) and incubated at 37°C for 10 min. Supernatants were carefully aspirated, and the same buffers but containing JC-1 (5  $\mu\text{g}/\text{ml}$ ) were added to the wells (50  $\mu\text{l}/\text{well}$ ). Wells in which FCCP (20  $\mu\text{M}$ ) was also added were considered as positive controls. Plate was incubated for 30 min, at 37°C in dark, supernatants were aspirated and fluorescence was read at 485/528 nm and 530/590 nm. Ratio between the two fluorescences was used to describe  $\Delta\Psi_m$  as published previously (29).

*Measurement of Mitochondrial  $\text{H}_2\text{O}_2$  Production* – To determine mitochondrial ROS production we used an Amplex red (Molecular Probes) assay (30). Crude

mitochondrial preparations were aliquoted (100  $\mu$ g/well) and pelleted onto a 96-well plate as described for measuring  $\Delta\Psi_m$ . Mitochondrial pellets were covered with Ca-EGTA respiration buffers with 0, 0.4 or 0.6  $\mu$ M (software calculated) free  $\text{Ca}^{2+}$  or  $\text{Ca}^{2+}$  uptake buffer with 150, 500 or 1000  $\mu$ M  $\text{Ca}^{2+}$  each supplemented with glutamate (10 mM), malate (10 mM), amplex red (50  $\mu$ M), horseradish peroxidase (0.01U/ml or 0.1U/ml) and with (for state 3) or without (for state 4) ADP (1.5 mM). Plate was read in the kinetic mode for 30 min at excitation/emission wavelengths 530/590nm at 37°C. Rates of  $\text{H}_2\text{O}_2$  production were determined using a standard curve.

*Statistical Analysis* – Results were analyzed using ANOVA, Student's *t* test or paired *t* test as indicated. Differences were considered significant if  $p \leq 0.05$ .

## Results

*Effects of  $\text{Ca}^{2+}$  on respiration in mitochondria from  $\text{STHdh}^{Q7/Q7}$  (wild-type) and  $\text{STHdh}^{Q111/Q111}$  (mutant) cells* – It has been shown previously that at the free concentrations higher than 1  $\mu$ M,  $\text{Ca}^{2+}$  causes strong inhibition of the oxidative phosphorylation (31). To determine the effects of  $\text{Ca}^{2+}$  on oxidative phosphorylation in mitochondria isolated from the cells expressing endogenous levels of wild-type ( $\text{STHdh}^{Q7/Q7}$ ) or mutant ( $\text{STHdh}^{Q111/Q111}$ ) huntingtin, we measured state 4 and state 3 respiration rates in respiration buffers containing increasing free  $\mu$ M  $\text{Ca}^{2+}$  concentrations. In these experiments, EGTA based respiration buffer was used for 0  $\mu$ M  $\text{Ca}^{2+}$  and  $\text{Ca}^{2+}$ -EGTA respiration buffers were prepared as described in “Materials and Methods”. At 0  $\mu$ M  $\text{Ca}^{2+}$ , we observed no differences in the state 4 or state 3 respiration rates between wild-type and mutant cells when glutamate plus malate (complex I substrate) or succinate



(complex II substrate) were used as substrates (Fig. 1A). As described earlier (31), with increasing free  $\mu\text{M Ca}^{2+}$  concentrations decreases in the state 3 rates were observed (Fig 1B). However, this decrease was more pronounced in the mitochondria from the mutant huntingtin expressing cells, reaching significance at lower  $\text{Ca}^{2+}$  concentrations than in the wild-type (Fig. 1B). State 4 rates increased with increasing  $\text{Ca}^{2+}$  concentrations, reaching significance only in the mutant at the highest  $\text{Ca}^{2+}$  concentration used (Fig. 1B). To describe overall changes in the respiration rates, we calculated Respiratory Control Ratios (RCRs) at the different  $\text{Ca}^{2+}$  concentrations. RCR was calculated as the ratio between state 3 and state 4 rates. A decrease in RCR was observed with increasing  $\text{Ca}^{2+}$  concentrations and was more pronounced in mitochondria from mutant cells, reaching significance at the lower  $\text{Ca}^{2+}$  concentrations than in the wild-type cells (Fig. 1C). These results suggest that mitochondria from  $\text{STHdh}^{\text{Q111/Q111}}$  (mutant) cells are more sensitive to  $\text{Ca}^{2+}$  induced changes in oxidative phosphorylation than mitochondria from  $\text{STHdh}^{\text{Q7/Q7}}$  (wild-type) cells.

*$\text{Ca}^{2+}$  uptake capacity in mitochondria from  $\text{STHdh}^{\text{Q7/Q7}}$  (wild-type) and  $\text{STHdh}^{\text{Q111/Q111}}$  (mutant) cells* – Several studies have suggested that there is reduced mitochondrial  $\text{Ca}^{2+}$  buffering capacity in HD. Panov et. al. demonstrated diminished  $\text{Ca}^{2+}$  uptake capacity in mitochondria from HD lymphoblast cell lines (7,13), and brain mitochondria from the full-length mutant huntingtin overexpressing mice (YAC72) (7) while others demonstrated diminished  $\text{Ca}^{2+}$  uptake in muscle mitochondria from R6/2 mice (32). In order to comprehensively describe the effects of  $\text{Ca}^{2+}$  on mitochondria in our model, we determined mitochondrial  $\text{Ca}^{2+}$  uptake capacity in  $\text{STHdh}^{\text{Q7/Q7}}$  (wild-type) and  $\text{STHdh}^{\text{Q111/Q111}}$  (mutant) cells. For these experiments we used a  $\text{Ca}^{2+}$  sensitive

electrode, as described in “Materials and Methods”. In a preliminary experiment, due to the fact that ER contamination is possible, we confirmed the mitochondrial nature of the  $\text{Ca}^{2+}$  uptake in our mitochondrial preparations, as the addition of uncoupler (FCCP) caused release of  $\text{Ca}^{2+}$ , and pretreatment of the cells with thapsigargin (which blocks the  $\text{Ca}^{2+}$  uptake pump of the ER, (33)) did not produce any change in the  $\text{Ca}^{2+}$  uptake capacity (data not shown). To determine, mitochondrial  $\text{Ca}^{2+}$  uptake, isolated mitochondria (1.5mg/2ml) were placed in a 37°C thermostatted chamber and challenged with 10 nmols  $\text{Ca}^{2+}$  pulses every 3 min. Representative traces are shown in figure 2A.  $\text{Ca}^{2+}$  uptake capacity was calculated as described in “Materials and Methods”. We observed that mitochondria from  $\text{STHdh}^{\text{Q111/Q111}}$  (mutant) cells have significantly diminished  $\text{Ca}^{2+}$  uptake capacity compared to mitochondria from  $\text{STHdh}^{\text{Q7/Q7}}$  (wild-type) cells (Fig. 2B). To determine the “initial uptake” rates we calculated the average of the rates after the second, third and fourth additions of  $\text{Ca}^{2+}$  and determined that the “initial uptake” rates were significantly diminished in the mitochondria from the mutant cells (Fig. 2C). These results indicate that mitochondria from  $\text{STHdh}^{\text{Q111/Q111}}$  (mutant) cells have a  $\text{Ca}^{2+}$  buffering defect, as they can take up less  $\text{Ca}^{2+}$  than the mitochondria from wild-type cells.

*Mitochondrial and cytosolic  $\text{Ca}^{2+}$  levels in  $\text{STHdh}^{\text{Q7/Q7}}$  (wild-type) and  $\text{STHdh}^{\text{Q111/Q111}}$  (mutant) cells* – In order to corroborate the decreased  $\text{Ca}^{2+}$  uptake capacity in mitochondria from mutant cells, we examined the mitochondrial  $\text{Ca}^{2+}$  levels in  $\text{STHdh}^{\text{Q7/Q7}}$  (wild-type) and  $\text{STHdh}^{\text{Q111/Q111}}$  (mutant) cells. For this purpose we used the mitochondrial specific  $\text{Ca}^{2+}$  sensitive dye (Rhod 2 - AM) (23,24) as described in “Materials and Methods”. In these experiments we determined that mitochondrial  $\text{Ca}^{2+}$

levels were similar in the two cell lines under basal conditions (Fig. 3B). Representative images are shown (Fig. 3A). In addition, we measured cytosolic and mitochondrial  $\text{Ca}^{2+}$  levels before and after the addition of mitochondrial uncoupler FCCP. Addition of FCCP resulted in a decrease of  $\Delta\Psi_m$  in both wild-type and mutant cells, respectively, as measured by Mitotracker red (data not shown)2. Similar cytosolic (Fig. 3C) and mitochondrial (Fig. 3D)  $\text{Ca}^{2+}$  levels in both cell lines were observed before and after the FCCP addition. These results are in agreement with previous reports showing that FCCP does not induce changes in the mitochondrial calcium levels in cortical neurons in the basal conditions (34). These results indicate that  $\text{STHdh}^{\text{Q111/Q111}}$  (mutant) cells do not exhibit any apparent perturbations in the mitochondrial calcium levels in basal conditions.

*Analysis of mitochondrial membrane integrity before and after  $\text{Ca}^{2+}$  addition in  $\text{STHdh}^{\text{Q7/Q7}}$  (wild-type) and  $\text{STHdh}^{\text{Q111/Q111}}$  (mutant) cells* –  $\text{Ca}^{2+}$  overload of mitochondria results in increased mitochondrial membrane permeability (35). In order to further study the cause of differences between mitochondria from wild-type and mutant cells in their sensitivity to  $\text{Ca}^{2+}$ , we wanted to determine if the decrease in respiration observed in the presence of free  $\mu\text{M}$   $\text{Ca}^{2+}$  concentrations was associated with increased permeability of the mitochondrial membrane. First, we analyzed the integrity of mitochondrial membrane in the basal conditions. NADH is the substrate for mitochondrial complex I. However, the inner mitochondrial membrane is not permeable to exogenous NADH (36). When pyruvate plus malate was added to provide reduced adenine dinucleotides (NADH,  $\text{FADH}_2$ ) inside the mitochondria we observed significant state 3 rates upon ADP addition (Fig. 4A). However, when NADH was used as the

respiratory substrate, we did not observe induction of state 3 respiration in mitochondria from any of the cell lines (Fig. 4A). Representative traces are shown (Fig. 4A). This indicates good integrity of mitochondrial inner membrane in basal conditions in mitochondria from both cell lines. It has been suggested that damage of the outer mitochondrial membrane results in the activation of alternative respiratory pathway in the presence of exogenous NADH and cytochrome c (37-40). In this pathway, NADH is oxidized at the outer mitochondrial membrane leading to reduction of exogenous cytochrome c. As described previously, if outer membrane is being compromised, cytochrome c will translocate to the complex IV and stimulate respiration (38). To assess mitochondrial membrane integrity, we measured the effects of NADH and cytochrome c on state 3 respiration in the absence or presence of  $\text{Ca}^{2+}$ . For these experiments, we chose  $\text{Ca}^{2+}$  concentration that caused a significant decrease in state 3 rate in the mitochondria from both cell lines. Experiments were carried out as described in "Materials and Methods". In the absence of  $\text{Ca}^{2+}$ , neither cytochrome c alone nor cytochrome c plus NADH had any effect on respiration (Fig. 4B). This indicated good integrity of the outer mitochondrial membrane in both cell lines. However in the presence of  $\text{Ca}^{2+}$ , when the state 3 respiration was decreased, cytochrome c plus NADH caused a significant increase in state 3 (Fig. 4B). Alamethicin, forms pores in the membrane, was used as a positive control for the method (not shown)<sup>2</sup>. Cytochrome c alone did not affect state 3 respiration in the presence of  $\text{Ca}^{2+}$  (Fig. 4B), suggesting that no substantial loss of cytochrome c is causing the decrease in state 3 rate. These results suggest that mitochondria from both wild-type and mutant cells do have good membrane integrity in the absence of  $\text{Ca}^{2+}$ . Further, the decrease in state 3 rates in the presence of  $\mu\text{M}$   $\text{Ca}^{2+}$

concentrations is associated with the increased permeability of mitochondrial membrane but not substantial loss of cytochrome c.

*Differential effects of  $\text{Ca}^{2+}$  on mitochondrial membrane potential ( $\Delta\Psi_m$ ) in  $\text{STHdh}^{Q7/Q7}$  (wild-type) and  $\text{STHdh}^{Q111/Q111}$  (mutant) cells* – To determine the effects of  $\text{Ca}^{2+}$  deregulation on  $\Delta\Psi_m$ , the ratiometric dye JC-1 was used (41). In these experiments, isolated mitochondria were incubated with increasing  $\text{Ca}^{2+}$  concentrations, keeping the same [mitochondrial mass/  $\text{Ca}^{2+}$  buffer volume] ratio as in the respiration experiments.  $\text{Ca}^{2+}$  concentrations used were – 0  $\mu\text{M}$  (EGTA based respiration buffer), two low  $\mu\text{M}$  concentrations: 0.4  $\mu\text{M}$ , 0.6  $\mu\text{M}$  (software calculated) that correspond to 1.1  $\mu\text{M}$ , 2.2  $\mu\text{M}$  ( $\text{Ca}^{2+}$  electrode determined) in figure 1B., at which decrease in state 3 respiration was observed, and 3 high  $\mu\text{M}$  concentrations: 150  $\mu\text{M}$ , 500  $\mu\text{M}$  and 1000  $\mu\text{M}$ , where 150  $\mu\text{M}$  corresponds approximately to the  $\text{Ca}^{2+}$  concentration at which we no longer observed  $\text{Ca}^{2+}$  uptake by the wild-type mitochondria (Fig. 2).  $\Delta\Psi_m$  was also measured in  $\text{Ca}^{2+}$  uptake buffer (Cab) which is respiration buffer without EGTA, and contains approximately 10  $\mu\text{M}$   $\text{Ca}^{2+}$  as determined by using the  $\text{Ca}^{2+}$  electrode.  $\Delta\Psi_m$  was determined as described in “Materials and Methods”. FCCP was used to induce maximal decrease of  $\Delta\Psi_m$ , as the positive control for the assay (Fig. 5). In the state 4 condition (ADP not added), we observed a  $\text{Ca}^{2+}$  concentration dependant decrease of  $\Delta\Psi_m$ . This decrease was significant in the mutant at as low as 0.4  $\mu\text{M}$ , but in the wild-type only at 500  $\mu\text{M}$   $\text{Ca}^{2+}$  (Fig. 5A). The significant difference between the two could be observed at 0.6  $\mu\text{M}$ , Cab (~10  $\mu\text{M}$ ), 150  $\mu\text{M}$  and 500  $\mu\text{M}$   $\text{Ca}^{2+}$ , and was about 80% at 0.6  $\mu\text{M}$  and 65% at 150  $\mu\text{M}$ . However, in the state 3 condition (ADP added) the significant difference in  $\Delta\Psi_m$  could be observed only starting at 150  $\mu\text{M}$  and was about 30% (Fig. 5B). These

results show that  $\Delta\Psi_m$  is significantly more sensitive to  $\text{Ca}^{2+}$  in  $\text{STHdh}^{\text{Q111/Q111}}$  (mutant) compared to  $\text{STHdh}^{\text{Q7/Q7}}$  (wild-type) cells. Also, this difference can be importantly attenuated by the presence of ADP.

*Effects of  $\text{Ca}^{2+}$  on  $\text{H}_2\text{O}_2$  production in mitochondria from  $\text{STHdh}^{\text{Q7/Q7}}$  (wild-type) and  $\text{STHdh}^{\text{Q111/Q111}}$  (mutant) cells* – Increased ROS production in mitochondria is usually associated with perturbations of electron transfer in the oxidative phosphorylation process (42) and has been described in conditions of increased mitochondrial membrane permeability (43). To assess the effects of  $\text{Ca}^{2+}$  on reactive oxygen species production (ROS) in the mitochondria from wild-type and mutant cells the Amplex Red assay was used (30). This assay measures  $\text{H}_2\text{O}_2$  production and was carried out as described in “Materials and Methods”. Isolated mitochondria were incubated with the increasing  $\text{Ca}^{2+}$  concentrations and  $\text{H}_2\text{O}_2$  production was measured in the course of incubation. The  $\text{Ca}^{2+}$  concentrations used were as described for  $\Delta\Psi_m$  experiments (Fig. 5). In the state 4, we observed  $\text{Ca}^{2+}$  concentration dependent increases in  $\text{H}_2\text{O}_2$  that reached significance at 1000  $\mu\text{M}$  in wild-type and at 500, 1000  $\mu\text{M}$  in mutant (Fig. 6A). No difference was observed when wild-type and mutants were compared at any of the data points (Fig. 6A). In the state 3 condition (ADP added), we observed increases in  $\text{H}_2\text{O}_2$  production with  $\text{Ca}^{2+}$  that reached significance only in the mutant at 1000  $\mu\text{M}$   $\text{Ca}^{2+}$  (Fig. 6B). The trend of increased  $\text{H}_2\text{O}_2$  production with increasing  $\text{Ca}^{2+}$  concentrations was similar to what was observed for  $\Delta\Psi_m$  change. At all  $\text{Ca}^{2+}$  concentrations, mutant mitochondria displayed a greater increase in  $\text{H}_2\text{O}_2$  production than wild-type (Fig. 6B). This increase was statistically significant at 0.4, 0.6, and 500  $\mu\text{M}$  (Fig. 6B). In these experiments, rotenone treated mitochondria were used as an assay positive control. As expected, in the wild-

type, rotenone treatment caused significant increase in  $\text{H}_2\text{O}_2$  production. Interestingly, mutant mitochondria generated significantly less  $\text{H}_2\text{O}_2$  upon rotenone treatment when compared to the wild-type.

*Effects of permeability transition pore (PTP) inhibitors on mitochondrial  $\text{Ca}^{2+}$  uptake capacity in  $\text{STHdh}^{\text{Q7/Q7}}$  (wild-type) and  $\text{STHdh}^{\text{Q111/Q111}}$  (mutant) cells –* Diminished  $\text{Ca}^{2+}$  uptake capacity in mutant could be explained by a lower threshold for PTP opening in the mutant cells. To test this hypothesis,  $\text{Ca}^{2+}$  uptake capacity in the presence of PTP inhibitors was measured. For these experiments, cyclosporine A plus ADP plus oligomycin was used, as this combination has been shown to be very efficient in inhibiting PTP in brain mitochondria (21). Addition of PTP inhibitors increased mitochondrial  $\text{Ca}^{2+}$  uptake capacity in both cell lines. This increase was greater and statistically significant in the mutant mitochondria (ANOVA, Tukey post test;  $p < 0.01$ ,  $n = 5$  for mutant and  $n = 8$  for mutant plus PTP inhibitors group) (Fig. 7). In the presence of PTP inhibitors, mitochondrial  $\text{Ca}^{2+}$  uptake capacity reduction was strongly attenuated in the mutant mitochondria, as the difference between the wild-type and mutant mitochondria no longer reached statistical significance (Fig. 7). These results suggest that  $\text{STHdh}^{\text{Q111/Q111}}$  (mutant) cells exhibit a lower threshold for PTP opening when compared to  $\text{STHdh}^{\text{Q7/Q7}}$  (wild-type) cells.

*Effects of  $\text{Ca}^{2+}$  on  $\Delta\Psi\text{m}$  and mitochondrial  $\text{Ca}^{2+}$  accumulation in  $\text{STHdh}^{\text{Q7/Q7}}$  (wild-type) and  $\text{STHdh}^{\text{Q111/Q111}}$  (mutant) cells in situ –* To determine the effects of changes in cytosolic  $\text{Ca}^{2+}$  levels on mitochondrial  $\text{Ca}^{2+}$  levels, cells were treated with a low concentration of 4-BrA23187 (1nM) which does not negatively impact cell viability (44). Cells were treated with the ionophore for 5 min, followed by 4  $\mu\text{mol}$   $\text{Ca}^{2+}$  additions,

approximately every 5 min, to obtain the increasing concentrations of  $\text{Ca}^{2+}$  in the medium (2, 4, 6 mM). With increasing  $\text{Ca}^{2+}$  concentrations a decrease in  $\Delta\Psi_m$  was observed as measured with CM-H2TMRos (27,28), and it was more pronounced in mutant cells (Fig. 8A). The difference in  $\Delta\Psi_m$  between wild-type and mutant cells was significant starting at 2mM  $\text{Ca}^{2+}$  in the media (Fig. 8A). This was in accordance with the results obtained in mitochondrial preparations as shown in figure 5. Mitochondrial  $\text{Ca}^{2+}$  accumulation was measured in the same experiments as  $\Delta\Psi_m$  using the mitochondrial specific  $\text{Ca}^{2+}$  sensitive dye (Rhod-2 AM). Starting mitochondrial  $\text{Ca}^{2+}$  levels are shown in figure 3. Interestingly, we observed an increased accumulation of  $\text{Ca}^{2+}$  in mitochondria from mutant cells when compared to wild-type (Fig. 8B). Mitochondrial  $\text{Ca}^{2+}$  levels were similar in wild-type during the course of experiment, while in mutant, mitochondrial  $\text{Ca}^{2+}$  levels increased and were significantly higher at 4 and 6 mM  $\text{Ca}^{2+}$  when compared to wild-type (Fig. 8B). These results show that in the live cells  $\text{Ca}^{2+}$  changes cause a significantly greater reduction in  $\Delta\Psi_m$  in  $\text{STHdh}^{\text{Q111/Q111}}$  (mutant) than in  $\text{STHdh}^{\text{Q7/Q7}}$  (wild-type) cells. Also, when cells are challenged with increasing  $\text{Ca}^{2+}$  loads, mitochondrial  $\text{Ca}^{2+}$  accumulation was greater in  $\text{STHdh}^{\text{Q111/Q111}}$  (mutant) than in  $\text{STHdh}^{\text{Q7/Q7}}$  (wild-type) cells.

### Discussion

In this study, we provide evidence for the first time that mitochondrial  $\text{Ca}^{2+}$  handling defects in cells of striatal origin that express endogenous levels of mutant huntingtin result in impairment of respiration, which could contribute to neuronal dysfunction and death in HD. Treatment of isolated mitochondria from mutant cells with



increasing  $\text{Ca}^{2+}$  concentrations, resulted in a significant decrease in state 3 respiration at lower  $\text{Ca}^{2+}$  than mitochondria from wild-type cells. Further, the  $\text{Ca}^{2+}$  dependent decrease of  $\Delta\Psi\text{m}$  was significantly greater in the mutant cells compared to the wild-type cells. However, the  $\Delta\Psi\text{m}$  defect was markedly attenuated in the presence of ADP. Additionally the mitochondrial  $\text{Ca}^{2+}$  uptake capacity in mutant cells was significantly lower than what was observed in mitochondria from wild-type cells, which was completely abolished by the presence of PTP inhibitors. In situ, mitochondrial  $\text{Ca}^{2+}$  levels were not different between wild-type and mutant cells in the basal conditions. Nonetheless, when the cells were challenged with increasing  $\text{Ca}^{2+}$  loads, mitochondria in the mutant cells accumulated more  $\text{Ca}^{2+}$  than mitochondria in the wild-type cells. Taken together these data demonstrate that the presence of mutant huntingtin at physiologically relevant levels results in impaired  $\text{Ca}^{2+}$  handling by mitochondria which negatively impacts their function and hence likely impairs proper neuronal function.

Excitotoxicity has been suggested as a key mechanism that is responsible for neurodegeneration in HD (45), and dysfunction at the level of the mitochondria could be a mediator of this toxicity. Mitochondrial dysfunction could result in an increase in the sensitivity of neurons to neurotransmitter glutamate, leading to  $\text{Ca}^{2+}$  induced cellular dysfunction and eventually cell death (the role of mitochondria in excitotoxicity examined and discussed in (46-48)). It has been shown previously that decreases in oxidative phosphorylation and state 3 rates are early events in excitotoxicity, and occur prior to the commitment to cell death (34). Moreover, it has been shown that free  $\mu\text{M}$   $\text{Ca}^{2+}$  concentrations cause significant decreases in oxidative-phosphorylation in isolated mitochondria (31). To determine if mutant huntingtin alters mitochondrial response to

$\text{Ca}^{2+}$ , we measured respiration rates in the presence of increasing  $\text{Ca}^{2+}$  concentrations in mitochondria from wild-type ( $\text{STHdh}^{\text{Q7/Q7}}$ ) and mutant huntingtin ( $\text{STHdh}^{\text{Q111/Q111}}$ ) expressing cells. We observed that the decrease in state 3 rate (ADP phosphorylation rate) occurred at significantly lower  $\text{Ca}^{2+}$  concentrations in mutant cells compared to wild-type cells, suggesting an increased sensitivity to  $\text{Ca}^{2+}$ .

Elevated mitochondrial  $\text{Ca}^{2+}$  levels are usually associated with the opening of PTP. However, the mechanism of the oxidative-phosphorylation decrease due to elevated  $\text{Ca}^{2+}$  levels is not quite clear (discussed in (34)). It has been suggested that permeabilization of the outer mitochondrial membrane leads to activation of an alternative respiratory pathway which utilizes exogenous NADH oxidation on the outer mitochondrial membrane and translocation of subsequently reduced cytochrome c to the inner membrane where it feeds into complex IV (37,38). In our study, addition of NADH and cytochrome c caused an increase in the state 3 rates in the presence of  $\text{Ca}^{2+}$ , but not in the absence, and cytochrome c alone did not increase state 3. These results indicate the  $\text{Ca}^{2+}$  induced decrease in oxidative-phosphorylation is associated with increased permeabilization of the mitochondrial membrane but not with substantial loss of cytochrome c.

In this study respiration rates were measured in mitochondria isolated from  $\text{STHdh}^{\text{Q7/Q7}}$  (wild-type) and  $\text{STHdh}^{\text{Q111/Q111}}$  (mutant) cells in KCl based EGTA containing respiration buffer, and no significant differences were observed. In our previous study, respiration rates were measured in digitonin permeabilized cells, in the sucrose based buffer without EGTA, and significant decrease in the state 3 rates was observed in  $\text{STHdh}^{\text{Q111/Q111}}$  (mutant) cells (18). In the light of current study, it is likely,

that the experimental conditions used in our previous study were permissive for the mutant huntingtin dependent mitochondrial defects. These conditions resulted in the deficits observed in state 3 rates for the mutant cells. Indeed it is likely that the presence of free  $\text{Ca}^{2+}$  in the buffers (e.g. from the sucrose) likely resulted in an increase in mitochondrial membrane permeability to a greater extent in the mutant cells than the wild-type cells which caused the observed differences in respiration.

It has been shown that huntingtin associates with the outer mitochondrial membrane (49). We tested the integrity of outer mitochondrial membrane in basal conditions. We found that mitochondria from both cell lines have a good outer mitochondrial membrane integrity as state 3 rates did not increase in the presence of NADH and cytochrome c. Inner mitochondrial membrane was of good integrity as well, since NADH (inner mitochondrial membrane impermeable) did not work as respiratory substrate. Also, state 4 rates were comparable in the two cell lines, indicating similar levels of inner membrane proton leakage. However, it is still possible that changes in the integrity of mitochondrial membrane due to mutant huntingtin are quite subtle and could not be detected with the methods we used.

Mutant huntingtin expressing cells (STHdh<sup>Q111/Q111</sup>) showed markedly enhanced  $\Delta\Psi_m$  reduction in response to increasing  $\text{Ca}^{2+}$  concentrations. Mitochondrial depolarization in response to  $\text{Ca}^{2+}$  is caused by  $\text{Ca}^{2+}$  uptake itself (partial and reversible depolarization) and by opening of the PTP when  $\text{Ca}^{2+}$  uptake capacity is exceeded (complete depolarization) (41). Since, in our experiments  $\Delta\Psi_m$  was measured in the population of mitochondria, determined  $\Delta\Psi_m$  values could indicate the portion of mitochondria undergoing PTP associated with complete depolarization or  $\Delta\Psi_m$  levels

present in the majority of mitochondria at specific  $\text{Ca}^{2+}$  concentrations. As previously described, ADP prevents PTP opening and stabilizes  $\Delta\Psi_m$  by the mechanism that includes binding and stabilization of adenine-nucleotide translocator (ANT) in the conformation that prevents PTP opening (50). The differences in  $\Delta\Psi_m$  reduction between wild-type and mutant cells were significantly attenuated in the presence of ADP. This suggested that differences in the threshold for PTP opening, significantly contributed to  $\Delta\Psi_m$  differences observed between wild-type and mutant cells.

The reduction of  $\Delta\Psi_m$  could be observed at as low as 0.4 and 0.6  $\mu\text{M}$   $\text{Ca}^{2+}$  (concentrations at which decreases in oxidative-phosphorylation were observed) in the mutant but not in the wild type cells. Since, in the respiration experiments (Fig. 1), respiration was first monitored in state 4 followed by the induction of state 3, the observed differences in the state 3 rates are likely due to the differences in the  $\Delta\Psi_m$  before the state 3 was induced. Indeed, no differences in  $\Delta\Psi_m$  were observed at 0.4 and 0.6  $\mu\text{M}$   $\text{Ca}^{2+}$  when measured in state 3 conditions.

ROS production could contribute to  $\text{Ca}^{2+}$  induced PTP opening (discussed in (43)). As described, determination of released  $\text{H}_2\text{O}_2$  is a common and the most reliable measure of mitochondrial ROS production (42). When added to isolated mitochondria,  $\text{Ca}^{2+}$  caused a dose dependent increase in the release of  $\text{H}_2\text{O}_2$ . However, no significant difference in released  $\text{H}_2\text{O}_2$ , between wild-type and mutant, was observed at different  $\text{Ca}^{2+}$  concentrations (state 4). Therefore, dramatic differences in  $\Delta\Psi_m$  and  $\text{Ca}^{2+}$  uptake capacity observed between wild-type and mutant are likely not caused by differences in the ROS production. However, in the presence of ADP (state 3), we observed higher levels of released  $\text{H}_2\text{O}_2$  in mutant, which reached significance at several data points.

Increased ROS in the presence of ADP would likely contribute to more pronounced decrease in state 3 rates observed in mutant mitochondria in the presence of  $\text{Ca}^{2+}$ . Unexpectedly, we observed reduced  $\text{H}_2\text{O}_2$  release from mutant mitochondria upon rotenone treatment. Our results suggest that ROS production is likely not the mechanism for reduced threshold for PTP opening in the mutant cells. However, there was a trend for mitochondria from mutant cells to exhibit altered ROS homeostasis compared to wild-type (modest increase in the presence of  $\text{Ca}^{2+}$  and ADP; decrease in the presence of rotenone).

In this paper we observed that mitochondria from mutant cells had reduced  $\text{Ca}^{2+}$  uptake capacity compared to mitochondria from wild type cells. As suggested in multiple papers, decreases in mitochondrial  $\text{Ca}^{2+}$  uptake capacity could be due to a decreased threshold for PTP opening (7,51). In fact, when mitochondria from mutant cells were treated with PTP inhibitors (cyclosporine A, ADP, oligomycin), the defect in  $\text{Ca}^{2+}$  uptake was almost abolished. Decreased mitochondrial  $\text{Ca}^{2+}$  uptake has already been reported in other HD models. Panov et.al reported decreased  $\text{Ca}^{2+}$  uptake in mitochondria from HD lymphoblast cell line, and brain mitochondria from full length huntingtin transgenic mice (YAC72) (7,13). Recently, attenuated  $\text{Ca}^{2+}$  uptake was reported in muscle mitochondria from R6/2 mice (32). Interestingly, recombinant truncated mutant huntingtin resulted in significant mitochondrial swelling at lower  $\text{Ca}^{2+}$  loads than truncated wild-type protein when added to isolated mouse liver mitochondria (49). This suggested that mechanism of mutant huntingtin induced mitochondrial dysfunction is possibly through its direct effects on mitochondria.

In situ experiments revealed similar mitochondrial  $\text{Ca}^{2+}$  levels in mutant and wild-type cells. When cells were given increasing  $\text{Ca}^{2+}$  loads, a significantly greater  $\Delta\Psi_m$  reduction was observed in the mutant cells, which was in agreement with the experiments done using isolated mitochondria. However, we also observed increased mitochondrial  $\text{Ca}^{2+}$  loading in mutant cells, as measured with Rhod-2 (Fig. 8B). At the first glance, this finding seems at odds with reduced  $\text{Ca}^{2+}$  uptake rates observed when mitochondrial  $\text{Ca}^{2+}$  uptake was measured in isolated mitochondria using a  $\text{Ca}^{2+}$  sensitive electrode (Fig. 2C). However, the rates determined in the isolated mitochondria likely represent the balance between  $\text{Ca}^{2+}$  uptake and  $\text{Ca}^{2+}$  release (due to PTP opening) rates. Additionally, when cells were treated with thapsigargin to inhibit  $\text{Ca}^{2+}$  uptake by the ER, mutant cells exhibited a significant decrease in mitochondrial  $\text{Ca}^{2+}$  uptake in comparison with wild-type cells<sup>2</sup>. Thapsigargin treatment produced approximately three fold higher cytosolic  $\text{Ca}^{2+}$  levels compared to ionophore plus  $\text{Ca}^{2+}$  treatment used in figure 8. These results indicated that cytosolic  $\text{Ca}^{2+}$  levels are a major factor in determining mitochondrial calcium uptake in the wild-type and mutant cells.

Using multiple mitochondrial functional assays, we demonstrated mitochondrial  $\text{Ca}^{2+}$  handling defect in mutant (STHdh<sup>Q111/Q111</sup>) cells. Interestingly, in situ experiments indicated an increased  $\text{Ca}^{2+}$  loading in mitochondria from mutant cells. It is not clear, at present, if this is related to the reduced PTP threshold observed in isolated mitochondria, or, if it is caused by perturbation in  $\text{Ca}^{2+}$  homeostasis elsewhere in the cells, and would, therefore, present additional burden to already compromised mitochondria. These possibilities will be explored in the future studies.

Given the increasing evidence of impaired mitochondrial  $\text{Ca}^{2+}$  buffering in HD, it is clear that elucidating the effects of mutant huntingtin on mitochondria will provide important clues for development of HD therapeutics. In the light of our current knowledge, successful PTP inhibition would be beneficial, but, as already discussed in terms of excitotoxicity (41), limiting mitochondrial  $\text{Ca}^{2+}$  uptake by manipulating its setpoint (through  $\text{Ca}^{2+}$ -uniporter inhibition or  $\text{Na}^{+}$ - $\text{Ca}^{2+}$  exchanger activation) would likely provide even greater benefits.

### References

1. (1993) *Cell* **72**, 971-983
2. Vonsattel, J. P., and DiFiglia, M. (1998) *J Neuropathol Exp Neurol* **57**, 369-384
3. Cattaneo, E., Rigamonti, D., Goffredo, D., Zuccato, C., Squitieri, F., and Sipione, S. (2001) *Trends Neurosci* **24**, 182-188
4. Landles, C., and Bates, G. P. (2004) *EMBO Rep* **5**, 958-963
5. Valera, A. G., Diaz-Hernandez, M., Hernandez, F., Ortega, Z., and Lucas, J. J. (2005) *Neuroscientist* **11**, 583-594
6. Tang, T. S., Tu, H., Chan, E. Y., Maximov, A., Wang, Z., Wellington, C. L., Hayden, M. R., and Bezprozvanny, I. (2003) *Neuron* **39**, 227-239
7. Panov, A. V., Gutekunst, C. A., Leavitt, B. R., Hayden, M. R., Burke, J. R., Strittmatter, W. J., and Greenamyre, J. T. (2002) *Nat Neurosci* **5**, 731-736
8. Gu, M., Gash, M. T., Mann, V. M., Javoy-Agid, F., Cooper, J. M., and Schapira, A. H. (1996) *Ann Neurol* **39**, 385-389
9. Mann, V. M., Cooper, J. M., Javoy-Agid, F., Agid, Y., Jenner, P., and Schapira, A. H. (1990) *Lancet* **336**, 749
10. Browne, S. E., Bowling, A. C., MacGarvey, U., Baik, M. J., Berger, S. C., Muqit, M. M., Bird, E. D., and Beal, M. F. (1997) *Ann Neurol* **41**, 646-653

11. Beal, M. F., Brouillet, E., Jenkins, B. G., Ferrante, R. J., Kowall, N. W., Miller, J. M., Storey, E., Srivastava, R., Rosen, B. R., and Hyman, B. T. (1993) *J Neurosci* **13**, 4181-4192
12. Brouillet, E., Hantraye, P., Ferrante, R. J., Dolan, R., Leroy-Willig, A., Kowall, N. W., and Beal, M. F. (1995) *Proc Natl Acad Sci U S A* **92**, 7105-7109
13. Panov, A., Obertone, T., Bennett-Desmelik, J., and Greenamyre, J. T. (1999) *Ann N Y Acad Sci* **893**, 365-368
14. Calabresi, P., Gubellini, P., Picconi, B., Centonze, D., Pisani, A., Bonsi, P., Greengard, P., Hipskind, R. A., Borrelli, E., and Bernardi, G. (2001) *J Neurosci* **21**, 5110-5120
15. Henshaw, R., Jenkins, B. G., Schulz, J. B., Ferrante, R. J., Kowall, N. W., Rosen, B. R., and Beal, M. F. (1994) *Brain Res* **647**, 161-166
16. Wallace, D. C. (1999) *Science* **283**, 1482-1488
17. Trettel, F., Rigamonti, D., Hilditch-Maguire, P., Wheeler, V. C., Sharp, A. H., Persichetti, F., Cattaneo, E., and MacDonald, M. E. (2000) *Hum Mol Genet* **9**, 2799-2809
18. Milakovic, T., and Johnson, G. V. (2005) *J Biol Chem* **280**, 30773-30782
19. Guidetti, P., Charles, V., Chen, E. Y., Reddy, P. H., Kordower, J. H., Whetsell, W. O., Jr., Schwarcz, R., and Tagle, D. A. (2001) *Exp Neurol* **169**, 340-350
20. Patton, C., Thompson, S., and Epel, D. (2004) *Cell Calcium* **35**, 427-431
21. Panov, A. V., Andreeva, L., and Greenamyre, J. T. (2004) *Arch Biochem Biophys* **424**, 44-52
22. Quintanilla, R. A., Munoz, F. J., Metcalfe, M. J., Hitschfeld, M., Olivares, G., Godoy, J. A., and Inestrosa, N. C. (2005) *J Biol Chem* **280**, 11615-11625
23. Collins, T. J., Lipp, P., Berridge, M. J., and Bootman, M. D. (2001) *J Biol Chem* **276**, 26411-26420
24. Darios, F., Muriel, M. P., Khondiker, M. E., Brice, A., and Ruberg, M. (2005) *J Neurosci* **25**, 4159-4168
25. Duchen, M. R. (2000) *Cell Calcium* **28**, 339-348
26. Krieger, C., and Duchen, M. R. (2002) *Eur J Pharmacol* **447**, 177-188



27. Krysko, D. V., Roels, F., Leybaert, L., and D'Herde, K. (2001) *J Histochem Cytochem* **49**, 1277-1284
28. Esposti, M. D., Hatzinisiriou, I., McLennan, H., and Ralph, S. (1999) *J Biol Chem* **274**, 29831-29837
29. Ruan, Q., Lesort, M., MacDonald, M. E., and Johnson, G. V. (2004) *Hum Mol Genet* **13**, 669-681
30. Chen, Q., Vazquez, E. J., Moghaddas, S., Hoppel, C. L., and Lesnefsky, E. J. (2003) *J Biol Chem* **278**, 36027-36031
31. Moreno-Sanchez, R. (1985) *J Biol Chem* **260**, 4028-4034
32. Gizatullina, Z. Z., Lindenberg, K. S., Harjes, P., Chen, Y., Kosinski, C. M., Landwehrmeyer, B. G., Ludolph, A. C., Striggow, F., Zierz, S., and Gellerich, F. N. (2006) *Ann Neurol* **59**, 407-411
33. Paschen, W., Doutheil, J., Gissel, C., and Treiman, M. (1996) *J Neurochem* **67**, 1735-1743
34. Kushnareva, Y. E., Wiley, S. E., Ward, M. W., Andreyev, A. Y., and Murphy, A. N. (2005) *J Biol Chem* **280**, 28894-28902
35. Forte, M., and Bernardi, P. (2005) *J Bioenerg Biomembr* **37**, 121-128
36. Voet, D., and Voet, J. G. (1995) *Biochemistry*, second edition Ed., John Wiley & Sons, Inc.
37. Bernardi, P., and Azzone, G. F. (1981) *J Biol Chem* **256**, 7187-7192
38. Lemeshko, V. V. (2001) *Arch Biochem Biophys* **388**, 60-66
39. La Piana, G., Marzulli, D., Consalvo, M. I., and Lofrumento, N. E. (2003) *Arch Biochem Biophys* **410**, 201-211
40. La Piana, G., Marzulli, D., Gorgoglione, V., and Lofrumento, N. E. (2005) *Arch Biochem Biophys* **436**, 91-100
41. Nicholls, D. G., and Ward, M. W. (2000) *Trends Neurosci* **23**, 166-174
42. Adam-Vizi, V. (2005) *Antioxid Redox Signal* **7**, 1140-1149
43. Brookes, P. S., Yoon, Y., Robotham, J. L., Anders, M. W., and Sheu, S. S. (2004) *Am J Physiol Cell Physiol* **287**, C817-833

44. Abramov, A. Y., and Duchen, M. R. (2003) *Cell Calcium* **33**, 101-112
45. Leegwater-Kim, J., and Cha, J. H. (2004) *NeuroRx* **1**, 128-138
46. Budd, S. L., Tenneti, L., Lishnak, T., and Lipton, S. A. (2000) *Proc Natl Acad Sci U S A* **97**, 6161-6166
47. Nicholls, D. G., Vesce, S., Kirk, L., and Chalmers, S. (2003) *Cell Calcium* **34**, 407-424
48. Khodorov, B. (2004) *Prog Biophys Mol Biol* **86**, 279-351
49. Choo, Y. S., Johnson, G. V., MacDonald, M., Detloff, P. J., and Lesort, M. (2004) *Hum Mol Genet* **13**, 1407-1420
50. Vergun, O., and Reynolds, I. J. (2005) *Biochim Biophys Acta* **1709**, 127-137
51. Bernardi, P. (1999) *Physiol Rev* **79**, 1127-1155

#### Footnotes

We thank Dr. P. Bernardi for suggestions and advice regarding outer mitochondrial membrane integrity experiments. This study was supported by NIH grant (NS041744).

<sup>1</sup>The abbreviations used are: HD, Huntington's disease;  $\Delta\Psi_m$ , mitochondrial membrane potential; PTP, permeability transition pore; 3-NP, 3-nitropropionic acid; HEPES, 4-(2-hydroxyethyl)piperazine-1-ethanesulfonic acid; BSA, bovine serum albumin; KRH, Krebs-Ringer-HEPES; CM-H2TMRos, MitoTracker® Red ; JC-1, 5,5',6,6'-tetrachloro-1,1',3,3'-tetraethylbenzimidazolylcarbocyanine iodide; RCR, respiratory control ratio; FCCP, carbonyl cyanide 4-(trifluoromethoxy)phenylhydrazone; ROS, reactive oxygen species; 4-BrA23187, 4-bromo A-23187, free acid; ANT, adenine nucleotide translocator.

<sup>2</sup>Unpublished observations

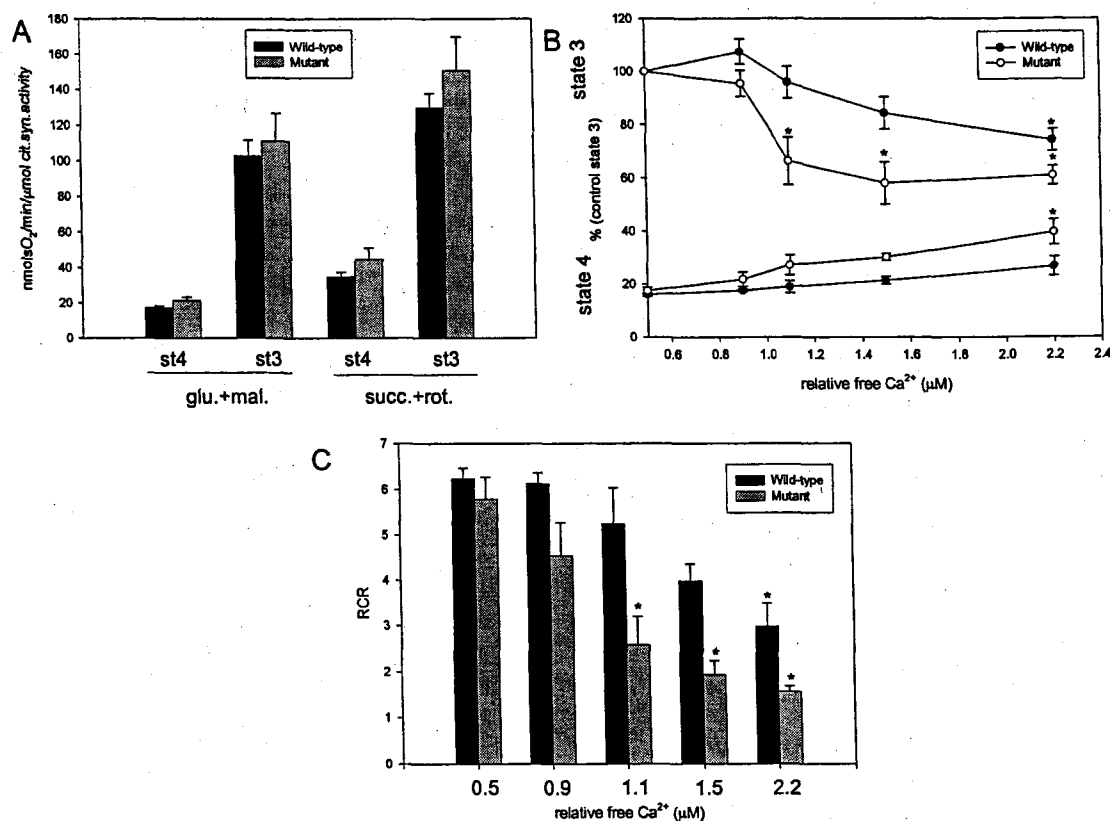


**Figure 1. Effects of Ca<sup>2+</sup> on respiration in mitochondria from STHdh<sup>Q7/Q7</sup> (wild-type) and STHdh<sup>Q111/Q111</sup> (mutant) cells.** **A**, State 4 (st4) and state 3 (st3) respiration rates measured in crude mitochondrial preparations in EGTA based respiration buffer. Crude mitochondria from wild-type and mutant cells were incubated with either glutamate plus malate (glu.+mal.) or succinate with rotenone (succ.+rot.) as respiratory substrates and respiration rates were determined as described under "Materials and Methods". Rates were normalized to citrate-synthase activity measured in the same samples. No significant differences were observed. **B**, Respiration rates measured in the presence of increasing free Ca<sup>2+</sup> concentrations. Crude mitochondria were resuspended in Ca-EGTA buffers with the indicated free Ca<sup>2+</sup> concentrations and state 4 and state 3 rates were determined as described in "Materials and Methods". Glutamate plus malate was used as the respiratory substrate. Results are expressed as percentage of the state 3 rates at 0 Ca<sup>2+</sup> for each of the cell lines. Significant decreases in state 3 rates at the low μM free Ca<sup>2+</sup> concentrations were observed, with the decreases occurring at the lower Ca<sup>2+</sup> concentrations in mitochondria from the mutant cells compared to wild-type mitochondria. State 4 rates showed a trend towards increasing with increasing free Ca<sup>2+</sup> concentrations, with significance being reached only at the highest Ca<sup>2+</sup> concentration used in the mutant cells. **C**, Respiratory control ratios (RCRs) in the presence of different free Ca<sup>2+</sup> concentrations were calculated as ratios between state 3 and state 4 rates presented in (B). The decrease in RCR reached significance at lower Ca<sup>2+</sup> concentrations in mutant cells than in the wild-type group. All data are mean ± S.E. of 3-4 independent experiments. For statistical analyses ANOVA followed by the Tukey post test (\*, p<0.05) was used.

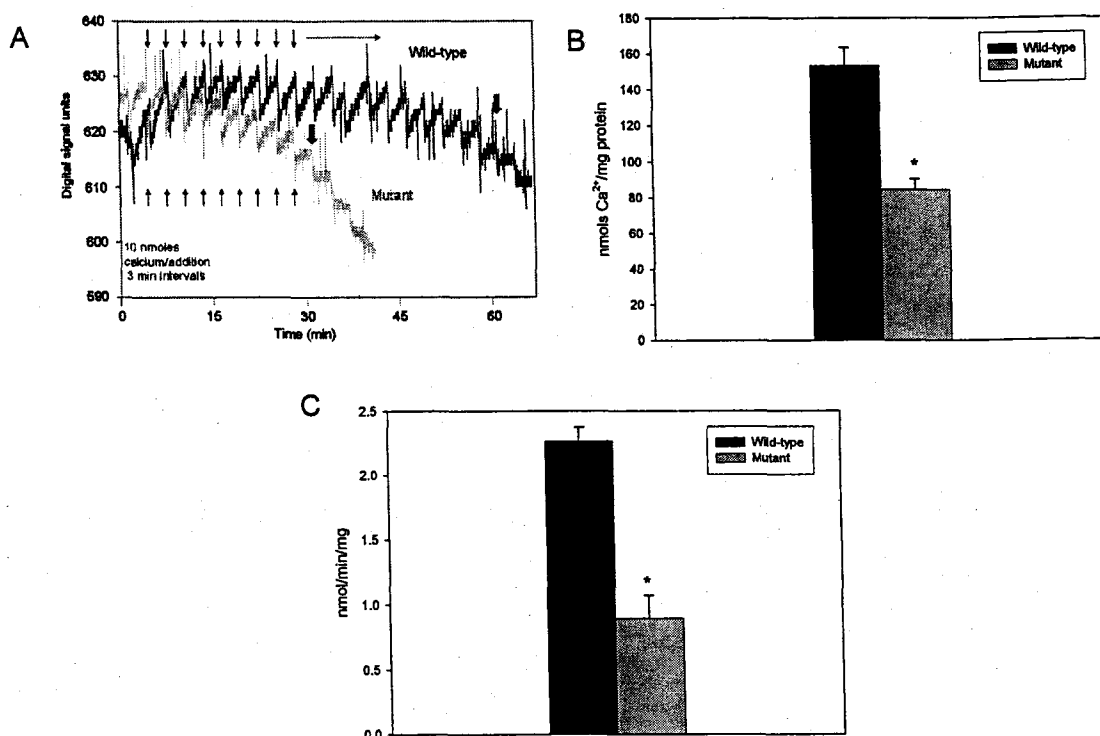
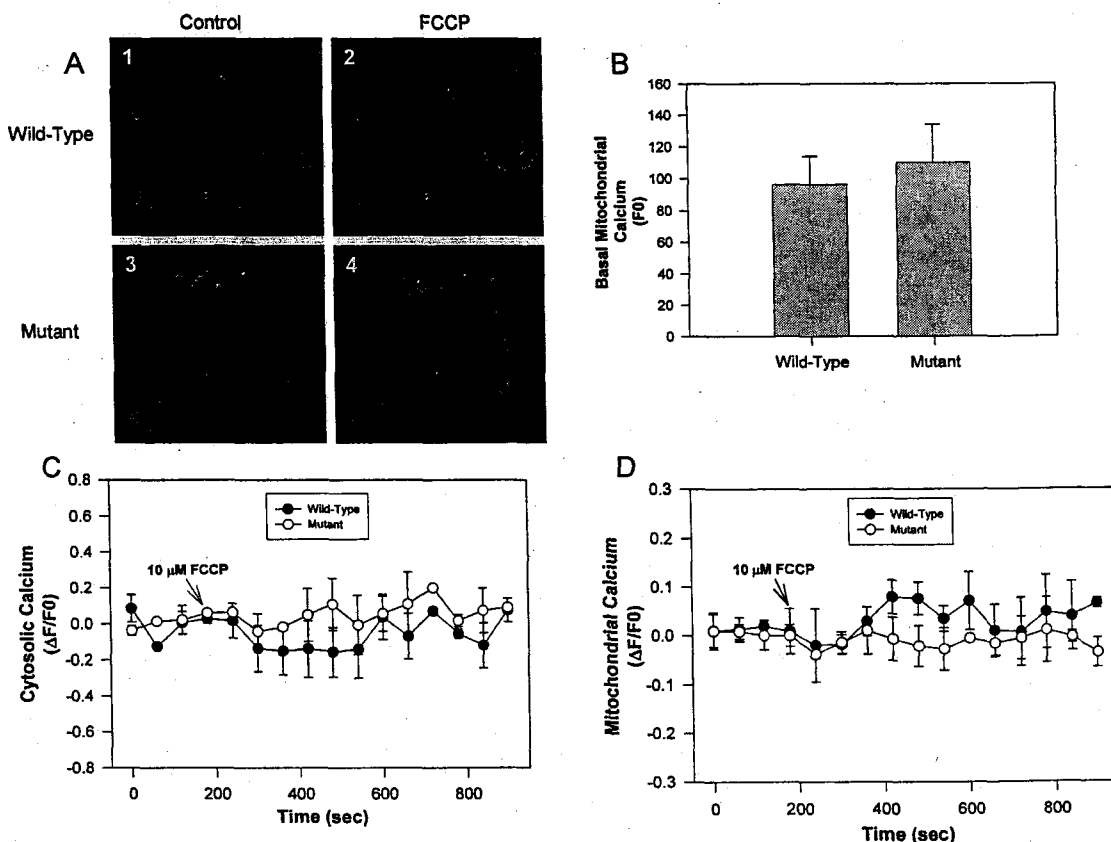
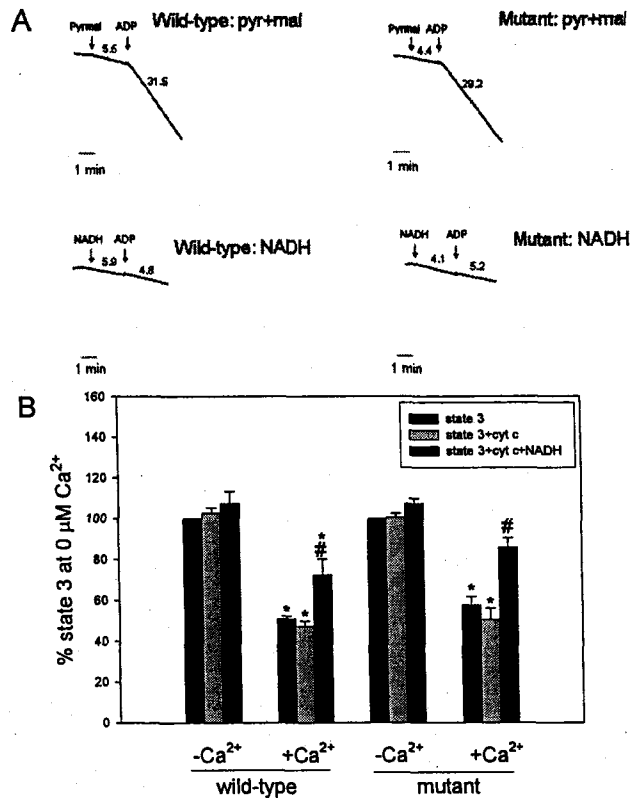


Figure 2.  $\text{Ca}^{2+}$  uptake capacity measured in mitochondria from  $\text{STHdh}^{\text{Q7/Q7}}$  (wild-type) and  $\text{STHdh}^{\text{Q111/Q111}}$  (mutant) cells. A, Representative traces of  $\text{Ca}^{2+}$  electrode recordings ( $\text{Ca}^{2+}$  uptake is reflected by an upward deflection of the trace). Small arrows are indicating  $\text{Ca}^{2+}$  additions. Large arrows indicate the last pulses included in the calculations. B,  $\text{Ca}^{2+}$  uptake capacities.  $\text{Ca}^{2+}$  uptake was measured using a  $\text{Ca}^{2+}$  sensitive electrode as described in "Materials and Methods". Crude mitochondria (1.5mg in 2ml) were given 10 nmol  $\text{Ca}^{2+}$  pulses every 3 min, until uptake could not be observed anymore.  $\text{Ca}^{2+}$  uptake capacities were calculated by multiplying the number of pulses by 10 nmol and normalizing it to mg protein. Significantly lower  $\text{Ca}^{2+}$  uptake capacity in mitochondria from mutant cells as compared to mitochondria from wild-type cells was observed. C, Initial  $\text{Ca}^{2+}$  uptake rates. Initial uptake rates were calculated by averaging rates of uptake after the second, third and fourth additions of  $\text{Ca}^{2+}$ . Initial  $\text{Ca}^{2+}$  uptake rates were significantly lower in mitochondria from mutant cells compared to wild-type cells. Data are mean  $\pm$  S.E. of 3 independent experiments. Student's t test (\*,  $p < 0.05$ ) was used for statistical analyses.



**Figure 3. Mitochondrial and cytosolic  $\text{Ca}^{2+}$  levels in  $\text{STHdh}^{\text{Q7/Q7}}$  (wild-type) and  $\text{STHdh}^{\text{Q111/Q111}}$  (mutant) cells.** **A**, Representative confocal photographs of wild-type and mutant cells labeled with Rhod-2 AM to determine mitochondrial  $\text{Ca}^{2+}$  levels. The pictures show the Rhod-2 AM staining of wild-type (1) and mutant cells (3) under control conditions and after treatment with 10  $\mu\text{M}$  FCCP for 30 min (see 2 and 4, respectively). **B**, Quantification of basal mitochondrial  $\text{Ca}^{2+}$  levels as fluorescence units. Quantification shows that mitochondrial  $\text{Ca}^{2+}$  levels in wild-type and mutant cells are not significantly different under resting conditions. Data are mean  $\pm$  S.E.,  $n = 6$  independent experiments. **C**, Wild-type and mutant cells were loaded with 5  $\mu\text{M}$  Fluo-3AM as an indicator of cytosolic  $\text{Ca}^{2+}$  levels. After 5 min of monitoring, 10  $\mu\text{M}$  FCCP was added to the cells in the recording chamber and the fluorescence intensity was monitored at 1 minute intervals for 30 min. The FCCP addition is indicated by the arrow in C. Data are mean  $\pm$  S.E.,  $n = 3$  independent experiments. **D**, Wild-type and mutant cells were loaded with Rhod-2 (10  $\mu\text{M}$ ) and the mitochondrial  $\text{Ca}^{2+}$  levels were measured before and after addition of FCCP. The FCCP addition is indicated by the arrow in D. FCCP addition did not cause any changes in mitochondrial  $\text{Ca}^{2+}$  levels. Data are mean  $\pm$  S.E.,  $n = 3$  independent experiments.



**Figure 4. Analysis of mitochondrial membrane integrity before and after  $Ca^{2+}$  addition to mitochondria from *STHdh*<sup>Q7/Q7</sup> (wild-type) and *STHdh*<sup>Q111/Q111</sup> (mutant) cells.** **A**, Integrity of the mitochondria in wild-type and mutant cells. Representative respiration traces are shown to demonstrate the inability of exogenous NADH (5 mM) (inner mitochondrial membrane impermeable) to act as a respiratory substrate in mitochondria from both wild-type and mutant cells. When pyruvate (10 mM) plus malate (10 mM) (pyr + mal) were used as respiratory substrates, a significant increase in O<sub>2</sub> consumption was observed upon ADP addition, while this was not the case when NADH was used. Numbers on the traces indicate O<sub>2</sub> consumption rates. **B**, Effects of cytochrome c (cyt c) or cytochrome c plus NADH (cyt c + NADH) on respiration before and after  $Ca^{2+}$  addition. Crude mitochondria were resuspended in respiration buffer without or with  $Ca^{2+}$  (0.6  $\mu$ M free  $Ca^{2+}$  as calculated by software) and respiration was measured as described in "Materials and Methods". Upon induction of state 3 for 2 min (state 3), cytochrome c was added and the rate measured for 2 min (state3+cyt c) and then NADH was added and the rate measured for additional 2 min (state3+cyt c+NADH). In the absence of  $Ca^{2+}$  neither cytochrome c nor cytochrome c plus NADH affected state 3 respiration. However, in the presence of  $Ca^{2+}$ , where significant decreases in state 3 rates were observed, cytochrome c plus NADH addition significantly increased respiration. Cytochrome c alone did not affect state 3 rates in the presence of  $Ca^{2+}$ . Data are mean $\pm$ S.E., n=4 independent experiments. For statistical analyses, we used ANOVA with Tukey post-test (\*, p<0.05, compared to state 3 -  $Ca^{2+}$ ; #, p<0.05, compared to state 3 +  $Ca^{2+}$ ).

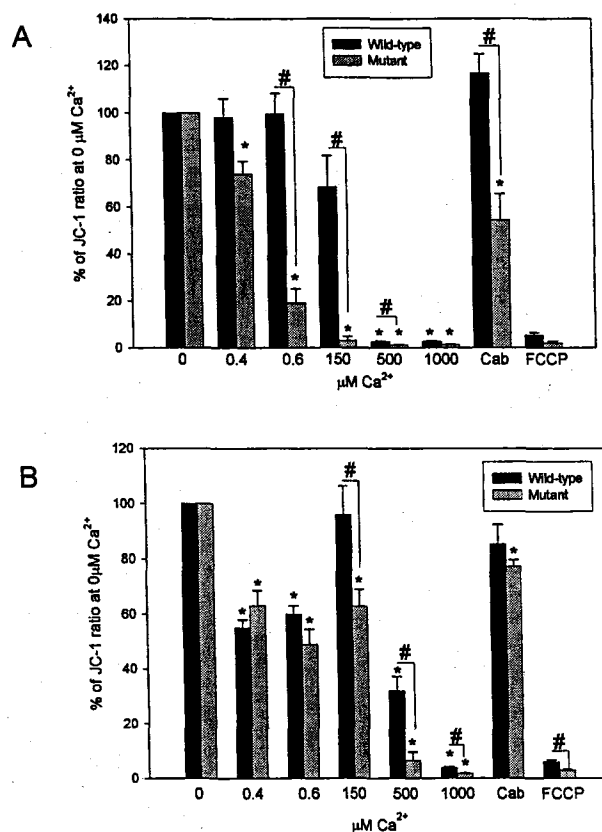
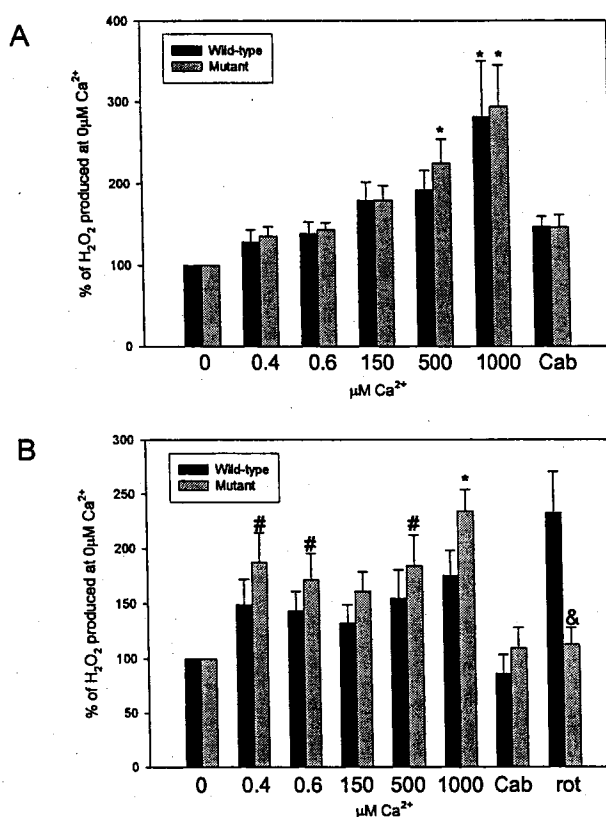


Figure 5. Differential effects of  $\text{Ca}^{2+}$  on mitochondrial membrane potential ( $\Delta\Psi_m$ ) in state 4 and state 3 conditions in  $\text{STHdh}^{Q7/Q7}$  (wild-type) and  $\text{STHdh}^{Q111/Q111}$  (mutant) cells. **A**, Effects of  $\text{Ca}^{2+}$  on  $\Delta\Psi_m$  in state 4.  $\Delta\Psi_m$  was measured in crude mitochondrial preparations using JC-1 as described in "Materials and Methods". In mutant cells  $\Delta\Psi_m$  was significantly reduced by as little as  $0.4 \mu\text{M Ca}^{2+}$  (software calculated), while in wild-type only at  $500 \mu\text{M Ca}^{2+}$  was a decrease in  $\Delta\Psi_m$  observed. "Cab" indicates measurements done in  $\text{Ca}^{2+}$  uptake buffer (respiration buffer without EGTA). FCCP was used as the positive control to induce a maximal decrease in  $\Delta\Psi_m$ . Data are mean  $\pm$  S.E.,  $n=3$  independent experiments. **B**, Effects of  $\text{Ca}^{2+}$  on  $\Delta\Psi_m$  in state 3. The presence of ADP (state 3) resulted in an attenuation of the differences between wild-type and mutant observed in state 4 conditions. Data are mean  $\pm$  S.E.,  $n=5$  independent experiments. For statistical analyses, we used ANOVA followed by Tukey post test (\*,  $p<0.05$ , compared to  $0 \mu\text{M Ca}^{2+}$ ) for each of the cell lines, and Student's  $t$  test (#,  $p<0.05$ ) to compare  $\Delta\Psi_m$  between the two cell lines at the different data points. Due to unequal variances, Welch correction applied for comparison between  $150 \mu\text{M}$  points in state 4.



**Figure 6. Effects of Ca<sup>2+</sup> on H<sub>2</sub>O<sub>2</sub> production in mitochondria from STHdh<sup>Q7/Q7</sup> (wild-type) and STHdh<sup>Q111/Q111</sup> (mutant) cells.** **A**, H<sub>2</sub>O<sub>2</sub> production in state 4. H<sub>2</sub>O<sub>2</sub> production was evaluated using the Amplex Red assay as described in "Materials and Methods". Ca<sup>2+</sup> induced increases in H<sub>2</sub>O<sub>2</sub> production and significance was reached at 1000 μM Ca<sup>2+</sup> in wild-type and at 500, 1000 μM Ca<sup>2+</sup> in mutant. "Cab" indicates measurements done in Ca<sup>2+</sup> uptake buffer (respiration buffer without EGTA). Results are mean ± S.E., n = 5 independent experiments. Statistical analyses were done using ANOVA followed by Tukey post-test (\*, p < 0.05, compared to 0 μM Ca<sup>2+</sup> for each cell line). **B**, H<sub>2</sub>O<sub>2</sub> production in state 3. Ca<sup>2+</sup> induced increases in H<sub>2</sub>O<sub>2</sub> production, and significance was reached only in mutant cells at 1000 μM Ca<sup>2+</sup>. When compared to wild-type cells, H<sub>2</sub>O<sub>2</sub> production upon Ca<sup>2+</sup> treatment was trending higher in mutant cells, reaching significance at 0.4, 0.6 and 500 μM Ca<sup>2+</sup> points when a paired t test analysis was done. Rotenone (Rot) addition was used in the assay as a positive control. Interestingly, in mutant cells H<sub>2</sub>O<sub>2</sub> production was significantly lower upon rotenone treatment compared to wild-type. Results are mean ± S.E., n = 4 independent experiments. Statistical analyses were done using ANOVA followed by Tukey post-test (\*, p < 0.05, compared to 0 μM Ca<sup>2+</sup> for each cell line), paired t test (#, p < 0.05) to compare the two cell lines at different data points, and Student's t test (&, p < 0.05) for rotenone treatment groups.



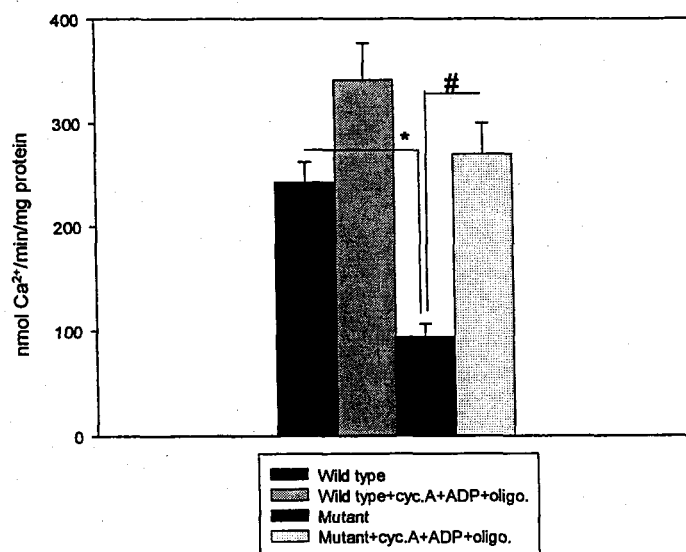
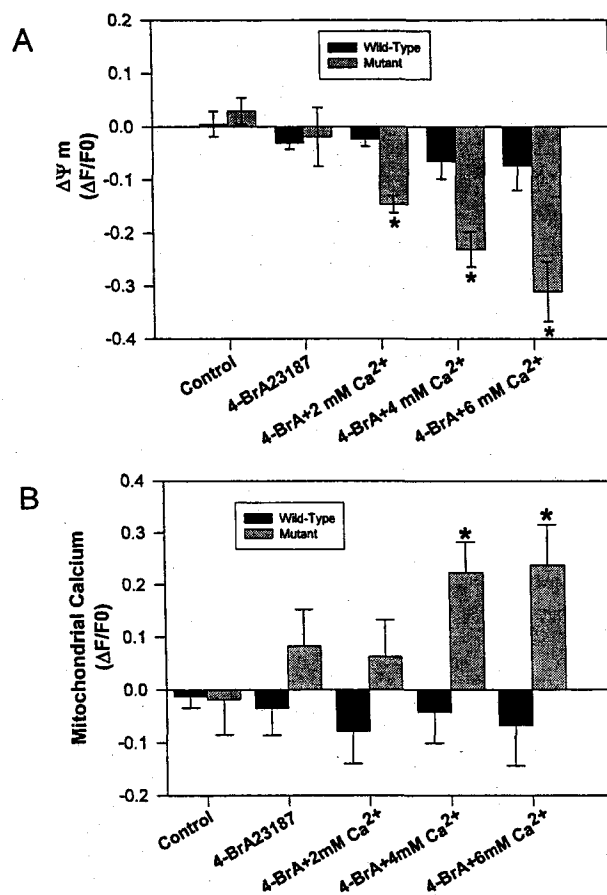


Figure 7. Effects of permeability transition pore (PTP) inhibitors on mitochondrial  $\text{Ca}^{2+}$  uptake capacity in  $\text{STHdh}^{Q7/Q7}$  (wild-type) and  $\text{STHdh}^{Q111/Q111}$  (mutant) cells. Mitochondrial  $\text{Ca}^{2+}$  uptake was measured as described in "Materials and Methods". A combination of cyclosporine A plus ADP plus oligomycin was used to inhibit PTP and was added to the mitochondrial suspension (1mg protein in 2ml volume) before  $\text{Ca}^{2+}$  additions. Additions of 20 nmols, 40 nmols, or 80 nmols  $\text{Ca}^{2+}$  were used in separate experiments but the regimen of  $\text{Ca}^{2+}$  additions was always the same for both cell types in a given experiment. Our results indicate that PTP inhibitors addition caused an increase in  $\text{Ca}^{2+}$  uptake capacity and this was significant for the mutant cells but not for the wild-type cells. In the absence of PTP inhibitors, mutant cells had a significantly decreased  $\text{Ca}^{2+}$  uptake capacity compared to the wild-type cells. In the presence of cyclosporine A plus ADP plus oligomycin the difference between wild-type and mutant was no longer significant. Data are mean  $\pm$  S.E.,  $n = 5 - 9$  independent measurements per group. Statistical analysis was done using ANOVA followed by Tukey post-test (\*, #,  $p < 0.05$ ).



**Figure 8. Effects of  $Ca^{2+}$  on  $\Delta\Psi_m$  and mitochondrial  $Ca^{2+}$  accumulation in STHdh<sup>Q7/Q7</sup> (wild-type) and STHdh<sup>Q111/Q111</sup> (mutant) cells in situ.** **A**, Wild-type and mutant cells were loaded with CMH2TMRos (200 nM) to measure changes in  $\Delta\Psi_m$ . Measurements were recorded at 1 min intervals and are shown as the  $\Delta F/F_0$  ratio. Wild-type (black bars) and mutant (gray bars) cells were exposed to 1 nM 4-BrA23187 in the presence of increasing  $Ca^{2+}$  concentrations. Quantification of mitochondrial membrane potential fluorescence, as relative units, shows significantly reduced  $\Delta\Psi_m$  in mutant cells pretreated with 4-BrA23187 at each  $Ca^{2+}$  concentration used in comparison to wild-type cells (\*,  $p < 0.05$ ;  $n=3$ ). Data are mean  $\pm$  S.E.  $n=3$  separate experiments, (\*  $p < 0.05$  by non-paired Student's *t*-test). **B**, Wild-type and mutant cells were loaded with Rhod-2 (10  $\mu$ M) and mitochondrial  $Ca^{2+}$  changes were measured in wild-type (black bars), and mutant cells (gray bars) exposed to 1 nM 4-BrA23187 in the presence of increasing  $Ca^{2+}$  concentrations. Addition of 1 nM 4-BrA23187 plus 4 mM  $CaCl_2$  induced a significant increase in the mitochondrial  $Ca^{2+}$  in mutant cells (\*,  $p < 0.05$ ;  $n=3$ ) (gray bars) in comparison to wild-type cells (black bars). Data are mean  $\pm$  S.E.  $n=3$  independent experiments, (\*  $p < 0.05$  by non-paired Student's *t*-test).

## CONCLUSIONS

There are numerous findings indicating that there is mitochondrial dysfunction in HD. In this dissertation, we analyzed the effects of mutant huntingtin on mitochondria in a genetically accurate cellular model of HD. In accordance with previous findings, we focused on the analyses of mutant huntingtin effects on the mitochondrial electron transport chain and mutant huntingtin effects on mitochondrial  $\text{Ca}^{2+}$  handling.

In order to determine the effects of mutant huntingtin on the complexes of the mitochondrial electron transport chain, we measured complex I, II, III and IV activities and determined their metabolic thresholds and spare capacities. According to our results, we concluded that mutant huntingtin does not affect the complexes of the electron transport chain. Our results indicate that impairments of the electron transport chain occur later in HD pathogenesis. Our findings are in agreement with a previous study showing that activities of electron transport chain complexes were not affected in presymptomatic and grade 1 (early stage) HD patients (96). The impairments of mitochondrial complexes II, III and IV found in the striatum of late stage HD patients could be the consequence of the oxidative stress that was demonstrated in HD (69,97,98). Further, gliosis was observed in both HD brains and transgenic HD mouse models (2,55), and activities of mitochondrial enzymes can vary among different cell types (99). Therefore, it is possible that the loss of neurons and increase in the number of glial cells could contribute to the observed reduction in mitochondrial complex activities in the striatum of late stage HD patients. It was reported, recently, that the onset of cell death in

primary embryonic striatal neurons expressing truncated mutant huntingtin (Htt171-82Q) coincides with a decrease in the expression of complex II catalytic subunits but not some other mitochondrial enzymes (complex V, complex IV) (100). Overexpression of complex II catalytic subunits, in this model, attenuated the execution phase of cell death (100). This finding also indicates that the complex II defect occurs in the later phases of HD pathogenesis.

We also analyzed mitochondrial  $\text{Ca}^{2+}$  handling. Our results strongly suggested that there is impaired mitochondrial  $\text{Ca}^{2+}$  handling in the mutant huntingtin expressing striatal cells. This is in agreement with several previous reports. Panov et. al. reported reduced  $\text{Ca}^{2+}$  uptake capacity in brain mitochondria from full-length mutant huntingtin transgenic mice (YAC 72) and HD lymphoblasts (30). Increased mitochondrial swelling was reported in liver mitochondria from 150/150 HD knock-in mice (73). Recently, reduced mitochondrial  $\text{Ca}^{2+}$  uptake was reported in muscle mitochondria from R6/2 mice (74). Since, we and others have shown impaired mitochondrial  $\text{Ca}^{2+}$  handling in the several different HD models, this impairment seems to be a fundamental effect of the expression of mutant huntingtin.

Respiration rates were similar between wild-type and mutant when measured in isolated mitochondria in EGTA based respiration buffer. This indicated that there is no intrinsic impairment of oxidative-phosphorylation in the mutant cells. However, a previous study reported reduced ATP levels in the mutant mitochondria, in situ (48). According to our results, factors other than mitochondrial ATP production machinery are responsible for this defect.

The survival time of neurons exposed to continuous NMDA stimulation inversely correlates with mitochondrial  $\text{Ca}^{2+}$  accumulation (82). The inhibition of mitochondrial  $\text{Ca}^{2+}$  uptake before NMDA stimulation resulted in restoration of cytosolic  $[\text{Ca}^{2+}]$  upon discontinuation of NMDA stimulation (82). However, if mitochondria actively accumulated  $[\text{Ca}^{2+}]$ , delayed  $\text{Ca}^{2+}$  deregulation culminating in cell death occurred, even after discontinuation of NMDA stimulation. These findings strongly suggested an important role for mitochondrial  $\text{Ca}^{2+}$  in excitotoxicity. Several effects of mitochondrial  $\text{Ca}^{2+}$  loading have been described and have also been determined in this dissertation: decrease in ATP production, decrease in  $\Delta\Psi_m$ , increase in ROS and PTP opening. It is a subject of great debate as to which of these effects are crucial for excitotoxicity. It has been shown that prolonged (~10 minutes) glutamate stimulation leads to decreased mitochondrial ATP production (78). Decreased mitochondrial ATP production leads to cellular ATP depletion likely causing further  $\text{Ca}^{2+}$  dysregulation by inhibiting ATP dependent  $\text{Ca}^{2+}$  extrusion ( $\text{Ca}^{2+}$ -ATP pump). Inhibition of the ATP dependent  $\text{Na}^+$ - $\text{K}^+$  pump would also contribute to excitotoxicity. Further, a strong correlation between the levels of cytosolic  $\text{Ca}^{2+}$  upon prolonged NMDA stimulation and mitochondrial depolarization was observed (77). This is believed to be either through the release of  $\text{Ca}^{2+}$  from mitochondria, inhibition of further  $\text{Ca}^{2+}$  uptake into mitochondria, or through ATP production inhibition. Interestingly, it was observed that glutamate causes markedly more mitochondrial depolarization in mature neurons compared with developing neurons (77). Increased ROS production has been described in excitotoxicity and it was suggested to mostly contribute to the late stages of excitotoxicity induced cell death (77). Opening of the PTP would lead to release of mitochondrial  $\text{Ca}^{2+}$ . Despite intensive research,

definitive evidence for PTP opening in excitotoxicity is lacking (77). This is mostly due to conflicting results about the protection provided by classic PTP inhibitors like cyclosporine A. But, it has been reported that brain mitochondria have altered response to conventional pore inhibitors (101-103).  $\text{Ca}^{2+}$  induced decreases in ATP production, decreases in  $\Delta\Psi_m$  and increases in ROS production that are evident during excitotoxicity, are often linked to PTP opening, though the final evidence is missing. The role of mitochondria in excitotoxicity is illustrated in figure 3.

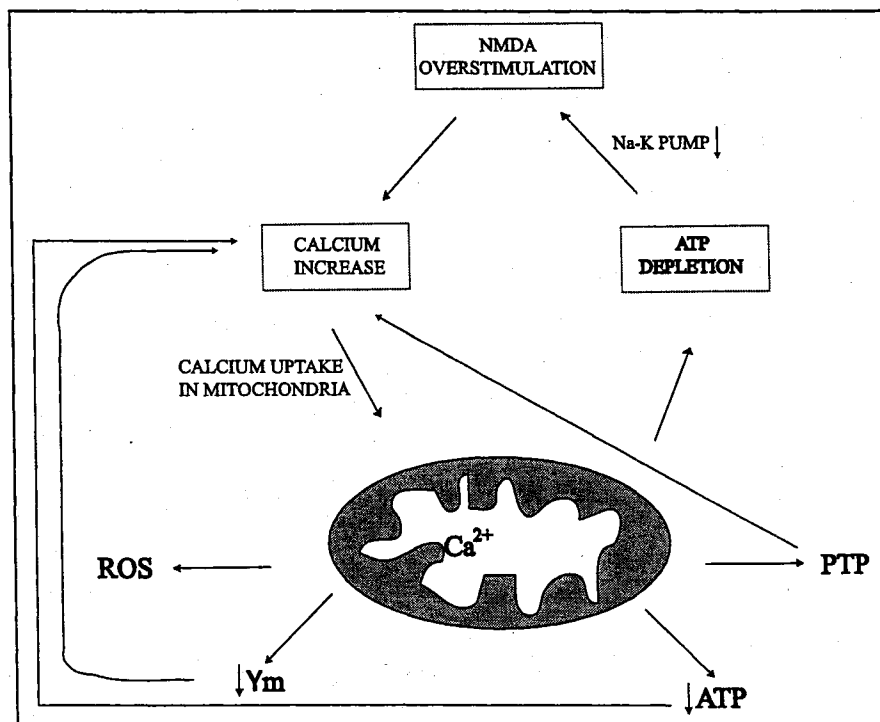


Figure 1. Role of Mitochondria in Excitotoxicity. Mitochondrial impairment leading to ATP depletion can initiate excitotoxicity by slowing the  $\text{Na}^+\text{-K}^+$  ATP dependent pump, causing plasma membrane depolarization and overstimulating NMDA receptors. Also, mitochondria play downstream, but crucial roles in excitotoxicity. Due to increases of cytosolic  $\text{Ca}^{2+}$  levels,  $\text{Ca}^{2+}$  enters mitochondria. Mitochondrial  $\text{Ca}^{2+}$  leads to a decrease of ATP production, mitochondrial depolarization (decrease of  $\Delta\Psi_m$ ), increase of ROS production and opening of PTP. Decreases in ATP, mitochondrial depolarization and PTP formation cause further  $\text{Ca}^{2+}$  deregulation culminating in cell death.

In our study, the effects of  $\text{Ca}^{2+}$  on the respiration of mitochondria isolated from mutant cells was significantly greater than the effects observed with mitochondria isolated from wild-type cells. Decreases in state 3 respiration could be caused by the collapse of  $\Delta\Psi_m$  due to  $\text{Ca}^{2+}$  induced PTP opening. We determined that the decrease in respiration was associated with increases in mitochondrial membrane permeability, but not substantial loss of cytochrome c. Therefore, the differences in respiration could be caused by increased sensitivity of mutant mitochondria to  $\text{Ca}^{2+}$  induced PTP opening. However, the decreases in respiration did not fully follow the decreases in  $\Delta\Psi_m$  (in state 4 or state 3). This would suggest a different major mechanism for the  $\text{Ca}^{2+}$  induced decrease in state 3 respiration. As suggested earlier,  $\text{Ca}^{2+}$  entering mitochondrial matrix could induce slowing of ATP-synthase (for each  $\text{Ca}^{2+}$  that enters mitochondria two protons fail to enter via ATP-synthase) (77,104). In our study, in situ experiments revealed increased uptake of  $\text{Ca}^{2+}$  in mutant mitochondria when only moderate increases of cytosolic  $\text{Ca}^{2+}$  were induced (ionophore plus  $\text{Ca}^{2+}$  treatment that caused an increase in cytosolic  $\text{Ca}^{2+}$  that was approximately a three fold lower than that observed with thapsigargin). It is not clear, at present, if increased  $\text{Ca}^{2+}$  uptake can be observed in isolated mitochondria at low  $\mu\text{M}$   $[\text{Ca}^{2+}]$ , which would suggest impairment at the level of mitochondrial  $\text{Ca}^{2+}$  uptake. If this were the case, respiration differences could, also, be caused by increased  $\text{Ca}^{2+}$  uptake by the mutant mitochondria. Alternatively the increased mitochondrial  $\text{Ca}^{2+}$  uptake observed in situ, could be caused by a  $\text{Ca}^{2+}$  homeostasis defect elsewhere in the cell (possible at the ER). When measured in permeabilized cells and in the absence of EGTA, we observed significantly reduced respiration in mutant mitochondria. Increased  $\text{Ca}^{2+}$  uptake in mutant mitochondria in the presence of ER



together with their increased sensitivity to  $\text{Ca}^{2+}$  would be a potential explanation for this result. The possibility of increased mitochondrial  $\text{Ca}^{2+}$  uptake in situ should be addressed in the future studies.

In in vitro experiments, we observed significantly reduced  $\text{Ca}^{2+}$  uptake capacity in mutant mitochondria compared to wild type mitochondria. This indicates a change in the balance between  $\text{Ca}^{2+}$  uptake and  $\text{Ca}^{2+}$  release. It could be caused by a decreased threshold for PTP opening in the mutant mitochondria. But, it could also be the result of a decrease in  $\Delta\Psi\text{m}$  and therefore a decrease in voltage dependent  $\text{Ca}^{2+}$  uptake in mutant mitochondria.

The most striking impairment revealed in this study, was the significant reduction of  $\Delta\Psi\text{m}$  in mutant mitochondria at low  $\mu\text{M}$   $\text{Ca}^{2+}$  concentrations in the absence of ADP and also in situ. As  $\text{Ca}^{2+}$  itself would only cause a transient depolarization, decreases in  $\Delta\Psi\text{m}$  indicate collapse of the proton gradient across the inner mitochondrial membrane due to  $\text{Ca}^{2+}$  induced permeabilization. Interestingly however, a significant decrease in  $\Delta\Psi\text{m}$  in mutant mitochondria was observed at a lower  $[\text{Ca}^{2+}]$  ( $\sim 1 \mu\text{M}$ ) than ceasing of the  $\text{Ca}^{2+}$  uptake ( $\sim 40 \mu\text{M}$ ). This suggests that the decrease in  $\Delta\Psi\text{m}$  is likely the cause of the significantly reduced  $\text{Ca}^{2+}$  uptake capacity in mutant mitochondria. In wild-type mitochondria, however, the decrease in  $\text{Ca}^{2+}$  uptake more closely followed decrease in  $\Delta\Psi\text{m}$ . In agreement with these observations, in HD lymphoblasts, but not in control lymphoblasts, mitochondrial depolarization occurred prior to high conductance PTP opening (as measured by alkalization of the incubation medium) (105). It is, therefore, possible that different  $\text{Ca}^{2+}$  induced changes lead to mitochondrial depolarization in wild-type and mutant cells, in the absence of ADP.

Oxidative stress has been demonstrated in HD brain and HD models. Addition of recombinant polyQ to isolated liver mitochondria was shown to cause increases in ROS production (106). In the course of our experiments, we did not find differences in the ROS production that could account for the observed mitochondrial  $\text{Ca}^{2+}$  handling defects.  $\text{Ca}^{2+}$  induced increases in ROS production were observed, but they did not correlate with the observed differences in  $\Delta\Psi_m$ .

The attenuation of the observed differences in mitochondrial  $\text{Ca}^{2+}$  handling by ADP (stabilizes ANT in the PTP unfavorable conformation) alone or together with cyclosporine A and oligomycin (combinations that potently inhibit PTP in brain mitochondria) (107) would suggest a reduced threshold for PTP opening as the cause of impaired mitochondrial  $\text{Ca}^{2+}$  handling in the mutant cells. It has been described that PTP operates in two conductance states (108). The high conductance state PTP is associated with mitochondrial  $\text{Ca}^{2+}$  overload leading to the opening of pore with conductivity up to 1.5kDa that results in mitochondrial swelling and release of cytochrome c. The low conductance state PTP is described as up to a 300Da pore (permeable to ions like  $\text{Ca}^{2+}$ ,  $\text{H}^+$ ,  $\text{K}^+$ ) associated, by several studies, to mitochondrial depolarization without swelling or release of cytochrome c (102,108). Low conductance PTP has been suggested to operate transiently under physiological conditions, as a mitochondrial  $\text{Ca}^{2+}$  release mechanism (108). Since, in our study, mutant mitochondria had decreased  $\Delta\Psi_m$  at low  $\mu\text{M}$   $\text{Ca}^{2+}$ , we would argue that mutant mitochondria exhibited opening of the low conductance PTP. Further, no release of cytochrome c was observed (not shown), which would also support this hypothesis.

The results in this dissertation suggest that mutant huntingtin directly or indirectly impairs mitochondrial  $\text{Ca}^{2+}$  buffering. The proposed model for the mutant huntingtin caused mitochondrial  $\text{Ca}^{2+}$  handling defect is shown in figure 4. This study did not find evidence for  $\text{Ca}^{2+}$  independent impairment of mitochondria by mutant huntingtin. The impairment of mitochondrial  $\text{Ca}^{2+}$  buffering could be a contributing mechanism to HD pathogenesis.

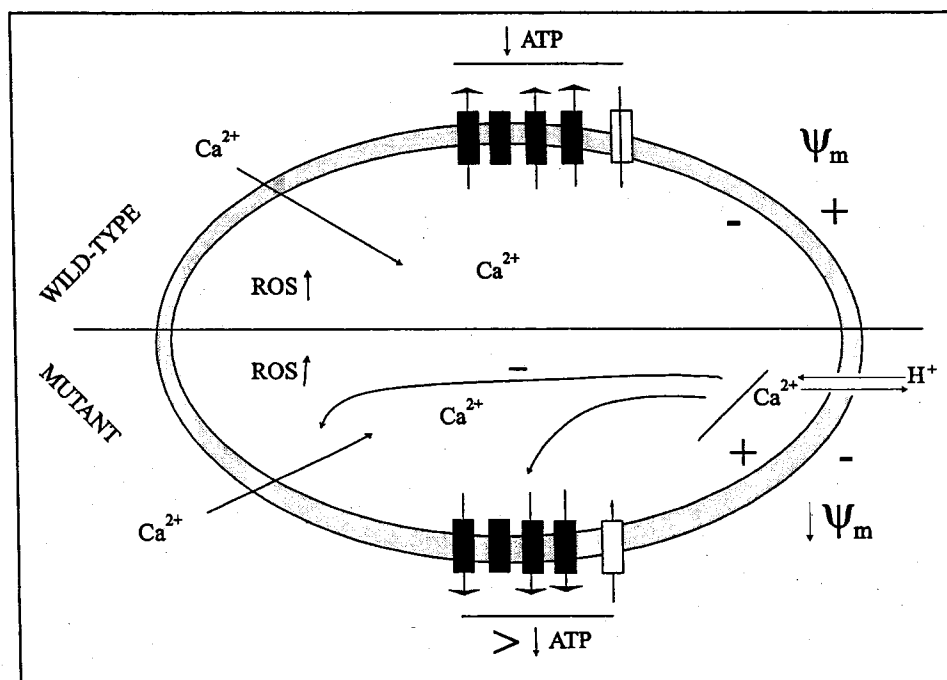


Figure 2. Proposed Model of the Mitochondrial  $\text{Ca}^{2+}$  Handling Defect in Mutant Huntingtin Expressing Cells. In the mutant mitochondria,  $\text{Ca}^{2+}$  that gets in stimulates prolonged opening of the low conductance PTP that results in  $\text{H}^+$  uptake and subsequently mitochondrial depolarization (decrease in  $\Delta\Psi_m$ ). Mitochondrial depolarization slows down the  $\text{Ca}^{2+}$  uptake causing an overall decrease in the  $\text{Ca}^{2+}$  uptake capacity. Also due to PTP opening, more  $\text{Ca}^{2+}$  is released, contributing further to the decrease in the  $\text{Ca}^{2+}$  uptake capacity. In both wild-type and mutant mitochondria,  $\text{Ca}^{2+}$  induces uncoupling of oxidative-phosphorylation (decrease of ATP producing (state 3) rate and to lesser extent increase of  $\text{H}^+$  leakage driven (state 4) rate). This results in decreases in ATP. The effects of  $\text{Ca}^{2+}$  on oxidative phosphorylation are more pronounced in mutant mitochondria due to PTP opening caused mitochondrial depolarization.  $\text{Ca}^{2+}$  induces increases in ROS production in both wild-type and mutant mitochondria. PTP opening did not affect ROS production in mutant mitochondria. Not shown on the model: Addition of ADP significantly protects against PTP opening in mutant mitochondria. In the presence of ADP, PTP opening and mitochondrial depolarization occur at much higher  $[\text{Ca}^{2+}]$  and more closely follow changes in the wild-type mitochondria.

Chronic administration of 3-NP (mitochondrial complex II inhibitor) to rodents and nonhuman primates causes pathology that resembles HD (51,52). 3-NP induced lesions can be attenuated by pretreatment with glutamate release inhibitor (109) or NMDA antagonist (MK-801) (110), suggesting that 3-NP causes excitotoxicity. The previous study showed that mutant huntingtin expressing cells (STHdh<sup>Q111/Q111</sup>) are more sensitive to 3-NP induced cell death than wild-type (STHdh<sup>Q7/Q7</sup>) cells (111). This was associated with greater mitochondrial depolarization in the mutant cells, and the cell death was attenuated by ruthenium red (Ca<sup>2+</sup>-uniporter inhibitor) (111). Findings from this dissertation strongly suggest that greater sensitivity of mutant cells to 3-NP is due to impaired mitochondrial Ca<sup>2+</sup> buffering in the mutant cells.

Future studies should be focused in two directions. Understanding the mechanism by which mutant huntingtin causes the mitochondrial Ca<sup>2+</sup> buffering defect and further understanding the significance of this defect in HD pathogenesis.

To understand the mechanism of the mitochondrial Ca<sup>2+</sup> buffering defect, one should take into consideration huntingtin localization in the cell. Since huntingtin associates with the outer mitochondrial membrane (73), its effects on mitochondria could be direct. This is strongly supported by the studies showing that recombinant polyQ, both without (fused to GST) or within huntingtin context (as part of huntingtin exon one) causes mitochondrial swelling at the lower Ca<sup>2+</sup> loads than control, when added to isolated liver mitochondria (72,73). Further, mutant huntingtin is also localized in the nucleus (95) and has been reported to affect transcription (15). Given that, it could affect mitochondrial function indirectly, through its nuclear toxicity, since the majority of mitochondrial proteins are nucleus encoded. Therefore, experiments should be designed

to further determine if the effects of mutant huntingtin on mitochondria are direct or indirect.

It has been shown that when mitochondria are incubated with trypsin, huntingtin disassociates from mitochondria (73). Trypsin did not affect integral outer mitochondrial membrane proteins such as VDAC (73). It would be useful to determine if pretreatment of mutant mitochondria with trypsin would attenuate the observed  $\text{Ca}^{2+}$  handling defects. The proper controls to determine the effects of trypsin on mitochondria should be included in the experiment.

As already described, ADP significantly attenuated  $\text{Ca}^{2+}$  induced decreases in  $\Delta\Psi_m$  in mutant mitochondria. Previously, it was demonstrated that mutant mitochondria have lower levels of both ADP and ATP (48). It was suggested that this is caused by impaired uptake of ADP in mitochondria (48). Functioning of ANT was not impaired and impaired signaling leading to ADP uptake was suggested as the cause of the defect (48). Cellular levels of ADP were higher in the mutant cells (48). It is, therefore, possible that mutant mitochondria have decreased thresholds for PTP opening due to lower content of adenine nucleotides. This is an appealing possibility and further research in this direction should be pursued. Interestingly the ATP/ADP ratio, as determined in human lymphoblasts, was inversely correlated to huntingtin CAG repeat length (both physiological and pathological range) (48). This suggested the possibility that huntingtin is involved in adenine nucleotides homeostasis.

In vitro studies showing that polyQ causes a reduced threshold for PTP opening in liver mitochondria suggested direct effects of polyQ on mitochondria (72,73). Therefore,

efforts should be put forth to analyze huntingtin interactions at the mitochondrial membrane.

Another line of research should go in the direction of further understanding of the significance of the mutant huntingtin induced mitochondrial  $\text{Ca}^{2+}$  handling defect. As we comprehensively described this defect in STHdh<sup>Q111/Q111</sup> cells, this cell line would be a good model for in situ studies. The primary neuronal cultures obtained from these mutant huntingtin knock-in mice should be used as well. Cells should be exposed to different schedules of glutamate treatments (single or repetitive, transient or prolonged) and the differences in cytosolic  $\text{Ca}^{2+}$  levels and mitochondrial functions (ATP production,  $\Delta\Psi_m$  and mitochondrial  $\text{Ca}^{2+}$  levels) should be analyzed at different time points. Survival and any other changes (morphology of primary neurons) should be monitored. Impaired  $\text{Ca}^{2+}$  homeostasis by mutant huntingtin has been observed at the level of the ER (29). Tang et.al. demonstrated that huntingtin associates with the inositol triphosphate receptor (Ip3R) that regulates  $\text{Ca}^{2+}$  release from the ER (29). Further, they demonstrated that mutant huntingtin but not wild-type stimulates activation of the Ip3R and release of  $\text{Ca}^{2+}$  from the ER. Given these findings, in situ experiments should also look for the changes in ER  $\text{Ca}^{2+}$  homeostasis.

Excitotoxicity has already been analyzed in some of the HD models. Full-length mutant huntingtin transgenic mice (YAC72) showed increased sensitivity to NMDA receptor induced excitotoxicity (86). However R6/2 mice were resistant to excitotoxicity (89), even though muscle mitochondria from R6/2 mice showed decreased  $\text{Ca}^{2+}$  uptake capacity (74). It was argued that this was due to reduced synaptic activity shown in these mice (112). In Q92 and Q111 knock-in mice, striatal mitochondria exhibited age-

dependent increases in resistance to  $\text{Ca}^{2+}$  induced depolarization, which could suggest activation of adaptation mechanisms (113). It was suggested that mitochondrial regeneration stimulated in stress conditions could be the mechanism of adaptation (113). It is therefore difficult to determine significance of excitotoxicity in vivo. Further characterization of other knock-in models (like 150/150) in regard to excitotoxicity would be of interest.

Mitochondrial  $\text{Ca}^{2+}$  buffering is important for spatio-temporal regulation of  $\text{Ca}^{2+}$  signaling. To our knowledge, no work has been done in analyzing possible perturbations of  $\text{Ca}^{2+}$  signal distribution in HD. Using  $\text{Ca}^{2+}$  imaging, it was discovered that mitochondria and the ER communicate through subsequent  $\text{Ca}^{2+}$  uptake and release that determines distribution and dynamics of  $\text{Ca}^{2+}$  signaling in the cell (38). It would be interesting to determine if  $\text{Ca}^{2+}$  signaling is affected in HD.

As already described in the introduction, HD is a complex neurodegenerative disease that likely involves several gained toxicities and some loss of normal huntingtin function. These effects could be parallel or consecutive or the combination of both. Revealing the schedule of events will be important for the development of successful therapies.

Mitochondrial trafficking impairment could work in parallel with mitochondrial defects to exacerbate neuronal sensitivity to glutamate. It was reported that huntingtin plays a role in axonal trafficking and that this function is impaired in HD (26). In that study, it was demonstrated that full-length mutant huntingtin causes impairment of mitochondrial trafficking in mammalian neurons both in culture and in vivo (26). Another study described impaired mitochondrial trafficking in cortical neurons



expressing either full-length or truncated mutant huntingtin and suggested that this is caused by mutant huntingtin aggregates causing mitochondria to accumulate adjacent to them and become immobilized (114). Impairment of mitochondrial trafficking would likely cause inadequate ATP supply in distal neuronal parts (dendrites and axons) what could additionally sensitize cells to excitotoxic insults.

Determination of consequent toxicities is crucial. As already mentioned, mitochondrial toxicity could be the consequence of mutant huntingtin induced transcriptional dysfunction. Histone deacetylase (HDAC) inhibitors, intended to balance decreases in histone acetylase activity (HAT) caused by mutant huntingtin, attenuated neurodegeneration in a *Drosophila* model of HD (115) and attenuated symptoms in R6/2 mice (116). These drugs are now entering clinical trials. It would be interesting to determine if HDAC therapy can attenuate mitochondrial defects.

Due to the importance of cellular  $\text{Ca}^{2+}$  homeostasis, mitochondrial  $\text{Ca}^{2+}$  buffering impairment likely plays important role in HD pathogenesis. Therefore, the development of treatments for this defect should be very beneficial. The most useful approach would be the tuning of the mitochondrial  $\text{Ca}^{2+}$  setpoint by inhibiting  $\text{Ca}^{2+}$  uptake and activating  $\text{Ca}^{2+}$  efflux pathways. Determination of the mechanism for this defect would provide additional solutions.

Since 1993, when it was discovered that HD is caused by the mutation in the huntingtin gene, remarkable progress has been made in understanding HD pathogenesis. We hope that the work presented in this dissertation provides a little contribution for further understanding of the disease and that the next thirteen years will bring successful HD therapeutics.

## LIST OF GENERAL REFERENCES

1. (1993) *Cell* **72**, 971-983
2. Vonsattel, J. P., and DiFiglia, M. (1998) *J Neuropathol Exp Neurol* **57**, 369-384
3. Hunter, J. M., Crouse, A. B., Lesort, M., Johnson, G. V., and Detloff, P. J. (2005) *J Neurosci Methods* **144**, 11-17
4. Kennedy, L., and Shelbourne, P. F. (2000) *Hum Mol Genet* **9**, 2539-2544
5. Kennedy, L., Evans, E., Chen, C. M., Craven, L., Detloff, P. J., Ennis, M., and Shelbourne, P. F. (2003) *Hum Mol Genet* **12**, 3359-3367
6. Huntington, G. (2003) *J Neuropsychiatry Clin Neurosci* **15**, 109-112
7. Nance, M. A., Mathias-Hagen, V., Breningstall, G., Wick, M. J., and McGlennen, R. C. (1999) *Neurology* **52**, 392-394
8. Nance, M. A., and Myers, R. H. (2001) *Ment Retard Dev Disabil Res Rev* **7**, 153-157
9. Katzung, B. G. (2000) *Basic and Clinical Pharmacology*, eight edition Ed., Appleton & Lange
10. DiFiglia, M., Sapp, E., Chase, K. O., Davies, S. W., Bates, G. P., Vonsattel, J. P., and Aronin, N. (1997) *Science* **277**, 1990-1993
11. Davies, S. W., Turmaine, M., Cozens, B. A., DiFiglia, M., Sharp, A. H., Ross, C. A., Scherzinger, E., Wanker, E. E., Mangiarini, L., and Bates, G. P. (1997) *Cell* **90**, 537-548
12. Hodgson, J. G., Agopyan, N., Gutekunst, C. A., Leavitt, B. R., LePiane, F., Singaraja, R., Smith, D. J., Bissada, N., McCutcheon, K., Nasir, J., Jamot, L., Li, X. J., Stevens, M. E., Rosemond, E., Roder, J. C., Phillips, A. G., Rubin, E. M., Hersch, S. M., and Hayden, M. R. (1999) *Neuron* **23**, 181-192
13. Schilling, G., Becher, M. W., Sharp, A. H., Jinnah, H. A., Duan, K., Kotzuc, J. A., Slunt, H. H., Ratovitski, T., Cooper, J. K., Jenkins, N. A., Copeland, N. G., Price, D. L., Ross, C. A., and Borchelt, D. R. (1999) *Hum Mol Genet* **8**, 397-407

14. Wheeler, V. C., White, J. K., Gutekunst, C. A., Vrbanac, V., Weaver, M., Li, X. J., Li, S. H., Yi, H., Vonsattel, J. P., Gusella, J. F., Hersch, S., Auerbach, W., Joyner, A. L., and MacDonald, M. E. (2000) *Hum Mol Genet* **9**, 503-513
15. Landles, C., and Bates, G. P. (2004) *EMBO Rep* **5**, 958-963
16. Valera, A. G., Diaz-Hernandez, M., Hernandez, F., Ortega, Z., and Lucas, J. J. (2005) *Neuroscientist* **11**, 583-594
17. Persichetti, F., Carlee, L., Faber, P. W., McNeil, S. M., Ambrose, C. M., Srinidhi, J., Anderson, M., Barnes, G. T., Gusella, J. F., and MacDonald, M. E. (1996) *Neurobiol Dis* **3**, 183-190
18. Mangiarini, L., Sathasivam, K., Seller, M., Cozens, B., Harper, A., Hetherington, C., Lawton, M., Trotter, Y., Lehrach, H., Davies, S. W., and Bates, G. P. (1996) *Cell* **87**, 493-506
19. Zeitlin, S., Liu, J. P., Chapman, D. L., Papaioannou, V. E., and Efstratiadis, A. (1995) *Nat Genet* **11**, 155-163
20. Nasir, J., Floresco, S. B., O'Kusky, J. R., Diewert, V. M., Richman, J. M., Zeisler, J., Borowski, A., Marth, J. D., Phillips, A. G., and Hayden, M. R. (1995) *Cell* **81**, 811-823
21. Duyao, M. P., Auerbach, A. B., Ryan, A., Persichetti, F., Barnes, G. T., McNeil, S. M., Ge, P., Vonsattel, J. P., Gusella, J. F., Joyner, A. L., and et al. (1995) *Science* **269**, 407-410
22. White, J. K., Auerbach, W., Duyao, M. P., Vonsattel, J. P., Gusella, J. F., Joyner, A. L., and MacDonald, M. E. (1997) *Nat Genet* **17**, 404-410
23. Cattaneo, E., Rigamonti, D., Goffredo, D., Zuccato, C., Squitieri, F., and Sipione, S. (2001) *Trends Neurosci* **24**, 182-188
24. Dragatsis, I., Levine, M. S., and Zeitlin, S. (2000) *Nat Genet* **26**, 300-306
25. Gauthier, L. R., Charrin, B. C., Borrell-Pages, M., Dompierre, J. P., Rangone, H., Cordelieres, F. P., De Mey, J., MacDonald, M. E., Lessmann, V., Humbert, S., and Saudou, F. (2004) *Cell* **118**, 127-138
26. Trushina, E., Dyer, R. B., Badger, J. D., 2nd, Ure, D., Eide, L., Tran, D. D., Vrieze, B. T., Legendre-Guillemain, V., McPherson, P. S., Mandavilli, B. S., Van Houten, B., Zeitlin, S., McNiven, M., Aebersold, R., Hayden, M., Parisi, J. E., Seeborg, E., Dragatsis, I., Doyle, K., Bender, A., Chacko, C., and McMurray, C. T. (2004) *Mol Cell Biol* **24**, 8195-8209

27. Zuccato, C., Tartari, M., Crotti, A., Goffredo, D., Valenza, M., Conti, L., Cataudella, T., Leavitt, B. R., Hayden, M. R., Timmusk, T., Rigamonti, D., and Cattaneo, E. (2003) *Nat Genet* **35**, 76-83
28. Valenza, M., Rigamonti, D., Goffredo, D., Zuccato, C., Fenu, S., Jamot, L., Strand, A., Tarditi, A., Woodman, B., Racchi, M., Mariotti, C., Di Donato, S., Corsini, A., Bates, G., Pruss, R., Olson, J. M., Sipione, S., Tartari, M., and Cattaneo, E. (2005) *J Neurosci* **25**, 9932-9939
29. Tang, T. S., Tu, H., Chan, E. Y., Maximov, A., Wang, Z., Wellington, C. L., Hayden, M. R., and Bezprozvanny, I. (2003) *Neuron* **39**, 227-239
30. Panov, A. V., Gutekunst, C. A., Leavitt, B. R., Hayden, M. R., Burke, J. R., Strittmatter, W. J., and Greenamyre, J. T. (2002) *Nat Neurosci* **5**, 731-736
31. Mann, V. M., Cooper, J. M., Javoy-Agid, F., Agid, Y., Jenner, P., and Schapira, A. H. (1990) *Lancet* **336**, 749
32. Gu, M., Gash, M. T., Mann, V. M., Javoy-Agid, F., Cooper, J. M., and Schapira, A. H. (1996) *Ann Neurol* **39**, 385-389
33. Browne, S. E., Bowling, A. C., MacGarvey, U., Baik, M. J., Berger, S. C., Muqit, M. M., Bird, E. D., and Beal, M. F. (1997) *Ann Neurol* **41**, 646-653
34. Wallace, D. C. (2005) *Annu Rev Genet* **39**, 359-407
35. Nicholls, D. G., and Ferguson, S. J. (2001) *Bioenergetics3*, Academic Press
36. Chalmers, S., and Nicholls, D. G. (2003) *J Biol Chem* **278**, 19062-19070
37. Forte, M., and Bernardi, P. (2005) *J Bioenerg Biomembr* **37**, 121-128
38. Rizzuto, R., Bernardi, P., and Pozzan, T. (2000) *J Physiol* **529 Pt 1**, 37-47
39. Kuhl, D. E., Phelps, M. E., Markham, C. H., Metter, E. J., Riege, W. H., and Winter, J. (1982) *Ann Neurol* **12**, 425-434
40. Kuhl, D. E., Metter, E. J., Riege, W. H., and Markham, C. H. (1984) *Ann Neurol* **15 Suppl**, S119-125
41. Kuhl, D. E., Markham, C. H., Metter, E. J., Riege, W. H., Phelps, M. E., and Mazziotta, J. C. (1985) *Res Publ Assoc Res Nerv Ment Dis* **63**, 199-209
42. Berent, S., Giordani, B., Lehtinen, S., Markel, D., Penney, J. B., Buchtel, H. A., Starosta-Rubinstein, S., Hichwa, R., and Young, A. B. (1988) *Ann Neurol* **23**, 541-546

43. Mazziotta, J. C., Phelps, M. E., Pahl, J. J., Huang, S. C., Baxter, L. R., Riege, W. H., Hoffman, J. M., Kuhl, D. E., Lanto, A. B., Wapenski, J. A., and et al. (1987) *N Engl J Med* **316**, 357-362
44. Kuwert, T., Lange, H. W., Boecker, H., Titz, H., Herzog, H., Aulich, A., Wang, B. C., Nayak, U., and Feinendegen, L. E. (1993) *J Neurol* **241**, 31-36
45. Grafton, S. T., Mazziotta, J. C., Pahl, J. J., St George-Hyslop, P., Haines, J. L., Gusella, J., Hoffman, J. M., Baxter, L. R., and Phelps, M. E. (1992) *Arch Neurol* **49**, 1161-1167
46. Jenkins, B. G., Koroshetz, W. J., Beal, M. F., and Rosen, B. R. (1993) *Neurology* **43**, 2689-2695
47. Jenkins, B. G., Rosas, H. D., Chen, Y. C., Makabe, T., Myers, R., MacDonald, M., Rosen, B. R., Beal, M. F., and Koroshetz, W. J. (1998) *Neurology* **50**, 1357-1365
48. Seong, I. S., Ivanova, E., Lee, J. M., Choo, Y. S., Fossale, E., Anderson, M., Gusella, J. F., Laramie, J. M., Myers, R. H., Lesort, M., and MacDonald, M. E. (2005) *Hum Mol Genet* **14**, 2871-2880
49. Parker, W. D., Jr., Boyson, S. J., Luder, A. S., and Parks, J. K. (1990) *Neurology* **40**, 1231-1234
50. Arenas, J., Campos, Y., Ribacoba, R., Martin, M. A., Rubio, J. C., Ablanedo, P., and Cabello, A. (1998) *Ann Neurol* **43**, 397-400
51. Beal, M. F., Brouillet, E., Jenkins, B. G., Ferrante, R. J., Kowall, N. W., Miller, J. M., Storey, E., Srivastava, R., Rosen, B. R., and Hyman, B. T. (1993) *J Neurosci* **13**, 4181-4192
52. Brouillet, E., Hantraye, P., Ferrante, R. J., Dolan, R., Leroy-Willig, A., Kowall, N. W., and Beal, M. F. (1995) *Proc Natl Acad Sci U S A* **92**, 7105-7109
53. Browne, S. E., and Beal, M. F. (2004) *Neurochem Res* **29**, 531-546
54. Brouillet, E., Guyot, M. C., Mittoux, V., Altairac, S., Conde, F., Palfi, S., and Hantraye, P. (1998) *J Neurochem* **70**, 794-805
55. Lin, C. H., Tallaksen-Greene, S., Chien, W. M., Cearley, J. A., Jackson, W. S., Crouse, A. B., Ren, S., Li, X. J., Albin, R. L., and Detloff, P. J. (2001) *Hum Mol Genet* **10**, 137-144
56. Carter, R. J., Lione, L. A., Humby, T., Mangiarini, L., Mahal, A., Bates, G. P., Dunnett, S. B., and Morton, A. J. (1999) *J Neurosci* **19**, 3248-3257

57. Bates, G. P., Mangiarini, L., Mahal, A., and Davies, S. W. (1997) *Hum Mol Genet* **6**, 1633-1637
58. Turmaine, M., Raza, A., Mahal, A., Mangiarini, L., Bates, G. P., and Davies, S. W. (2000) *Proc Natl Acad Sci U S A* **97**, 8093-8097
59. Tabrizi, S. J., Workman, J., Hart, P. E., Mangiarini, L., Mahal, A., Bates, G., Cooper, J. M., and Schapira, A. H. (2000) *Ann Neurol* **47**, 80-86
60. Jenkins, B. G., Klivenyi, P., Kustermann, E., Andreassen, O. A., Ferrante, R. J., Rosen, B. R., and Beal, M. F. (2000) *J Neurochem* **74**, 2108-2119
61. Truckenmiller, M. E., Namboodiri, M. A., Brownstein, M. J., and Neale, J. H. (1985) *J Neurochem* **45**, 1658-1662
62. Bates, T. E., Strangward, M., Keelan, J., Davey, G. P., Munro, P. M., and Clark, J. B. (1996) *Neuroreport* **7**, 1397-1400
63. Andreassen, O. A., Dedeoglu, A., Ferrante, R. J., Jenkins, B. G., Ferrante, K. L., Thomas, M., Friedlich, A., Browne, S. E., Schilling, G., Borchelt, D. R., Hersch, S. M., Ross, C. A., and Beal, M. F. (2001) *Neurobiol Dis* **8**, 479-491
64. Dedeoglu, A., Kubilus, J. K., Yang, L., Ferrante, K. L., Hersch, S. M., Beal, M. F., and Ferrante, R. J. (2003) *J Neurochem* **85**, 1359-1367
65. Wyss, M., and Kaddurah-Daouk, R. (2000) *Physiol Rev* **80**, 1107-1213
66. Adam-Vizi, V. (2005) *Antioxid Redox Signal* **7**, 1140-1149
67. Brookes, P. S., Yoon, Y., Robotham, J. L., Anders, M. W., and Sheu, S. S. (2004) *Am J Physiol Cell Physiol* **287**, C817-833
68. Tabrizi, S. J., Cleeter, M. W., Xuereb, J., Taanman, J. W., Cooper, J. M., and Schapira, A. H. (1999) *Ann Neurol* **45**, 25-32
69. Perez-Severiano, F., Rios, C., and Segovia, J. (2000) *Brain Res* **862**, 234-237
70. Choo, Y. S., Mao, Z., Johnson, G. V., and Lesort, M. (2005) *Neurosci Lett* **386**, 63-68
71. Panov, A., Obertone, T., Bennett-Desmelik, J., and Greenamyre, J. T. (1999) *Ann NY Acad Sci* **893**, 365-368
72. Panov, A. V., Burke, J. R., Strittmatter, W. J., and Greenamyre, J. T. (2003) *Arch Biochem Biophys* **410**, 1-6

73. Choo, Y. S., Johnson, G. V., MacDonald, M., Detloff, P. J., and Lesort, M. (2004) *Hum Mol Genet* **13**, 1407-1420
74. Gizatullina, Z. Z., Lindenberg, K. S., Harjes, P., Chen, Y., Kosinski, C. M., Landwehrmeyer, B. G., Ludolph, A. C., Striggow, F., Zierz, S., and Gellerich, F. N. (2006) *Ann Neurol* **59**, 407-411
75. Leegwater-Kim, J., and Cha, J. H. (2004) *NeuroRx* **1**, 128-138
76. Nicholls, D. G. (2004) *Curr Mol Med* **4**, 149-177
77. Khodorov, B. (2004) *Prog Biophys Mol Biol* **86**, 279-351
78. Kushnareva, Y. E., Wiley, S. E., Ward, M. W., Andreyev, A. Y., and Murphy, A. N. (2005) *J Biol Chem* **280**, 28894-28902
79. Henneberry, R. C., Novelli, A., Cox, J. A., and Lysko, P. G. (1989) *Ann N Y Acad Sci* **568**, 225-233
80. Novelli, A., Reilly, J. A., Lysko, P. G., and Henneberry, R. C. (1988) *Brain Res* **451**, 205-212
81. Zeevalk, G. D., and Nicklas, W. J. (1991) *J Pharmacol Exp Ther* **257**, 870-878
82. Nicholls, D. G., Vesce, S., Kirk, L., and Chalmers, S. (2003) *Cell Calcium* **34**, 407-424
83. Dure, L. S. t., Young, A. B., and Penney, J. B. (1991) *Ann Neurol* **30**, 785-793
84. Albin, R. L., Young, A. B., Penney, J. B., Handelin, B., Balfour, R., Anderson, K. D., Markel, D. S., Tourtellotte, W. W., and Reiner, A. (1990) *N Engl J Med* **322**, 1293-1298
85. Ferrante, R. J., Kowall, N. W., Cipolloni, P. B., Storey, E., and Beal, M. F. (1993) *Exp Neurol* **119**, 46-71
86. Zeron, M. M., Hansson, O., Chen, N., Wellington, C. L., Leavitt, B. R., Brundin, P., Hayden, M. R., and Raymond, L. A. (2002) *Neuron* **33**, 849-860
87. Petersen, A., Chase, K., Puschban, Z., DiFiglia, M., Brundin, P., and Aronin, N. (2002) *Exp Neurol* **175**, 297-300
88. Hansson, O., Castilho, R. F., Korhonen, L., Lindholm, D., Bates, G. P., and Brundin, P. (2001) *J Neurochem* **78**, 694-703
89. Hickey, M. A., and Morton, A. J. (2000) *J Neurochem* **75**, 2163-2171

90. Schiefer, J., Landwehrmeyer, G. B., Luesse, H. G., Sprunken, A., Puls, C., Milkereit, A., Milkereit, E., and Kosinski, C. M. (2002) *Mov Disord* **17**, 748-757
91. Hansson, O., Guatteo, E., Mercuri, N. B., Bernardi, G., Li, X. J., Castilho, R. F., and Brundin, P. (2001) *Eur J Neurosci* **14**, 1492-1504
92. Laforet, G. A., Sapp, E., Chase, K., McIntyre, C., Boyce, F. M., Campbell, M., Cadigan, B. A., Warzecki, L., Tagle, D. A., Reddy, P. H., Cepeda, C., Calvert, C. R., Jokel, E. S., Klapstein, G. J., Ariano, M. A., Levine, M. S., DiFiglia, M., and Aronin, N. (2001) *J Neurosci* **21**, 9112-9123
93. Waxman, E. A., and Lynch, D. R. (2005) *Neuroscientist* **11**, 37-49
94. Brustovetsky, T., Purl, K., Young, A., Shimizu, K., and Dubinsky, J. M. (2004) *Exp Neurol* **189**, 222-230
95. Trettel, F., Rigamonti, D., Hilditch-Maguire, P., Wheeler, V. C., Sharp, A. H., Persichetti, F., Cattaneo, E., and MacDonald, M. E. (2000) *Hum Mol Genet* **9**, 2799-2809
96. Guidetti, P., Charles, V., Chen, E. Y., Reddy, P. H., Kordower, J. H., Whetsell, W. O., Jr., Schwarcz, R., and Tagle, D. A. (2001) *Exp Neurol* **169**, 340-350
97. Browne, S. E., Ferrante, R. J., and Beal, M. F. (1999) *Brain Pathol* **9**, 147-163
98. Bogdanov, M. B., Andreassen, O. A., Dedeoglu, A., Ferrante, R. J., and Beal, M. F. (2001) *J Neurochem* **79**, 1246-1249
99. Chretien, D., Rustin, P., Bourgeron, T., Rotig, A., Saudubray, J. M., and Munnich, A. (1994) *Clin Chim Acta* **228**, 53-70
100. Benchoua, A., Trioulier, Y., Zala, D., Gaillard, M. C., Lefort, N., Dufour, N., Saudou, F., Elalouf, J. M., Hirsch, E., Hantraye, P., Deglon, N., and Brouillet, E. (2006) *Mol Biol Cell* **17**, 1652-1663
101. Brustovetsky, N., and Dubinsky, J. M. (2000) *J Neurosci* **20**, 8229-8237
102. Brustovetsky, N., and Dubinsky, J. M. (2000) *J Neurosci* **20**, 103-113
103. Chinopoulos, C., Starkov, A. A., and Fiskum, G. (2003) *J Biol Chem* **278**, 27382-27389
104. Wang, G. J., Randall, R. D., and Thayer, S. A. (1994) *J Neurophysiol* **72**, 2563-2569



105. Panov, A. V., Lund, S., and Greenamyre, J. T. (2005) *Mol Cell Biochem* **269**, 143-152
106. Puranam, K. L., Wu, G., Strittmatter, W. J., and Burke, J. R. (2006) *Biochem Biophys Res Commun* **341**, 607-613
107. Panov, A. V., Andreeva, L., and Greenamyre, J. T. (2004) *Arch Biochem Biophys* **424**, 44-52
108. Ichas, F., and Mazat, J. P. (1998) *Biochim Biophys Acta* **1366**, 33-50
109. Schulz, J. B., Matthews, R. T., Henshaw, D. R., and Beal, M. F. (1996) *Neuroscience* **71**, 1043-1048
110. Kim, G. W., Copin, J. C., Kawase, M., Chen, S. F., Sato, S., Gobbel, G. T., and Chan, P. H. (2000) *J Cereb Blood Flow Metab* **20**, 119-129
111. Ruan, Q., Lesort, M., MacDonald, M. E., and Johnson, G. V. (2004) *Hum Mol Genet* **13**, 669-681
112. Klapstein, G. J., Fisher, R. S., Zanjani, H., Cepeda, C., Jokel, E. S., Chesselet, M. F., and Levine, M. S. (2001) *J Neurophysiol* **86**, 2667-2677
113. Brustovetsky, N., LaFrance, R., Purl, K. J., Brustovetsky, T., Keene, C. D., Low, W. C., and Dubinsky, J. M. (2005) *J Neurochem* **93**, 1361-1370
114. Chang, D. T., Rintoul, G. L., Pandipati, S., and Reynolds, I. J. (2006) *Neurobiol Dis*
115. Steffan, J. S., Bodai, L., Pallos, J., Poelman, M., McCampbell, A., Apostol, B. L., Kazantsev, A., Schmidt, E., Zhu, Y. Z., Greenwald, M., Kurokawa, R., Housman, D. E., Jackson, G. R., Marsh, J. L., and Thompson, L. M. (2001) *Nature* **413**, 739-743
116. Hockly, E., Richon, V. M., Woodman, B., Smith, D. L., Zhou, X., Rosa, E., Sathasivam, K., Ghazi-Noori, S., Mahal, A., Lowden, P. A., Steffan, J. S., Marsh, J. L., Thompson, L. M., Lewis, C. M., Marks, P. A., and Bates, G. P. (2003) *Proc Natl Acad Sci U S A* **100**, 2041-2046

**GRADUATE SCHOOL  
UNIVERSITY OF ALABAMA AT BIRMINGHAM  
DISSERTATION APPROVAL FORM  
DOCTOR OF PHILOSOPHY**



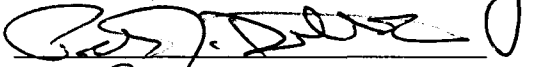


**Name of Candidate** Tamara Milakovic

**Graduate Program** Cell Biology

**Title of Dissertation** Delineating the Effects of Mutant Huntingtin on Mitochondria

I certify that I have read this document and examined the student regarding its content. In my opinion, this dissertation conforms to acceptable standards of scholarly presentation and is adequate in scope and quality, and the attainments of this student are such that he may be recommended for the degree of Doctor of Philosophy.

**Dissertation Committee:**

Name	Signature
<u>Gail V. Johnson</u> , Chair	<u></u>
<u>Shannon M. Bailey</u>	<u></u>
<u>Peter J. Detloff</u>	<u></u>
<u>Richard S. Jope</u>	<u></u>
<u>Mathieu J. Lesort</u>	<u></u>

**Director of Graduate Program** 

**Dean, UAB Graduate School** 

**Date** 6/14/06